FIELD STUDY OF NATURAL GROUND WATER

RECHARGE IN A SEMI ARID LOWLAND

Daniel B. Stephens
Associate Professor of Hydrology

and

Robert G. Knowlton, Jr., James McCord, and Warren Cox
Graduate Research Assistants
New Mexico Institute of Mining and Technology
Department of Geoscience/Research & Development Division

TECHNICAL COMPLETION REPORT

Project No. 1345679

May 1986

New Mexico Water Resources Research Institute

in cooperation with

Department of Geoscience/Research & Development Division
New Mexico Institute of Mining and Technology

The research on which this report is based was financed in part by the United States Department of the Interior, through the New Mexico Water Resource Research Institute.

Project Numbers:

DISCLAIMER

The purpose of Water Resources Research Institute technical reports is to provide a timely outlet for research results obtained on projects supported in whole or in part by the institute. Through these reports, we are promoting the free exchange of information and ideas and hope to stimulate thoughtful discussion and action that may lead to resolution of water problems. The WRRI, through peer review of draft reports, attempts to substantiate the accuracy of information contained in its reports, but the views expressed are those of the author(s) and do not necessarily reflect those of the WRRI or its reviewers.

TABLE OF CONTENTS

LIST OF FIGURES

LIST OF FIGURES (CONTINUED)

LIST OF TABLES

ABSTRACT

A desert area near Socorro, New Mexico was studied to determine the amount of recharge that could occur by direct infiltration of precipitation. Recharge variability due to topography, vegetation and surficial geology was also studied. Except on the dune slopes, the depth to the water table is shallow, on the order of several meters. The instrumentation network included a meteorological station, soil-moisture sensors, and observation wells. Data were collected from as early as November 1982, but the network was not complete until about September 1983.

Precipitation during both summer and winter generates soil-water movement below the root zone. At one location, recharge calculated from Darcy's equation is at least 4 cm/yr, or roughly 20 percent of mean annual precipitation. By calculation of deep drainage at 15 locations, during a 19 month period, the amount of precipitation that may become recharge may vary by an order of magnitude due to the combined effects of vegetation, topography and soil type. Even when the potential for evaporation greatly exceeds the available precipitation, significant amounts of rainfall may infiltrate thick, unconsolidated soils to become recharge. This finding is in contrast to previous speculation by some hydrologists and geologists that groundwater recharge in dry climates is negligible.

Infiltration of precipitation is strongly affected by topography. Tracer experiments on sandy hillslopes clearly show evidence for lateral movement even in the absence of an underlying low-permeable horizon. Lateral flow in the unsaturated zone is also believed to cause substantial variability in moisture content within a homogeneous sand dune. Hydrologic models and water budgets of sloping terrain should recognize the significance of lateral flow in topographically convergent areas. Such areas would be expected to be areas of enhanced recharge potential.

INTRODUCTION

The rate of replenishment of ground water is called recharge. In the basin and range physiographic province, ground water recharge may occur by infiltration of runoff and snow melt in mountain terrain, by infiltration through channels of surface waters, or by deep percolation of irrigation water and natural precipitation. This study is concerned with that portion of ground-water recharge that is derived from the infiltration of natural precipitation over extensive areas.

The quantification of natural ground-water recharge can be very important. Planners and engineers need to know the amount of water available in aquifers for planning and designing projects. Government agencies need this information for water-resource management purposes. If an aquifer has an appreciable amount of recharge, it may be managed as a renewable resource. If the aquifer has a negligible recharge rate, it has been the accepted practice to "mine" the ground water from the aquifer over a certain period of time, say 40 years.

Another reason to study ground-water recharge is to predict ground-water quality impacts from waste disposal seepage. There have been proposals for storing hazardous wastes in desert environments, under the premise that recharge, and therefore seepage rates, are negligible (Winograd 1981; Longmire et al. 1981; Hawley 1983). If recharge is significant, seepage from hazardous wastes could eventually contaminate the underlying aquifer.

To date there have been many recharge studies in humid regions and in irrigated agricultural areas. Natural ground-water recharge in arid or semi-arid regions has been studied by only a few investigators who have found differing results. Some investigators suggest that recharge is negligible and others indicate that recharge may be a significant percentage of the annual precipitation.

The purpose of this project is to better understand the physical processes influencing areal recharge from precipitation in a semi-arid lowland watershed in New Mexico. To this end, soil-water instrumentation was emplaced throughout a small basin north of Socorro. This instrumentation was placed in 15 different locations so that differences in soil water movement due to vegetative cover, slope, and soil type could be analyzed. The types of instrumentation include tensiometers for measuring pressure heads, access tubes for measuring water content profiles with a neutron probe, thermistors for measuring temperature-depth profiles, observation wells for measuring water table elevations, and a weather station for measuring meteorological conditions.

Two methods were employed to calculate recharge. The first is based on Darcy's equation and the second is based on temperature gradients. An approximate method, which is based upon moisture content measurements, was also applied. Tracer experiments on hillslopes and flatlands were conducted to determine the direction of fluid movement following a precipitation event.

RELATED RESEARCH

Soil-water movement was studied in this project through a variety of methods. These include estimations of fluid and temperature fluxes, and tracer experiments. A number of previous studies have used one or more of these methods to estimate recharge.

For example, Enfield et al. (1973) evaluated soil-water potential and temperature data from a site in the south-central desert of Washington state and suggested that less than 1 cm/yr of water was recharging the underlying aquifer. In the High Plains of Colorado, Klute et al. (1972) found, using neutron moisture logging, that when an unvegetated fine-textured soil was covered with a coarse-textured sand, moisture moved to depths exceeding the depth logged, about 3 m. In contrast, for a plot covered with native grass vegetation, they found no measurable increase in moisture below 120 cm, following precipitation events and inferred that virtually no recharge occurred in such areas. In this same general area of Colorado Reddel (1967) estimated recharge rates from field methods on the order of 1 cm/yr; locally, however, in sandy areas where the soil-water pressure head is high, much larger recharge rates may occur.

Dincer et al. (1974) studied natural recharge rates in sand dunes in Saudi Arabia using tritium. Their results indicate that recharge may comprise about 25 percent of the 8 cm of annual precipitation. Allison et al. (1985) used chloride concentrations from core samples to determine that recharge to a cleared sand dune area is as much as 1.4 cm/yr in a semi-arid area in south Australia where mean annual precipitation is about 30 cm/yr.

Meyboom (1966), through the use of water level hydrographs, estimated recharge to be approximately 7.5 percent of the annual precipitation on the Saskatchewan prairies in Canada. Boyle and Saleem (1979) studied temperature profiles in wells in northeast Illinois which penetrate a multiple aquifer system and concluded that the recharge rate across the aquitard was between 7.8 and 31.0 cm/yr.

Maxey and Eakin (1949) devised a method for use in the desert basins of Nevada to predict ground-water recharge. They assumed that ground-water discharge from a basin was essentially equal to the ground-water recharge coming into the basin. They then estimated that in areas where there was less than 20.3 cm/yr of precipitation, the recharge rate was essentially zero. Watson et al. (1976) did a follow up study to the Maxey-Eakin technique. Using multiple and linear regression models, they estimated that as much as 3.4 percent of precipitation could become recharge in areas where precipitation was less than 20.3 cm/yr.

An interesting study by Sammis et al. (1982) compared three different techniques for estimating ground-water recharge on irrigated agricultural land near Phoenix, Arizona. Their three methods were the hydraulic, temperature profile, and tritium analyses, which yielded rates of 18, 9, and 40 cm/yr respectively. Averaging all three estimates yields a predicted recharge of 22 cm/yr.

Besides the physical or chemical means of estimating recharge, some researchers have utilized mathematical models to assist them in their predictions. For example, Freeze (1969) conducted numerical simulations of natural infiltration ground-water recharge and discharge for various hypothetical application rates to analyze moisture redistribution and recharge. No comparisons were made to field data. Hanks et al. (1969) simulated laboratory column data to make estimates of infiltration, redistribution, drainage and evaporation.

Krishnamurthi et al. (1977) used a mathematical model to simulate natural ground-water recharge on the High Plains of Colorado where mean precipitation is about 37 cm/yr. They claimed good comparison of results to actual water level data, and presented a graph showing five years of simulated recharge rates, with values calculated monthly. These recharge rates were on the order of 1 cm/yr. Longenbaugh (1975) made computer estimates of natural recharge in this same area of Colorado. He used field soil-moisture data for his simulations and concluded that recharge was approximately 6.1 cm/yr.

Gupta et al. (1978) developed a model for estimating soil-water movement, with the main emphasis on evapotranspiration. The model calibrations and predictions from their study were for irrigated crops. Jensen (1983) presented an in-depth modeling study of unsaturated flow in two irrigated agricultural areas. He showed good correlation between model results and field data. Kirkham and Gee (1983) presented field and model results showing approximately 20 percent of the precipitation in the Washington state desert regions is recharge, as a result of an unusually wet period.

Higuchi (1984) used numerical simulation results with field data for a humid region in Japan. He demonstrated that upward moisture fluxes occur above the 35cm depth following precipitation events, but that below this depth there is generally downward moisture flow. Thermal gradients are the cause of this upward moisture flux, while the general lack of diurnal temperature changes at depth yields a downward flux.

This is not a complete list of the studies done to date related to this project. However, it does show that there is a need to expand the field data base in arid or semi-arid environments in order to predict more accurately the amount of recharge that may be available.

SITE SELECTION AND DESCRIPTION

The site is located approximately 24 kilometers north of Socorro, New Mexico, within the Sevilleta National Wildlife Refuge, approximately 4.8 kilometers west of Interstate 25 along the Rio Salado (figure 1). The Rio Salado is an ephemeral, braided stream with a broad, shallow channel. The instrumented area is on the south side of the Rio Salado, occupying a small area of only 1.3 square kilometers.

One reason for selecting this area was the variability in topography, vegetation, and, to a lesser extent, soil type. Machette (1978) identified four separate soil mapping units within the area (figure 2), all of which are sandy texture. The topography of this basin is shown in figure 2 along with the locations of the instrumentation sites. The vegetation types have been identified courtesy of Ted Stans, refuge manager. Principal shrubs include: indigo bush, four-wing saltbush, snakeweed, sacatone, annual mustard, creosote bush, and mesquite; other plant species include: gramma grass, spectacle pod, nightshade, desert willow, primrose, globe mallow, sand sage, bind weed, scorpion plant, indian rice grass, prickly pear, yucca, salt cedar, and juniper. No complete study has been undertaken to evaluate the variation of rooting patterns for these plants; however, this information is important to recharge, and a very detailed investigation of moisture flow to an indigo bush is in progress.

Most of the basin shows little evidence of surface runoff outside the Rio Salado channel. Annual precipitation at the site is about 21 cm/yr. Most of the surface soils are quite permeable and therefore facilitate rapid infiltration of precipitation. Where the surface water runoff is negligible, almost all the precipitation that falls must either evapotranspire or recharge the underlying aquifer at a depth of several meters. This characteristic of the site simplifies the analysis of recharge.

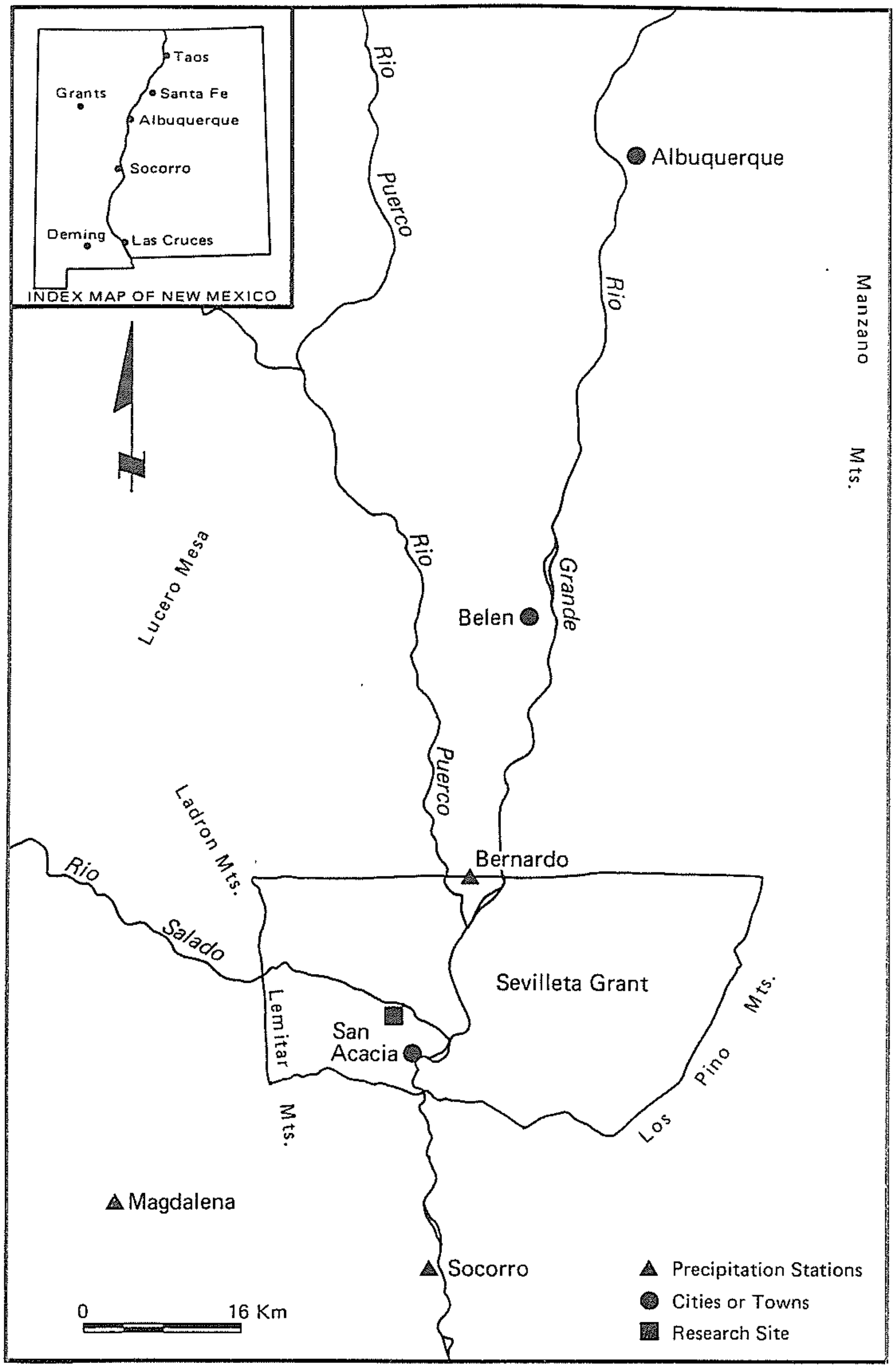

Figure 1. Location Map.

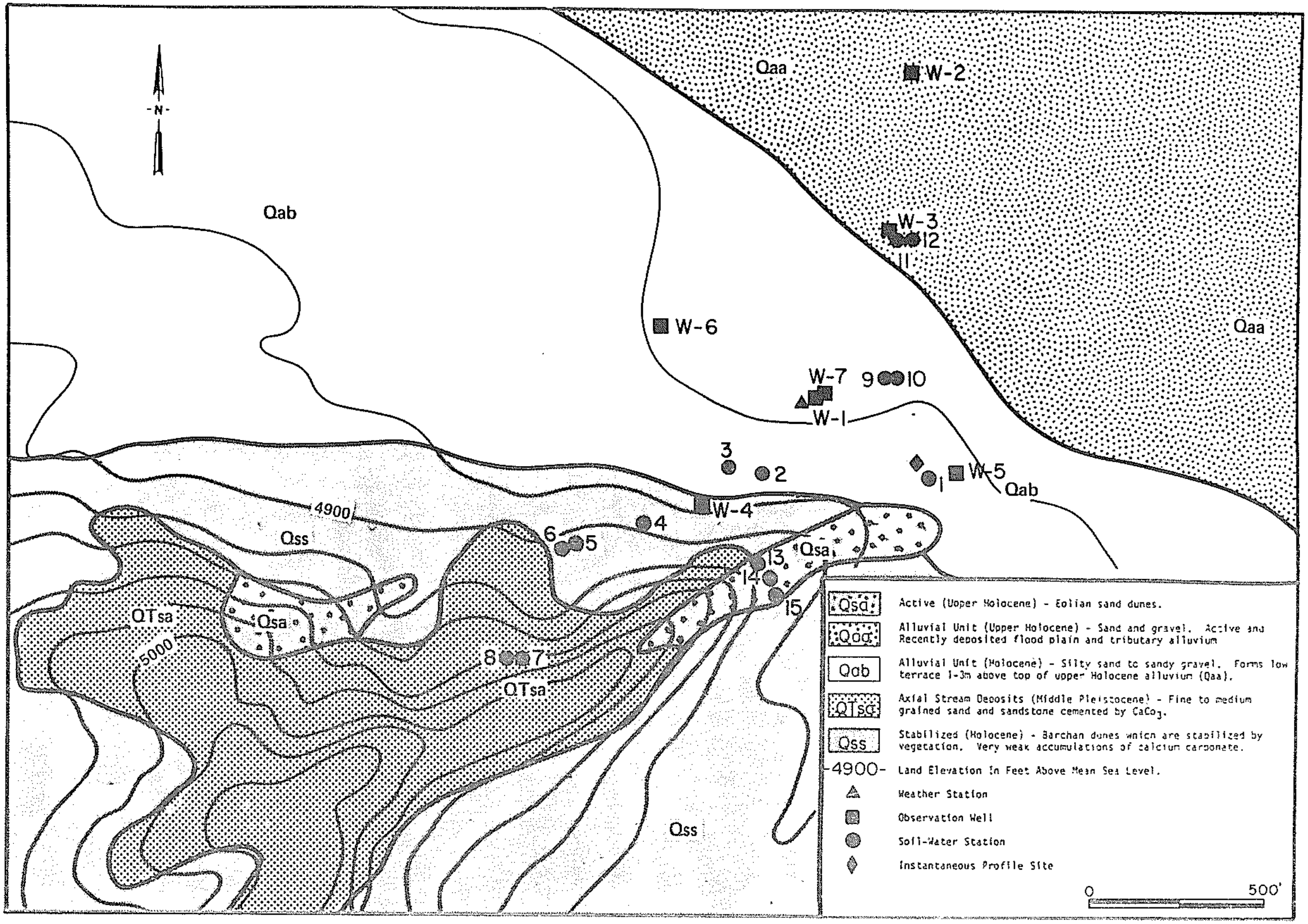

Figure 2. Geologic Map Showing Instrumentation Sites.

SITE INSTRUMENTATION

The research site has been instrumented with a weather station, two additional recording rain gauges, three recording observation wells, four non-recording observation wells, and 15 soil-moisture stations. In addition, soil-moisture station number 1 includes subsurface thermistors. These instrument locations are shown in figure 2.

Weather Stations

The weather station is comprised of a number of meteorological instruments including: a tipping bucket rain gauge with accuracy to 0.02cm; a hygrothermograph with temperature, relative humidity, and barometric pressure sensors; a mechanical pyranograph for measuring solar radiation; and an evaporation pan equipped with a maximum-minimum thermometer, a totalizing anemometer for reading cumulative wind velocities, and a hook gauge with accuracy to 0.001cm. The weather station is located near the center of the basin along the access road, for ease of maintenance. Figure 3 shows a photograph of the weather station and the physical setting.

The two additional rain gauges were set at opposite ends of the basin, one near the head of the basin on the south, and one on a sand bar within the river channel. The gauge in the river channel was identical to the tipping bucket gage at the weather station. The third gauge is a weighing type with accuracy to 0.12 cm. The purpose of installing three rain gauges was to determine whether there is any significant variability in precipitation characteristics as may be expected from thunderstorms, for example.

Observation Wells

As shown in figure 2, seven wells at the site monitor water level fluctuations. All wells were drilled with a Mobile B-30 drill rig. Each was

Figure 3. The Weather Station and Surrounding Vegetation.

drilled to a depth of about 150 cm below the water table, except well 7. Well 7 was drilled to 17.1 m and a well point was set at 10.7 m, about 7 m below the water table.

Wells 1, 3, and 4 were constructed from 15 cm diameter PVC casing with 150 cm of number 20 slot PVC screen. These wells are equipped with water level recorders. Well 2 was constructed from 5 cm diameter PVC pipe which was slotted by hack saw in the bottom 150 cm. Wells 5, 6, and 7 were constructed from 5 cm diameter galvanized steel pipe with 90 cm of wire wrapped number 20 slot screen at the bottom. The spatial arrangement of the observation wells is designed to permit the water level data to be used in calculations of areal recharge, as well as recharge from the Rio Salado channel.

Soil Moisture Monitoring

The soil-moisture station sites were chosen on the basis of soil type, slope, and vegetative cover. The station locations are shown by number in figure 2. Each station consists of a set of laboratory-assembled tensiometers installed in the field to depths ranging from 30 cm to 244 cm below land surface. If the water table depth was more shallow than 244 cm, the deepest tensiometer was set just above the water table. The tensiometers were inserted with the aid of a tensiometer insertion tool. Special care was taken to ensure that the annular space was properly backfilled and that the porous cup was in good contact with the surrounding media. Proper saturation of the porous cup was also considered a crucial step in obtaining good contact with the porous media.

From November 1982 through November 1983 site number 1 had mercury manometer tensiometers. After this time, pressure in the tensiometer was determined by inserting a hypodermic needle, which is attached to a pressure transducer, through a septum rubber stopper on the top of the tensiometer.

The early versions of the tensiometers were constructed according to the specifications of Marthaler et al. (1983) (figure 4), and later in the project a commercially available tensiometer was used (Soil Measurements Systems, Inc., Las Cruces, NM). This manometer system provided rapid and reliable measurements of soil-water potential.

Each soil-moisture station also included a neutron access tube. The neutron access tubes were installed to a depth of 5.8 meters whenever possible. Exceptions occurred where the water table was more shallow, or bedrock was encountered, and at station 1 prior to September 1983 when the depth of the access tube was only 2.1 m. The bottoms of the tubes were plugged with rubber stoppers.

The aluminum access tubing was set by hand augering a 5 cm diameter hole to the proper depth and backfilling with native material. Care was taken to ensure a proper and complete backfill occurred. Stations 11 and 12 required the use of the drill rig for their installation due to the size of the cobbles within the soil profile.

The neutron probe used at the beginning of the project was a Troxler model 3222 depth moisture gauge with a 10 millicurie source. Electronic breakdowns occurred during the winter of 1983-1984. After the end of April 1984, a Campbell Pacific Nuclear, model 503, with a 50 millicurie americium-beryllium source was used for all moisture measurements The probes were calibrated using gravimetric analyses by collecting insitu samples from the access tube core holes and by collecting samples outside the access tubes in some instances.

For calibrating the Troxler neutron probe, 13 data points were used which covered a range of volumetric water contents from 0.063 to 0.35 cm^3/cm^3. A linear regression (y=mx+b) of volumetric water content (y) and neutron probe data (x) gives a slope of 0.895, intercept of -3.36 and r^2 = 0.99. The

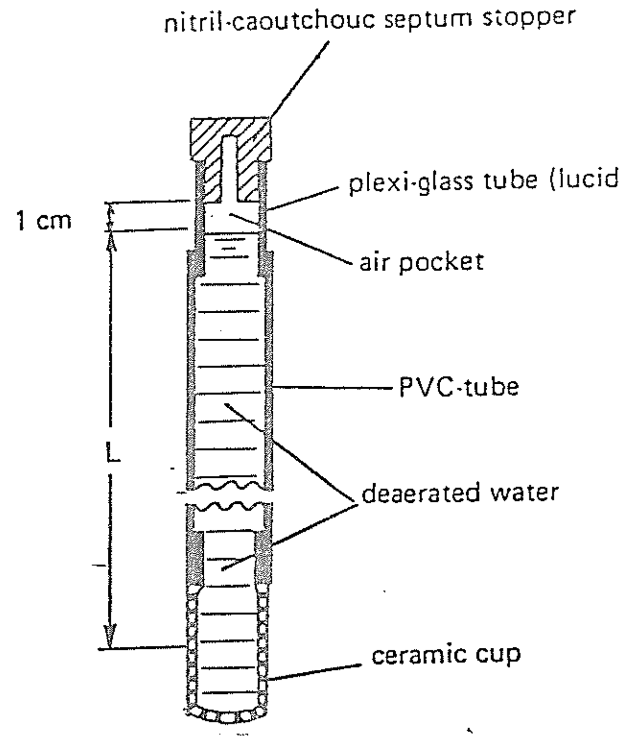

A) TENSIOMETER SETUP

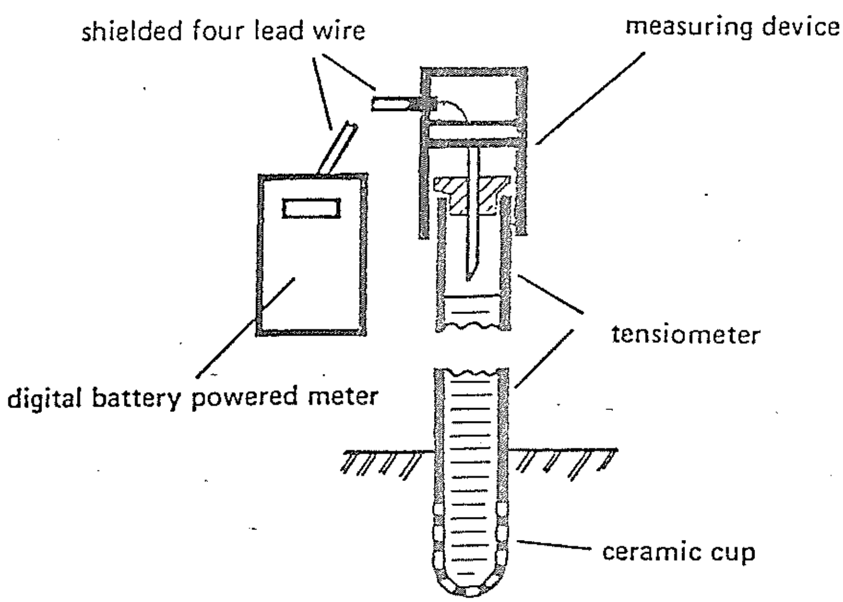

B) MONITORING SETUP

FIGURE 4 - Schematic of Tensiometer Used with the Portable Pressure Transducer

CPN probe was calibrated using 46 data points ranging in value of volumetric water content from 0.056 to 0.382 cm^3/cm^3. The samples included those from the project area and another location comprised of silty sand. Logarithmic transformations of the dependent variables used in a linear regression equation were found to give the best fit to observed data, particularly in the dry range. The equation has the form $\ln y = a + b \ln x$, where a is 0.275, b is 1.32, and x and y are the neutron probe readings and volumetric water contents, respectively. The r^2 value of this equation is 0.967.

Table 1 summarizes the characteristics of the soil moisture monitoring stations shown in figure 2. Soil-mosture station 1 was established in November 1982. This station was set up near the previous research site used for borehole infiltration tests by Stephens et al. (1983). Station 1 is located in a soil type that is near the transition between the active sand dune and the Holocene fluvial deposits along the old floodplain.

Stations 2, 3, 9, and 10 are located in the floodplain in the soil type listed by Machette (1978) as an alluvial deposit of the Holocene age. Stations 2 and 10 are located in sparsely vegetated areas. Each set of paired soil-moisture stations located in sparse and dense vegetation, are within about 10 meters of each other. Stations 2 and 3 are located near the boundary between the old alluvial floodplain and the stabilized eolian sand deposits. In parts of the old alluvial flood plain there is a noticeably finer grained surface soil texture, and correspondingly a greater plant density, than in the eolian deposits.

Stations 4, 5, 6, 7, and 8 are located in the stabilized Holocene eolian deposits. However, station 4 is located near the outcrop of the Santa Fe Formation sandstone, a consolidated axial stream deposit that is slightly

TABLE 1. Summary of Soil-Water Monitoring Station Characteristics

STATION	PREDOMINANT LITHOLOGY	TOPOGRAPHIC CONDITION	VEGETATION
1	Eolian and Alluvial Sand	Flat	Sparse
2	Alluvial Clay and Sand	Flat	Sparse
3	"	"	Dense
4	Stabilized Eolian Sand	Hillslope	Sparse
5	"	Base of Hillslope	Sparse
6	"	"	Dense
7	"	Hillslope	Sparse
8	"	"	
9	Alluvial Sand and Clay	Flat (old flood plain)	Dense
10	"	"	Sparse
11	Alluvial Sand Gravel and Silt	Flat (active channel)	Sparse
12	"	"	Dense
13	Active Eolian Sand	Slope on Dune	None
14	"	Crest of Dune	"
15	"	Swale on Dune	"

weathered at this location. The intent of setting the neutron tube near the bedrock surface underlying the eolian deposits was to monitor interflow within the unconsolidated material above the bedrock. The depth to bedrock at this point is about 3.5 meters. Stations 5 and 6 are located near the base of the slope, whereas stations 7 and 8 are located high on the slope near the weighing-type rain gauge. Stations 6 and 8 are more densely vegetated than stations 5 and 7.

Two stations, 11 and 12, are located in an alluvial deposit of the upper Holocene age, within the modern flood plain of the Rio Salado, just inside the river channel bank. Station 11 is sparsely vegetated and station 12 is more densely vegetated in a salt cedar thicket.

The active eolian sand dune on the southeast side of the basin was also instrumented. Stations 13, 14, and 15 define a transect across the dune from west to east. These dune sands are at least 5.8 m thick, based on hand augering. This contrasts with Machette's estimate of a thickness usually less than 2 meters.

The axial stream deposits of the Santa Fe Formation, the source material for the active dune, could not be instrumented with available equipment due to their consolidated nature.

Soil Temperature

At station 1, soil temperature was recorded to an accuracy of about 0.5°C by thermistors (Model MC-312, Soiltest, Inc., Evanston, IL) placed in the soil at 30 cm depth intervals to 214 cm below land surface. The thermistors were calibrated in the laboratory before installation.

MONITORING PROCEDURES

The instrumentation at the study site was monitored either continuously, via recording charts and cassettes, or semi-weekly through manual observations. The three recording observation wells, hygrothermograph, three precipitation gauges, and the radiometer all have seven day recording charts and were changed once a week. The evaporation pan instrumentation and soil thermistors at station 1 were read semi-weekly. The non-recording observation wells were also measured twice a week.

The tensiometers were recorded semi-weekly and filled when necessary with de-aired, distilled water. The water was de-aired in the field by bubbling helium through it.

Early in the program during the winter months, temperatures were cold enough to freeze and crack some of the plastic tops on the tensiometers. These cracks permitted the tensiometers to lose vacuum and drain water into the soil, thus locally disturbing the natural flow field. This problem was overcome by filling the tensiometers with a 40 percent solution of ethylene glycol in de-aired, distilled water. Under laboratory conditions, no significant differences were observed between pressure head in tensiometers filled with the ethylene glycol solution, and tensiometers filled only with distilled water.

The water content was monitored weekly at each soil-moisture station. The first neutron tube was installed at station 1 in November 1982 to a depth of 213 cm. Measurements were made in 15 cm increments from about 30 cm to 198 cm of depth below land surface. In September 1983 this neutron access tube was replaced with a 580 cm deep tube. Measurements were made in 15 cm increments from 30 cm to 274 cm depth and in 30 cm increments from 274 cm to 549 cm depths. Monitoring soil moisture at the other stations also began in late summer of 1983 and followed similar procedures. Monitoring the 15 stations with a neutron probe was very time consuming and tedious. Therefore, roughly half the sites were measured during each semi-weekly trip to the field.

HYDRAULIC CHARACTERISTICS

In situ unsaturated hydraulic conductivity was determined by the instantaneous profile method (Hillel et al. 1972) at a location about 10 m west of station 1 (figure 2). A 2m x 2m area, void of vegetation, was leveled and bermed with sand. Tensiometers were placed in the center of the area at 30 cm depth intervals to 153 cm. For monitoring moisture content by the neutron scattering method, a 5 cm diameter aluminum access tube was emplaced in the center of the plot to a depth of about 3m. The neutron probe (Troxler, Model 3222) readings were calibrated against gravimetric data over a wide range of water contents. Water was pumped from the underlying alluvial aquifer, through a flow meter, and into the impoundment. The depth of ponding ranged from 5.2 to 6.8 cm. After five hours of infiltration, the pressure head and water content profiles remained approximately constant. The steady infiltration rate corrected to $20^{o}C$ was 1.0×10^{-2} cm/s by measuring the rate of decline in the ponding depth after the water supply line was closed, and the flow rate was 8.5×10^{-3} cm/s by flow meter measurements. During an 18-day drainage period, the plot was covered with plastic to prevent evaporation. Hydraulic conductivity was calculated by a graphical procedure described by Hillel (1980).

The relationship between the natural log of calculated hydraulic conductivity and water content in Figure 5 is nearly linear in the range of insitu water contents (less than about 11 percent); a linear regression through this segment gives $K(\theta) = 0.11 \;\; n K + 0.21$ ($r^2 = 0.71$). Unsaturated hydraulic conductivity versus pressure head is shown in figure 6. A linear regression fit through data from all depths gives $K(\psi) = 0.5601 \exp (0.02030\psi)$, with ψ in centimeters of water and $r^2 = 0.88$. These insitu results are consistent with conductivities calculated from a flownet procedure (Stephens 1985) and with

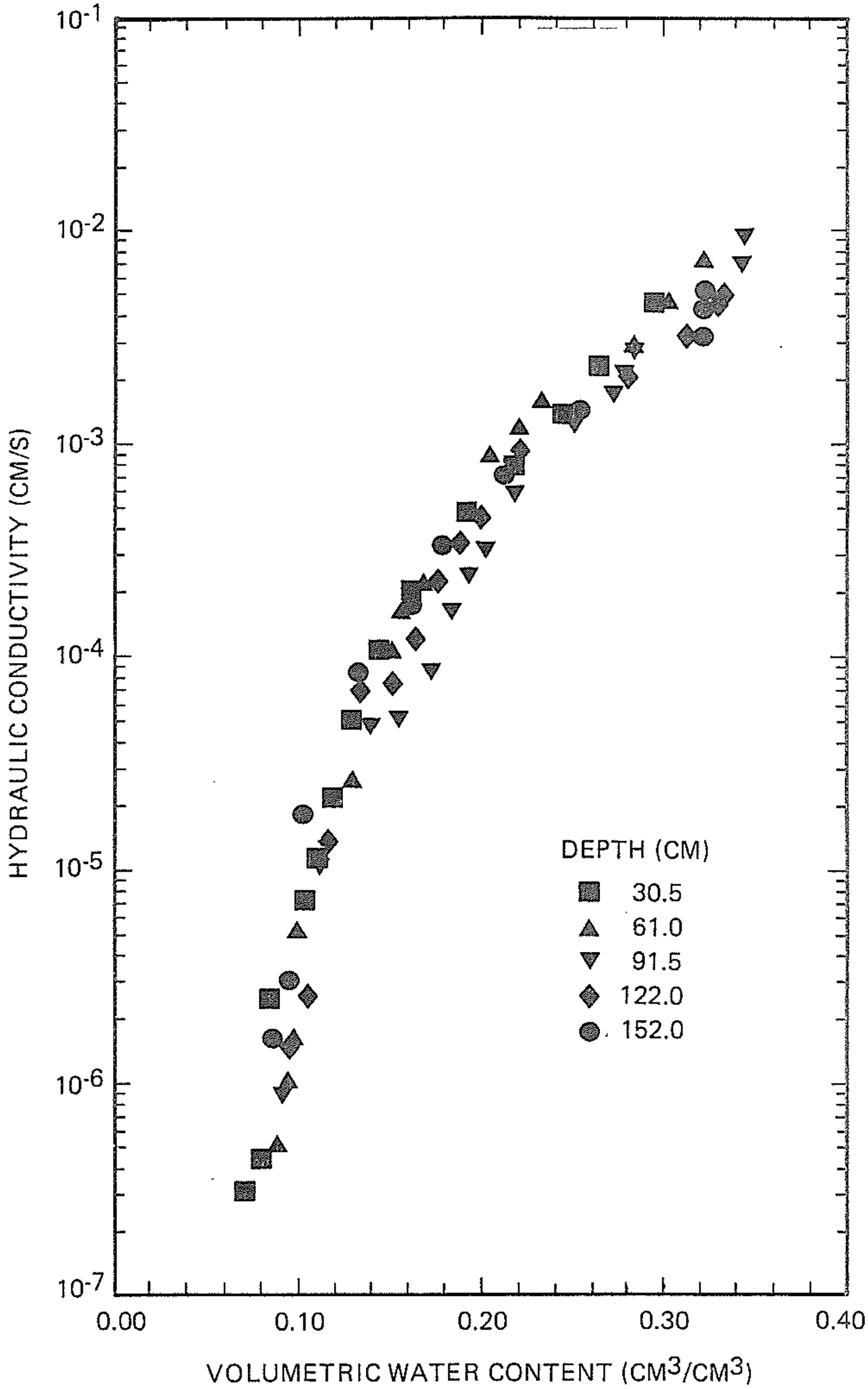

Figure 5. K versus Water Content Data from Instantaneous Profile Test.

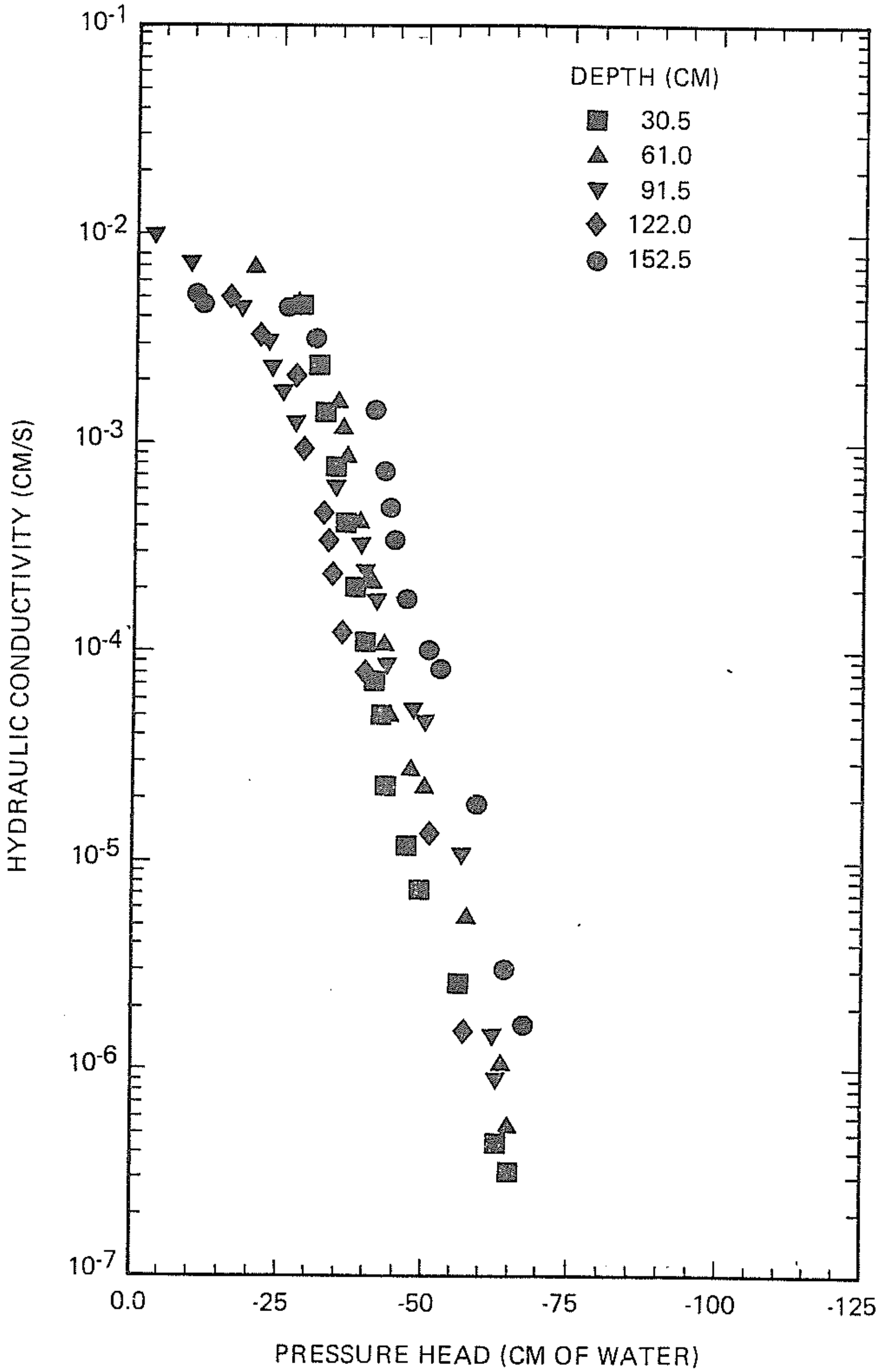

Figure 6. K versus Pressure Head Data from Instantaneous Profile Test.

conductivities calculated from soil-water retention data on cores from the impoundment (Stephens and Rehfeldt 1985).

An analysis of errors associated with calculating unsaturated hydraulic conductivity (e.g., Fluhler et al. 1976) indicates that the 95 percent confidence interval ranges from about $\pm$ 60 percent at 0.33 cm^3cm^{-3} to about $\pm$19 percent at about 0.075 cm^3cm^{-3}. However, there is another source of error in the hydraulic condfuctivities determined from the instantaneous profile test. The test was conducted during the month of February when soil temperatures within the test interval averaged 8 to 9°C prior to infiltration of water which had a temperature of 17 to 20°C. For this report, no temperature corrections were applied to fluxes determined in situ. If a viscosity (temperature) correction were applied to calculated fluxes, the unsaturated hydraulic conductivities would increase by perhaps 30 percent compared to values shown in figures 5 and 6. Thus, neglecting other sources of error, recharge values calculated herein would be conservatively low. Unsaturated hydraulic conductivity expressed as a function of pressure head is likely to exhibit some hysteresis. This is especially true for this sand where the pressure head becomes relatively large. It should be kept in mind that K-ψ is obtained during drainage in the instantaneous profile method. At a given pressure head, the unsaturated hydraulic conductivity during drainage may be greater than that during wetting. As a result, if recharge is calculated from pressure head during a wetting cycle, then the actual value of recharge would be smaller than the calculated value. On the other hand, no significant hysteresis in K-θ is expected at any field water content less than saturation.

For determining saturated hydraulic conductivity in the vertical direction, thin-walled shelby tube samples (7.3 cm diameter x 61 cm) were collected about 1 m west of the soil-water monitoring station from land

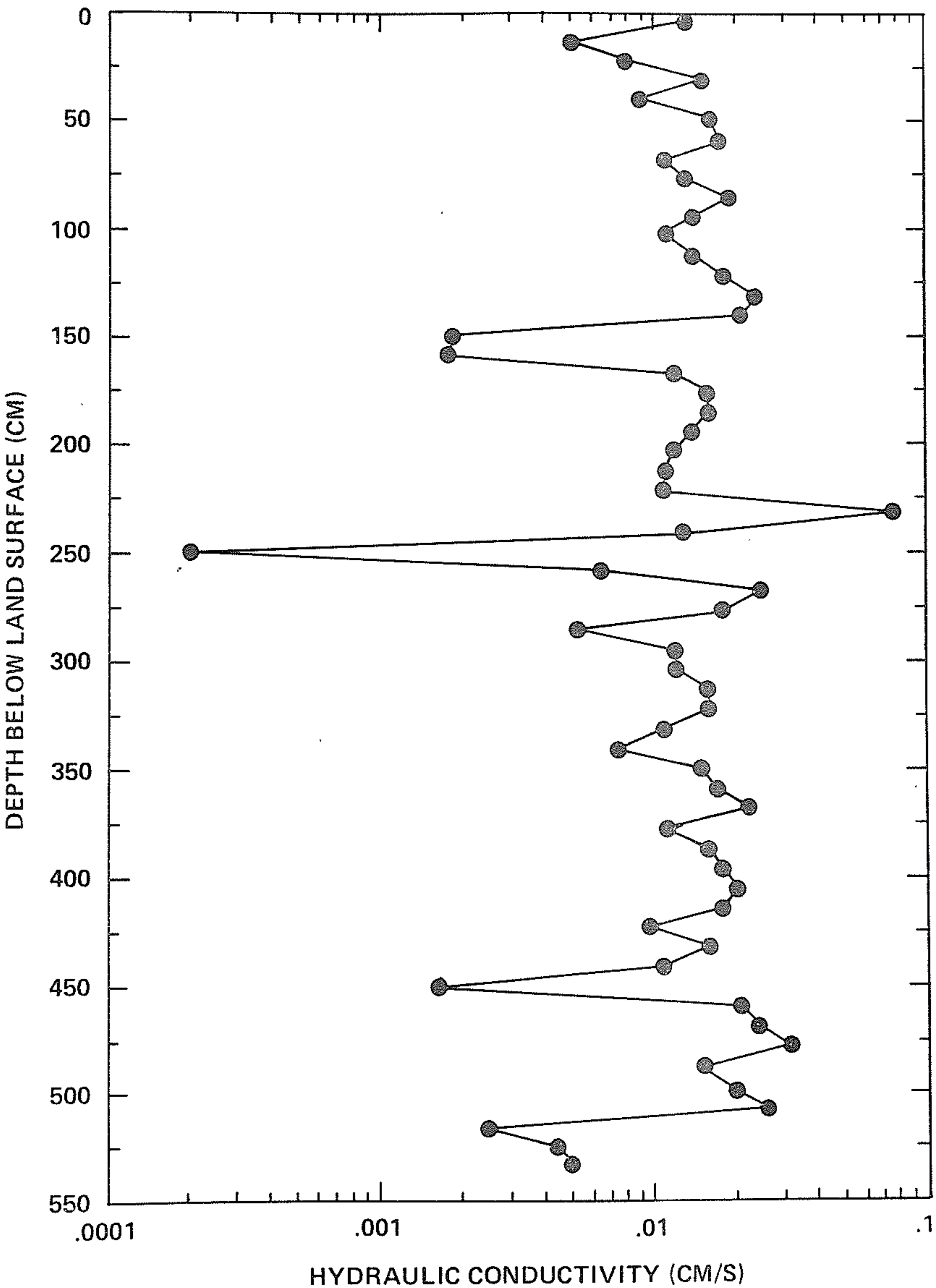

Figure 7. Depth versus Saturated Hydraulic Conductivity from the Shelby Tube Permeameter.

surface to 5.33 m depths using a Mobil B-30 drill rig with hollow stem flight augers. The samples were returned to the laboratory and fitted with manometers at about 9 cm intervals by drilling through the wall of the tube. To minimize entrapped air during wet-up, carbon dioxide was injected through the samples, followed by tap water from a constant head reservoir. Infiltration was allowed to procede until manometer fluid levels stabilized, and then flow rate and gradients were determined to calculate conductivity by Darcy's equation. On the average, the profile of saturated conductivity, shown in figure 7, is similar to one described a few tens of meters to the west by Byers and Stephens (1983) which was obtained from constant head permeameter analyses on 100 cc core samples. The average conductivity results from laboratory tests are in good agreement with insitu ponding experiments, borehole infiltration tests, and air-entry permeameter experiments in the same soil described by Stephens et al. (1983).

The soil-moisture characteristic curve (also referred to as the θ-ψ curve) was determined using the 100 cc 'undisturbed' soil samples (pF rings) and the hanging column method (Vomocil 1965). The method was used for both imbibition and drainage. Figure 8 shows the results from the 30.5 cm depth, including the effect of hysteresis. The results are similar to those from other depths and are typical of unconsolidated sands.

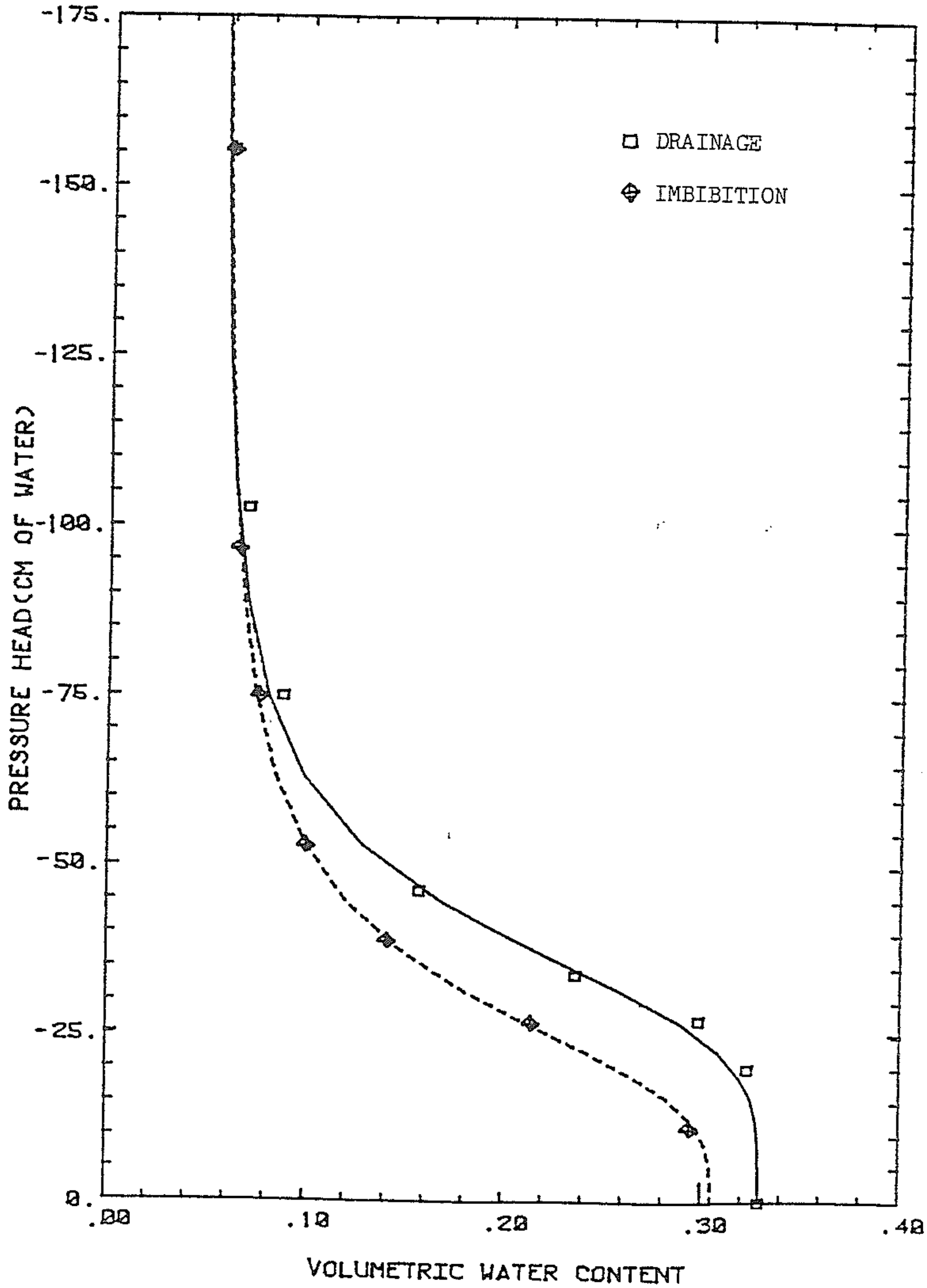

FIGURE 8. - Pressure Head versus Water Content for the 30.5cm Depth

METHODS OF ANALYSIS OF RECHARGE

Hydrodynamic Approach

This report is concerned with estimating the flux of deep percolation of precipitation through the unsaturated zone that may recharge the ground-water table. The assumption is made that any downward flux of water below the root zone eventually will reach the water table. One method of estimating this flux at a particular depth is by Darcy's equation:

$$q = K(\psi) \times i \tag{1}$$

where q = Darcian flux, [L/T]

$K(\psi)$ = vertical unsaturated hydraulic conductivity as a function of pressure head, [L/T]

i = vertical hydraulic gradient, [L/L].

The tensiometric data from soil-moisture station 1 were used to calculate the hydraulic gradient over a discrete time interval. An average value of pressure head over this time interval was used to determine the corresponding value of unsaturated hydraulic conductivity (figure 6). The effective average hydraulic conductivity for the profile is estimated by both a harmonic and a geometric mean. A harmonic mean may be expected to better characterize the hydraulic conductivity of a horizontally stratified medium when vertical infiltration occurs.

The unsaturated hydraulic conductivity was also estimated from the neutron moisture data at station 1. The Darcian flux was set equal to the unsaturated hydraulic conductivity corresponding to the average water content over a particular depth interval, by assuming a unit hydraulic gradient within the profile.

Temperature Gradient Method

The temperature gradient approach (Stallman 1963) was also used for estimating the recharge flux. The assumptions behind the derivation of this technique was originally developed for determining vertical leakage across aquitards where the porous medium was saturated, homogeneous, and isotropic. Boyle and Saleem (1979) give a good discussion on how to use this technique.

Sammis et al. (1982) showed how this method could be used in the vadose zone with good results. The methods assumes a steady state temperature distribution, and therefore a uniform seepage velocity in the vertical direction. Two separate equations are solved to estimate the seepage velocity. The first equation to be used is solved iteratively for the term B, where:

$$\frac{Tz - To}{Tl - To} = \frac{\exp(Bz/L) - 1}{\exp(B) - 1} \qquad (2)$$

Tz = temperature at depth z

To = temperature at depth z = 0

Tl = Temperature at depth z = L

L = vertical distance over which temperatures are observed

This value of B is then used in the following equation to solve for the seepage velocity, V_z:

$$V_z = \frac{k\ B}{Co\ Po\ L} \qquad (3)$$

k = thermal conductivity of the medium, Cal/cm-sec-°C

Po = density of the medium at field saturation, g/cm^3

Co = specific heat of water, Cal/gm-°C

Negative values of B indicate upward flow, positive value indicate downward flow and a zero value indicates no flow.

After solving for the seepage velocity, the average water content, θ, was used to estimate the Darcian velocity, or recharge flux, from the following equation:

$$q_T = V_z \times \theta \tag{4}$$

This technique was applied to the temperature data gathered from soil-moisture station 1 at the 152, 183, and 213cm depths. At these depths there are minor diurnal temperature fluctuations, and significant seasonal temperature changes. In any given season the temperature data were usually collected at about the same time each day. This should minimize diurnal fluctuations in the data. Temperatures for each depth are averaged for the period of record; thus, transient effects are neglected.

Deep Drainage

In the soil profile, moisture content may vary seasonally due to infiltration of precipitation, but over the long term moisture content is fairly constant, with inflows balancing outflows. In an interval of the profile below the root zone, the outflows will be due to drainage which will eventually become recharge. The outflow from the profile below the root zone can be determined from the moisture content profiles. To calculate deep drainage, q_D, we used the equations:

$$q = \frac{1}{t} \int_0^t q_L dt \tag{5}$$

$$q_L = \int_{z_1}^{z_2} \left(\frac{\partial\theta}{\partial t}\right) dz \approx \sum_{z_1}^{z_2} \left(\frac{\Delta\theta}{\Delta t}\right) \Delta z \tag{6}$$

where $\Delta\theta_L$ is the decrease in water content within depth interval Δz during time period Δt. Only losses of water which occurred between periods of measurement (usually weekly) were accounted for in this approach. The approach is conservative in that there may be periods of near steady-state flow and deep percolation when there is no measurable change in moisture content.

Bromide Tracer Experiments

An experimental technique applied in this study is the use of a bromide tracer in measuring average water particle velocities, or seepage velocities, after natural precipitation events. The basic concept employed here has been applied by other researchers, such as Jury et al. (1982) and Saffigna et al. (1977). Bromide is a highly soluble ion which very rarely occurs in nature in any appreciable amounts. It is easily detected with the use of a relatively inexpensive bromide ion-specific electrode.

Flatlands. In the field, 15 cm diameter PVC columns were installed near station 1 by driving them about 30 cm into the soil until the top of each column was flush with land surface. The top 1 cm of soil was then removed from the column and 5.0 g of bromide ($CaBr_2 \cdot 2H_2O$) was distributed over this surface. The previously removed soil was then placed on top of the column to protect the tracer from blowing away. The columns were then left in place until after a precipitation event occurred. A few days after the event, the columns were pulled from the soil, capped at both ends, and then brought back to the laboratory for analysis.

As soon as the columns were brought into the lab the soil was removed in 1 cm intervals, the soil samples placed in beakers, weighed, then put in the oven to dry. After 24 hours of drying at 105°C the samples were taken out and weighed to determine the water content.

Then, a known volume of distilled water and ISA (Ionic Strength Adjuster) solution was added to each soil sample. Each sample was stirred thoroughly, while the bromide electrode was lowered into the solution to determine the bromide concentration. According to previous studies by Warrick et al. (1971), the depth of the wetting front, Z_{wf}, during a period of uniform infiltration, could be calculated from the following approximation:

$$Z_{wf} = (K(\theta_0) \times t)/(\theta_0 - \theta_i) \tag{7}$$

where $K(\theta_0)$ is the hydraulic conductivity behind the wetting front in units of [L/T], t is the time over which infiltration has occurred, θ_0 is the volumetric water content behind the wetting front, and θ_i is the initial water content.

The bromide concentration profile should show the maximum depth of infiltration of the bromide salt due to the precipitation. Warrick et al. (1971) showed that the solute front will lag behind the wetting front, owing to the displacement of water initially in the profile by the infiltrating precipitation. The vertical extent of the bromide solution, an indication of the actual depth of infiltration of the precipitation, may be approximated with the following equation:

$$Z_s = (K(\theta_0) \times t)/(\theta_0) \tag{8}$$

<u>Hillslope</u>. The site of the hillslope tracer experiments lies approximately 30 m east of station 7 as shown on figure 2. The site is sparsely vegetated and the subsurface materials consist of stabilized eolian sands. The ground surface slopes 23 degrees to the north and small scale eolian bedding structures are also found. These bedding structures are parallel to sub-parallel with the ground surface, dipping about 24 to 28 degree dip to the north.

Initially, three trenches were dug 30 cm wide by 60 cm deep. Sheets of plastic were laid against both side walls of the trenches (not the bottom) and the trenches were then backfilled with the excavated sand. Calcium bromide was placed in the three trenches at a different depth in each trench: 1 cm, 15 cm, and 50 cm, respectively. Following a major rain event, soil samples were collected along the length of the trench. These soil samples were then tested in the laboratory to determine bromide concentration using a specific ion electrode.

Subsequently, experiments were repeated in the "undisturbed" materials between the backfilled trenches. The bromide tracer was placed at a 1 cm, 15 cm, and 50 cm depth at each different location. This time, however, the tracer was applied as a 30 cm long horizontal line source at each site. Following two rainfall events in October 1984, each location was sampled along a transect downslope from the middle of the line source. After another rainfall event, which occurred about three weeks following the first events, the soils were sampled again.

RESULTS

Meterological Data

Temperature. The mean daily temperatures averaged over the month are shown in figure 9. The maximum recorded daily temperatures was 37°C on September 27, 1984, and the minimum daily temperature was -16.1°C on February 4, 1985. Freezing temperatures were common from late November through January, as evidenced by ice on the evaporation pan. Figure 10 shows soil temperatures near station 1 to depths of 213 cm, and average montly temperatures are given in table 2. The thermistor at 122 cm did not produce reliable results and was omitted from the records. Where monthly average temperatures were required at the 122 cm depth, they were calculated from the arithmetic average of temperatures from the 92 and 153 cm depths.

Pan Evaporation. The mean monthly potential evaporation data are shown in figure 11, based on measurements of pan evaporation corrected with a class A pan coefficient of 0.7. For 1984, the total potential lake evaporation was about 160 cm. This amount of evaporation is reasonably close to the long-term annual estimate of 178 cm by the U.S. Department of Agriculture (1972).

Winds are usually persistent at the site. The wind velocity averages 5 to 6 km/hr during the late winter and spring, and only about 1 to 2 km/hr in the fall. The relative humidity is generally low.

Precipitation. Figure 12 illustrates the pattern of precipitation at the site during the period of measurement. There appear to be significant differences between stations, as shown more clearly in table 3. The flatland gage, a tipping bucket type, appears to record less precipitation than the hillslope gage, a weighing type of gage. Reasons for this difference may be due to calibration errors or natural variability of precipitation. From

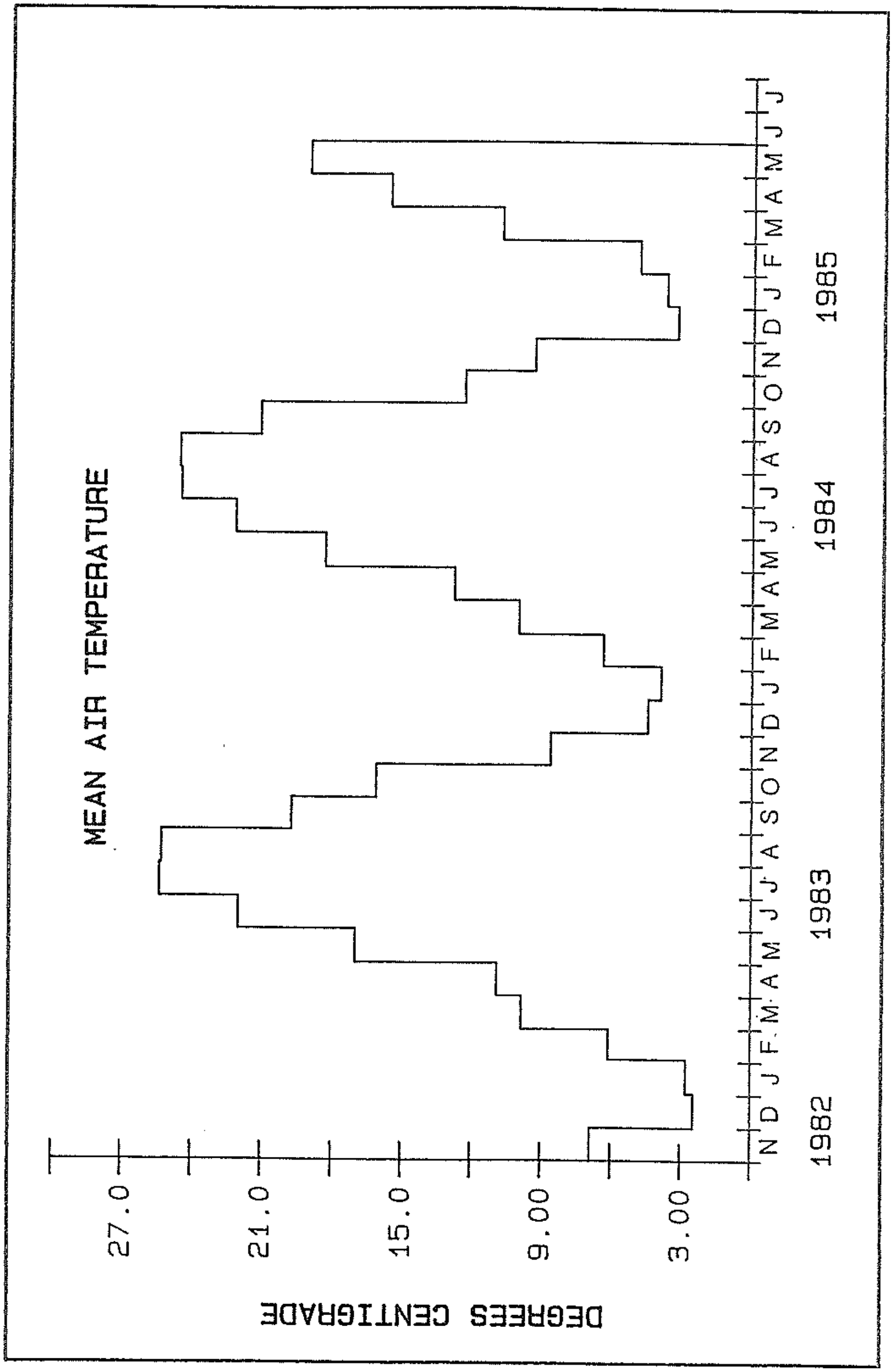

Figure 9. Mean Monthly Air Temperature at the Site.

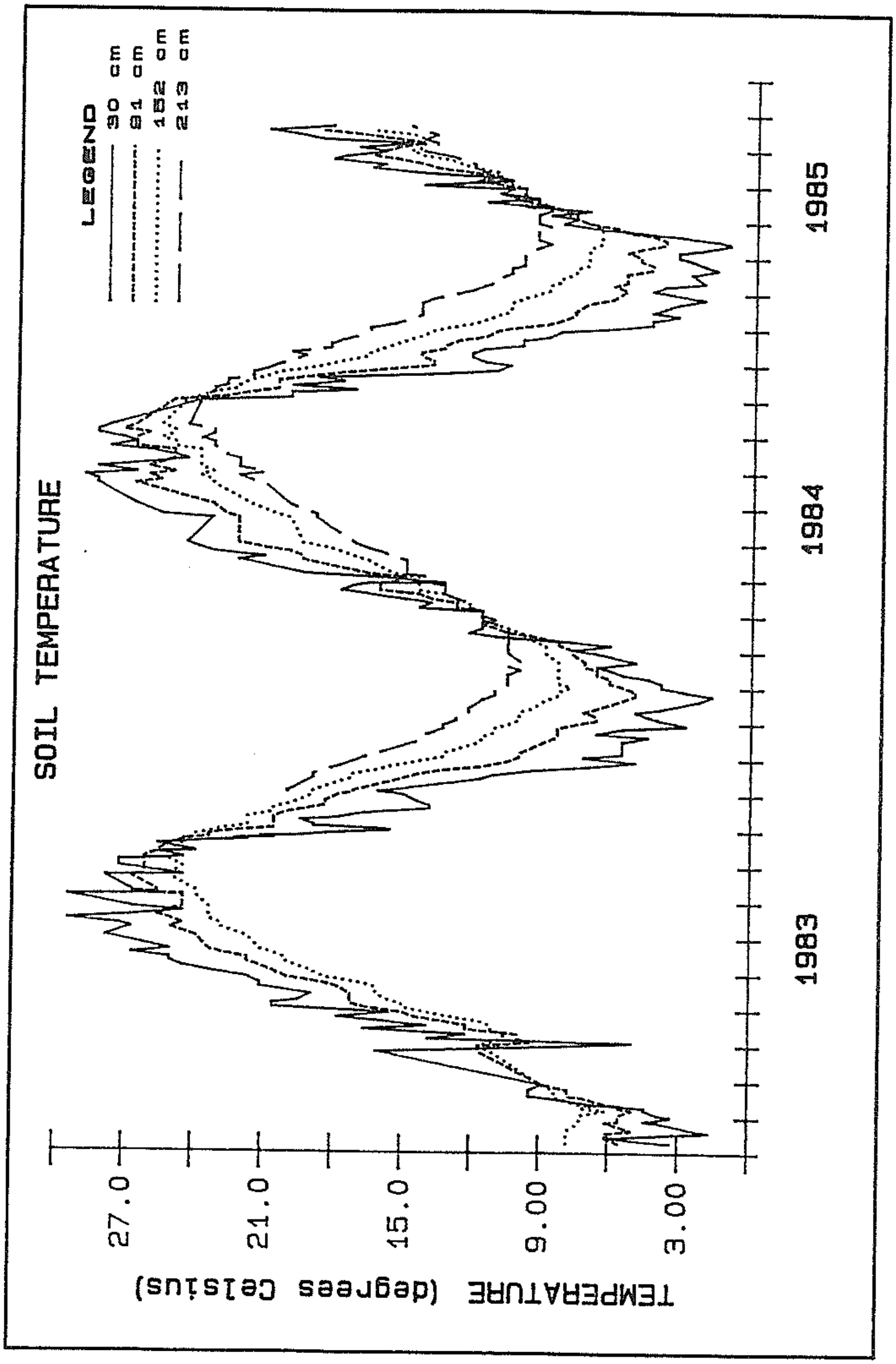

Figure 10. Soil Temperature Near Station 1.

TABLE 2. AVERAGE MONTHLY SOIL TEMPERATURE IN DEGREES CELSIUS

Month	Depth (cm) 92	153	183	214
1/83	5.6	7.3	9.3	---
2/83	8.2	8.7	9.4	---
3/83	10.3	11.0	11.1	---
4/83	15.1	13.6	12.8	---
5/83	20.2	18.5	17.1	---
6/83	23.9	21.8	20.3	---
7/83	25.4	23.8	22.5	---
8/83	26.0	24.9	23.9	---
9/83	22.3	23.0	22.9	---
10/83	17.5	19.1	19.7	---
11/83	11.2	14.5	15.8	18.2
12/83	7.3	10.3	11.6	13.7
1/84	5.9	8.3	9.2	11.5
2/84	8.3	9.0	9.4	10.4
3/84	12.4	11.9	11.7	11.2
4/84	16.4	14.9	14.2	13.5
5/84	21.0	18.6	17.3	16.6

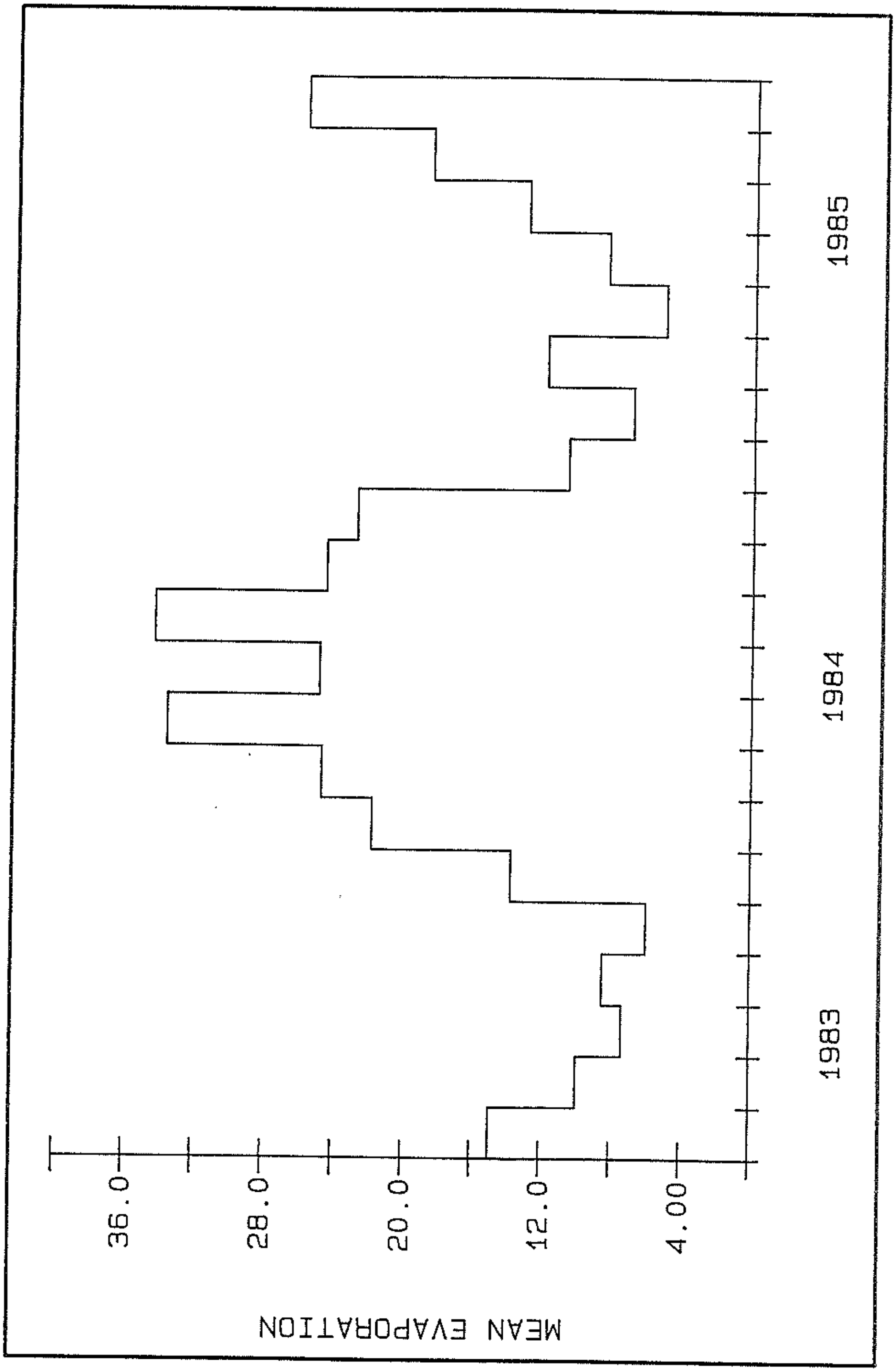

Figure 11. Mean Monthly Potential Evaporation in Centimeters.

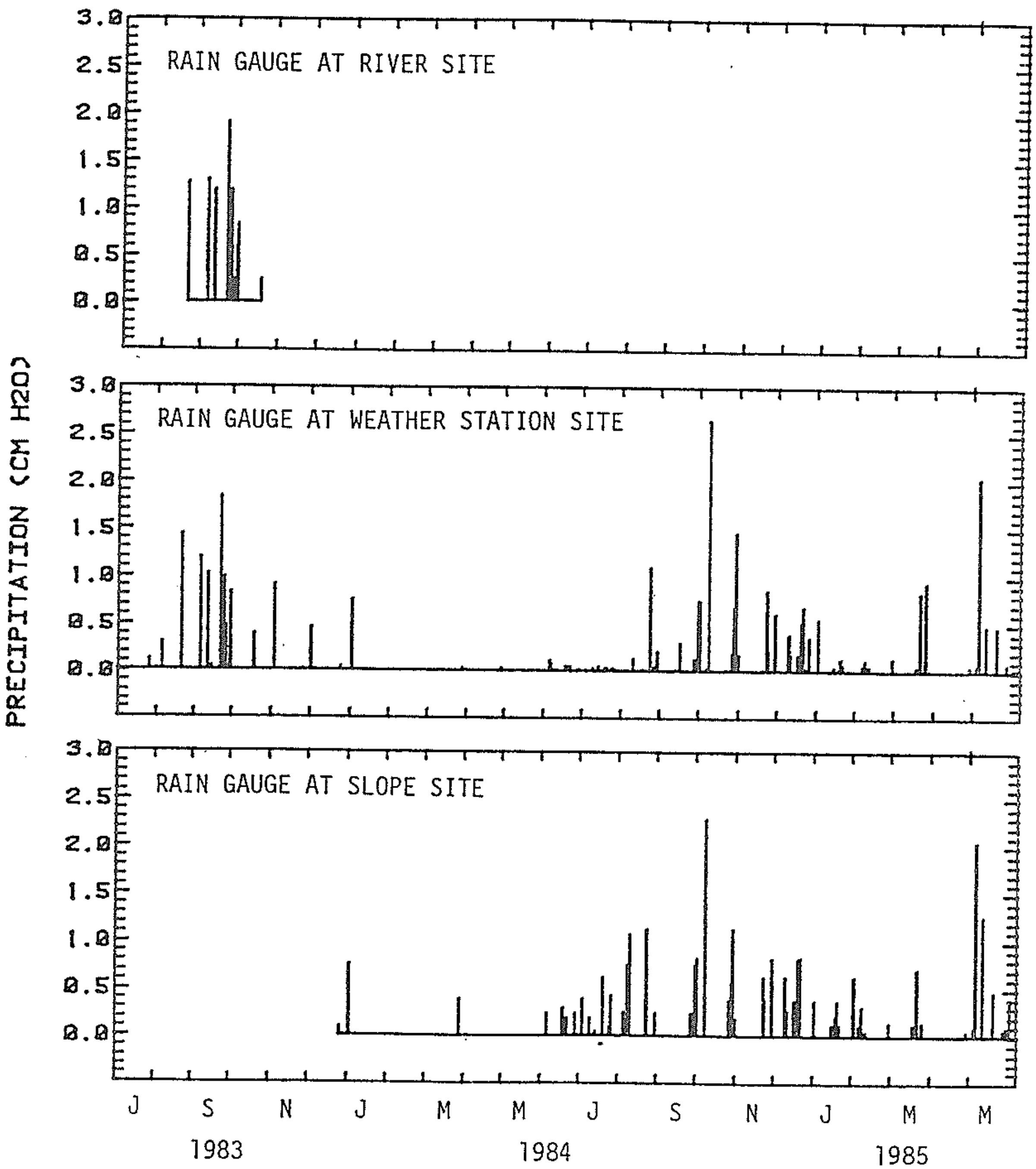

Figure 12. Daily Precipitation at the Site.

TABLE 3. RECORDS OF PRECIPITATION

PRECIPITATION (cm)

	Period of Record	Hillside Gage	Flatland Gage	River Gage	Socorro (departure)	Bernardo
1982	NOV.	----	----	----	1.55(+0.74)	2.13
	DEC.	----	----	----	3.78(+2.39)	2.85
1983	JAN.	----	----	----	4.62(+3.94)	5.79
	FEB.	----	----	----	3.45(+2.57)	1.17
	MAR.	----	----	----	0.89(+0.03)	0.64
	APR.	----	----	----	0.51(-0.46)	0.23
	MAY	----	----	----	1.27(-0.36)	0.30
	JUNE	----	----	----	0.05(-1.42)	1.09
	JULY	----	0.12	----	0.94(-2.31)	1.40
	AUG.	----	1.79	1.27	3.86(-0.33)	1.02
	SEP.	----	6.09	5.99	5.51(+2.29)	3.38
	OCT.	----	1.24	1.28	2.21(-0.56)	2.90
	NOV.	----	0.95	----	2.41(+1.60)	1.32
	DEC.	0.10	0.51	----	0.28(-1.12)	1.02
1984	JAN.	0.76	0.78	----	1.85(+1.17)	0.20
	FEB.	0.00	0.00	----	0.00(-0.89)	0.00
	MAR.	0.04	0.04	----	0.00(-0.86)	0.46
	APR.	0.00	0.04	----	0.68(-0.28)	0.51
	MAY	0.00	0.00	----	0.31(-0.61)	0.08
	JUNE	1.30	0.58	----	1.47(---)	1.63
	JULY	1.82	0.28	----	4.22(+0.51)	6.17
	AUG.	4.12	1.53	----	3.66(-0.53)	6.05
	SEP.	1.84	2.23	----	1.88(-1.35)	2.18
	OCT.	4.58	5.25	----	5.94(+3.18)	5.31
	NOV.	1.88	1.72	----	2.06(+1.24)	1.60
	DEC.	3.69	3.15	----	5.86(+4.47)	5.38
1985	JAN.	1.62	0.39	----	2.26(+1.58)	1.88
	FEB.	0.53	0.35	----	0.61(-0.28)	0.71
	MAR.	0.99	1.83	----	----	----
	APR.	2.22	2.20	----	----	----
	MAY	2.41	1.11	----	----	----
JUNE'84-MAY'85		27.00	20.62	----	----	----
CALENDER YR.'84		20.03	15.60	----	27.94	31.57
AVE. 1962-1984		----	----	----	23.32	19.91
MAX. 1962-1984		----	----	----	35.48(1972)	35.36(1974)
MIN. 1962-1984		----	----	---	12.88(1970)	10.72(1964)

August to October 1983, very good agreement was observed between a tipping bucket precipitation gage placed near the river channel and the tipping bucket gage at the weather station; unfortunately, the gage near the river was destroyed in a large runoff event. Nevertheless, the total precipitation at the site averages much less than that at Socorro or Bernardo, as indicated by precipitation for calendar year 1984 in table 3. Depending upon which 12-month period is selected for averaging, annual precipitation may range from about 15.6 to 27.0 cm for the two gages at the site.

Although the total precipitation at the Sevilleta site is less than that measured at Bernardo and Socorro, the monthly precipitation patterns are very similar, as indicated in table 3. Figure 13 shows that precipitation during the winter of 1982 and winter of 1984 were considerably above normal. At Socorro, the spring and early summer of 1983 and the period from about February 1984 through September 1984 were very dry; in contrast, the precipitation for December 1984 was more than 420 percent above normal. At the site, total precipitation was less than 0.04 cm for the four month period of February through May 1984. However, on the average, annual precipitation during the period of record at the site probably was well within the extreme annual events, based on long-term records from Socorro and Bernardo.

Figure 14 shows the ratio of precipitation to potential evaporation. A ratio less than unity indicates that precipitation is less than potential evaporation. On a monthly basis, the potential evaporation is always greater than precipitation. In the winter the monthly potential evaporation is about twice the precipitation, and in the summer the potential evaporation is more than about 14 times the precipitation.

Soil Moisture Content Measurements

Moisture content data through May 1984 for station 1 are shown in figure

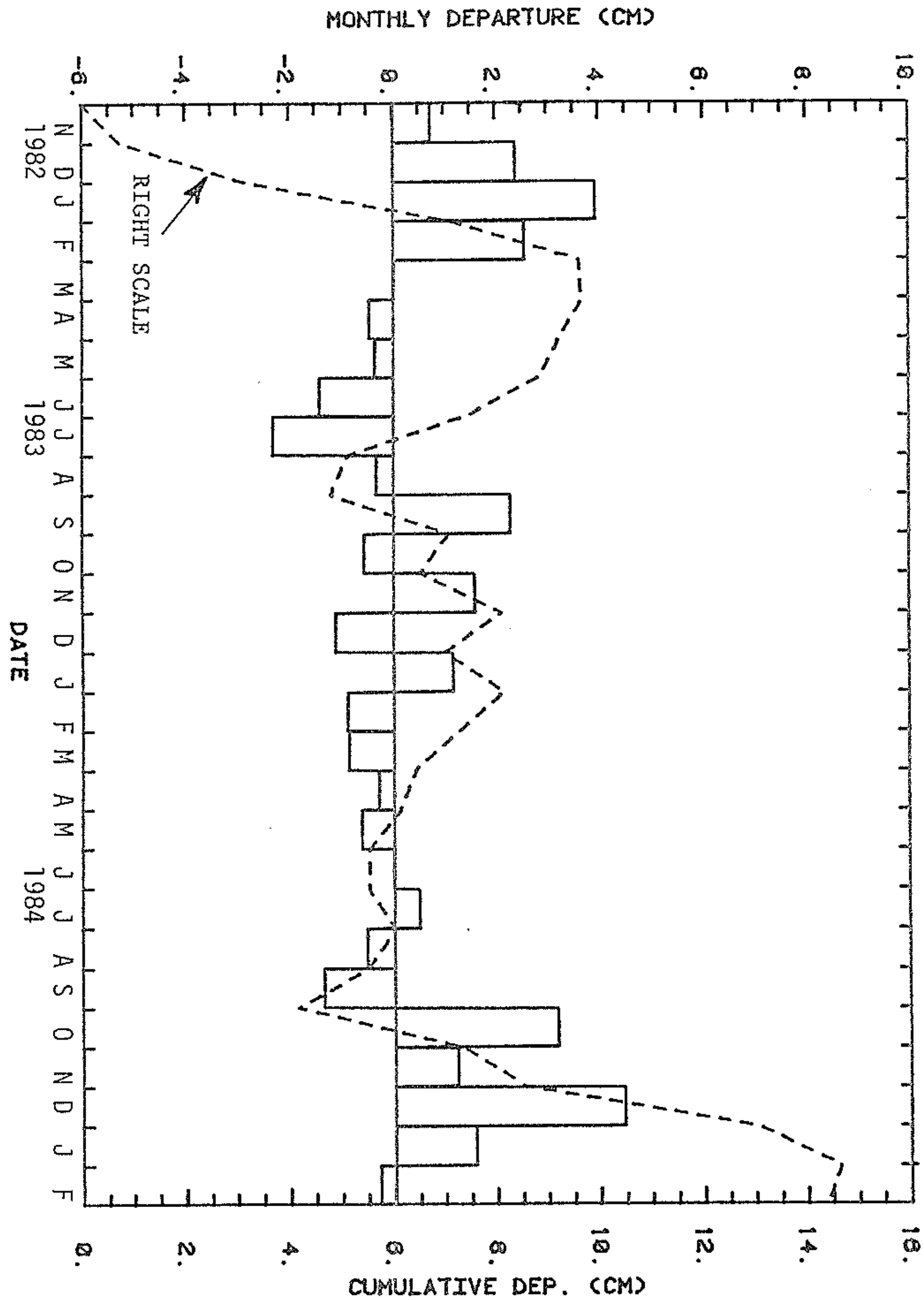

Figure 13. Monthly Departure and Cumulative Departure from Normal Precipitation at Socorro.

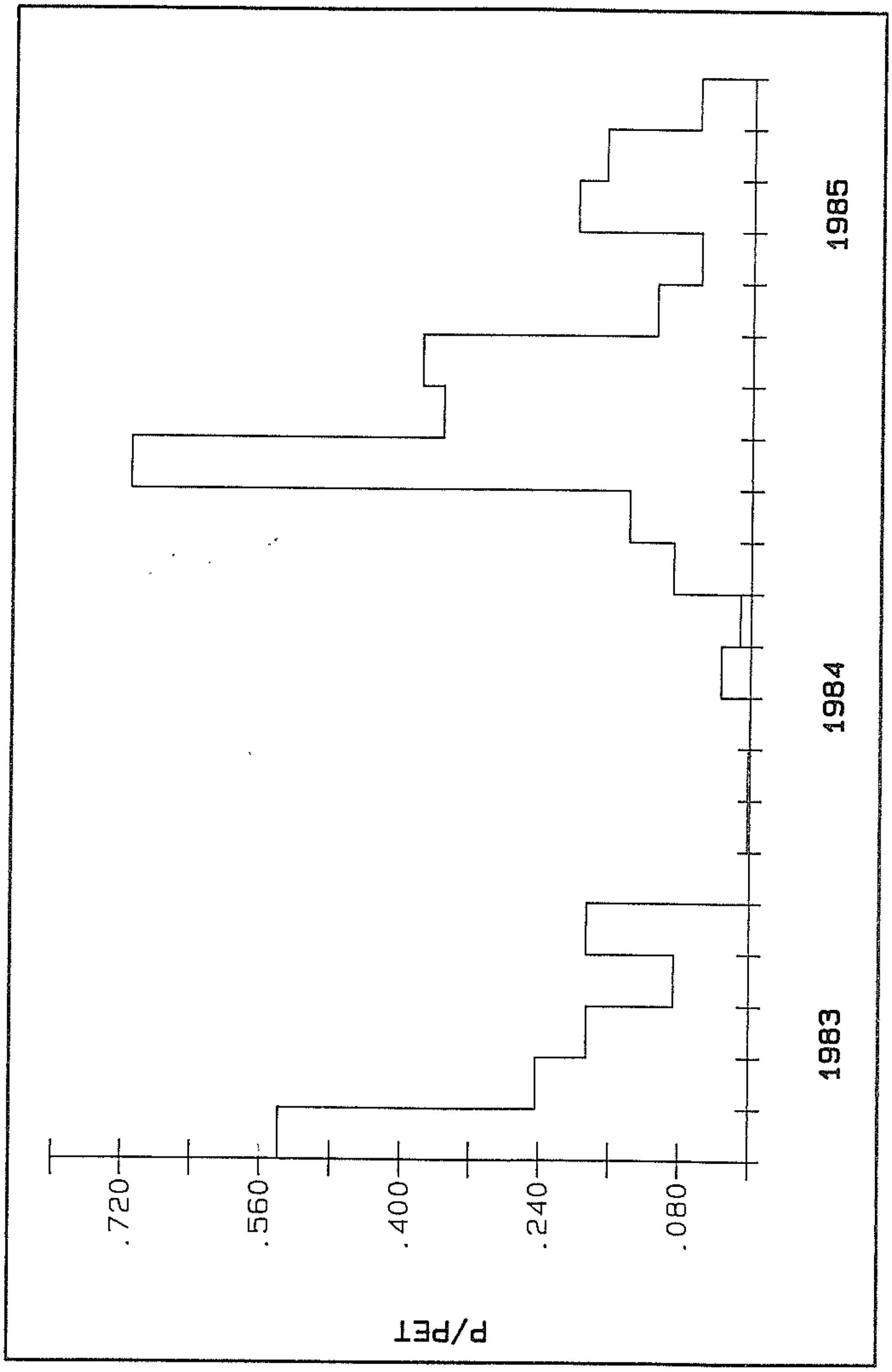

Figure 14. Ratio of Precipitation to Potential Evaporation.

15. To depths of at least 180 cm, the trends in soil moisture in figure 15 clearly correlate with the drought during the spring and early summer of 1983 and the subsequent summer rains. The long period of decreasing moisture in early 1983 ended in approximately August of that year, concurrent with the commencement of significant thunderstorm events. These data suggest that precipitation causes moisture to move rapidly through the profile to depths of at least 180 cm, even during periods when the evapotranspiration rate is at a maximum. Below this depth the pulses of soil moisture due to precipitation are not as well defined (figure 15). This may be attributed to the gap in data caused by mechanical breakdown of the neutron probe, the influence of a rising water table (obvious at the 549 cm depth), heterogeneity within the profile, and possibly water withdrawal by vegetation.

Relatively deep soil moisture movement is also shown to occur shortly after precipitation events. For example, the soil moisture content profile following a series of storms in October 1984 is shown for station 1 in figure 16, and for all of the other stations in figures 17 through 19. In combination, these storms delivered about 4.8 cm of rainfall, or about 24 percent of the long term mean annual precipitation. At station 1, in a lowland, the fall and winter precipitation caused a buildup of moisture below the estimated depth of rooting, 150 cm. By numerical integration of the moisture profile obtained on January 24, 1985, (figure 16), the increase in soil moisture from September 1984 through January 1985 (9.9 cm) is nearly equal to total precipitation (10.2 cm) which was recorded at the site in that same time period.

Figures 17 through 19 illustrate the variability in moisture penetration following the storm events of October 1984. In figure 17, stations 2 and 3 are located in the lowland, stations 10 and 9 are near the base of a slope, and 11 and 12 are in the active channel (figure 2). Stations 2, 10 and 11 are

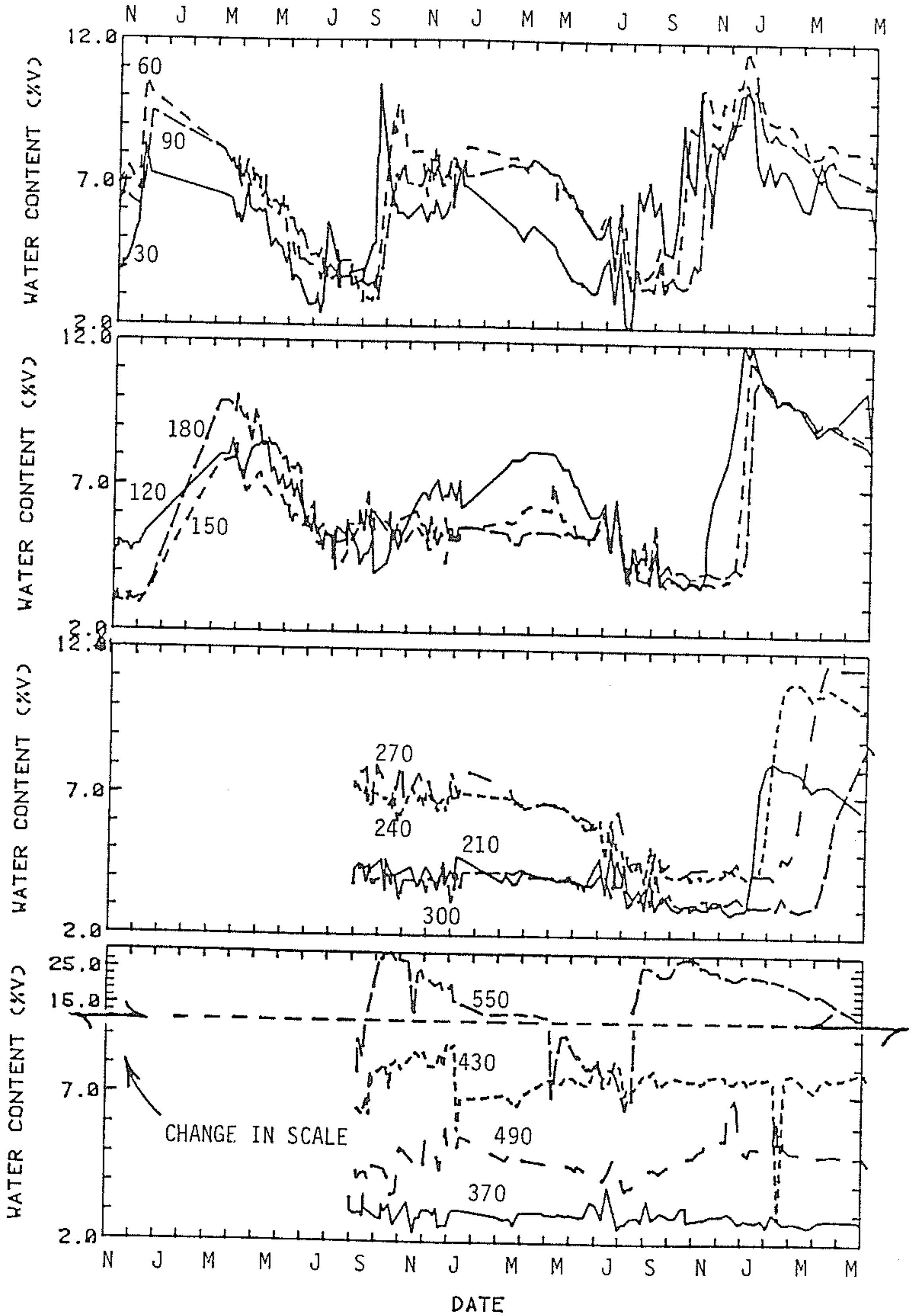

Figure 15. Moisture Content at Station 1, 1982-1985.

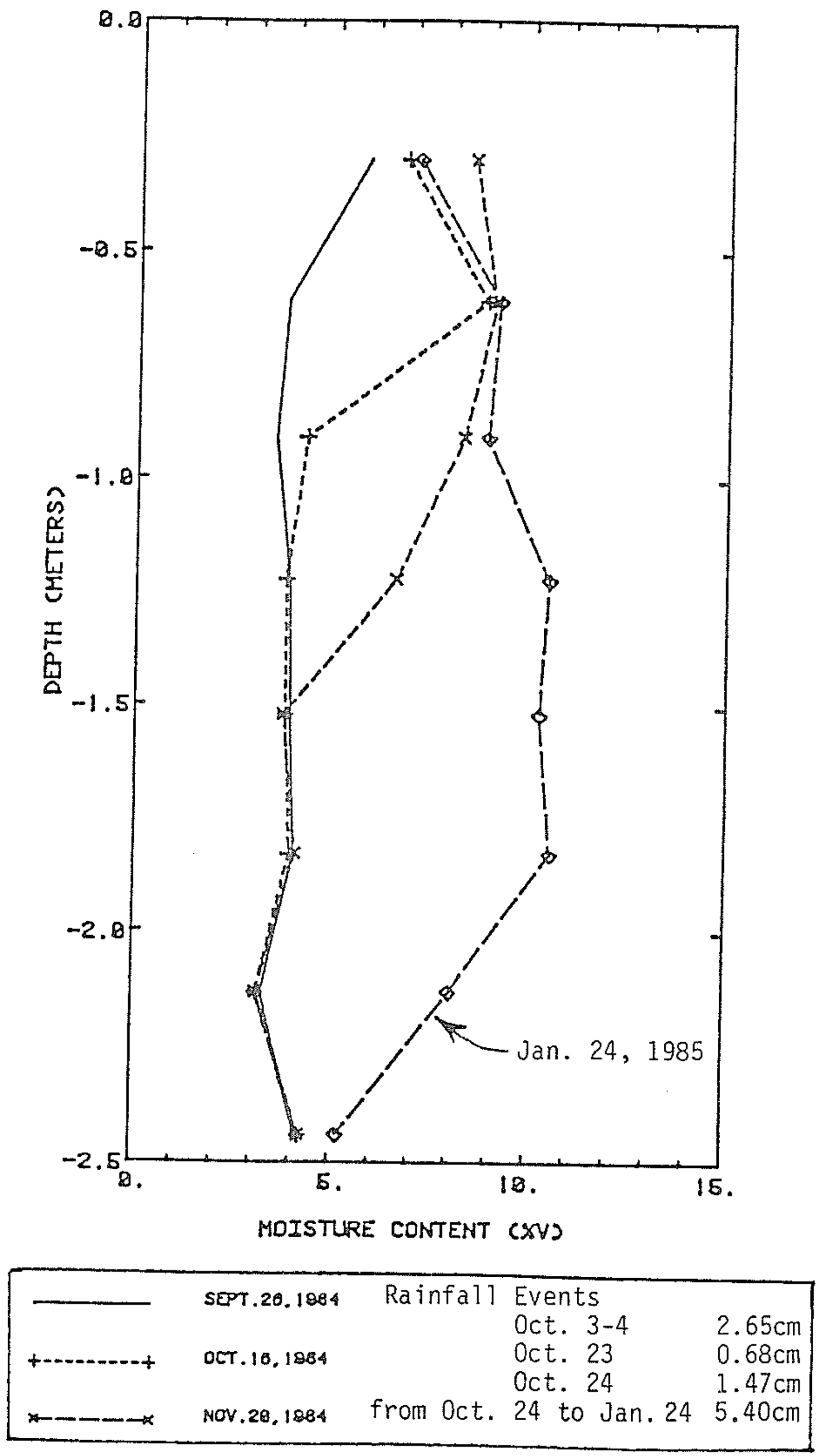

Figure 16. Moisture Content Profile in Alluvium at Station 1 Following a Storm Sequence.

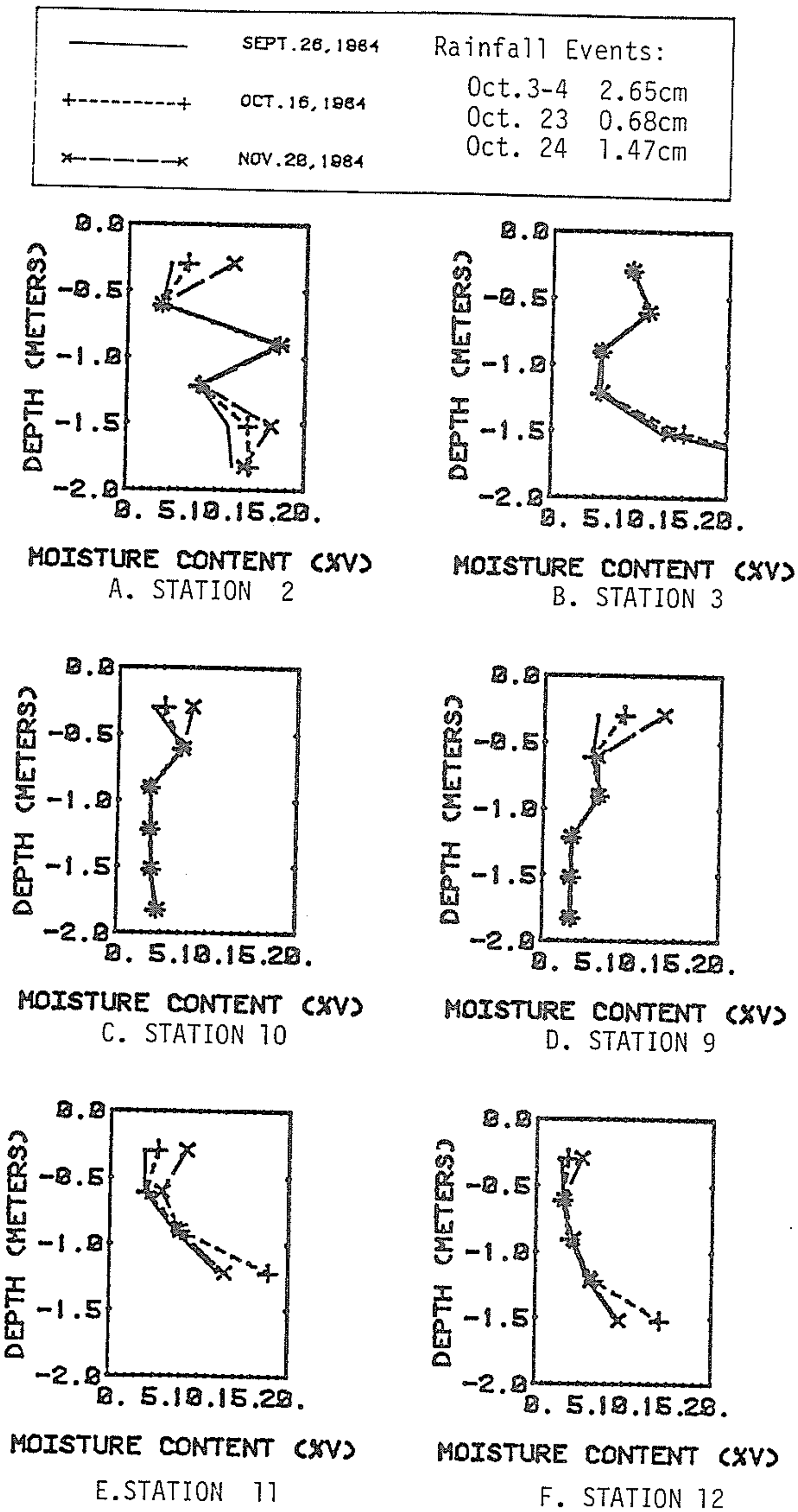

Figure 17. Moisture Content Profile in Alluvium at Station 1 Following a Storm Sequence. Stations 2, 10, and 11 are sparsely vegetated.

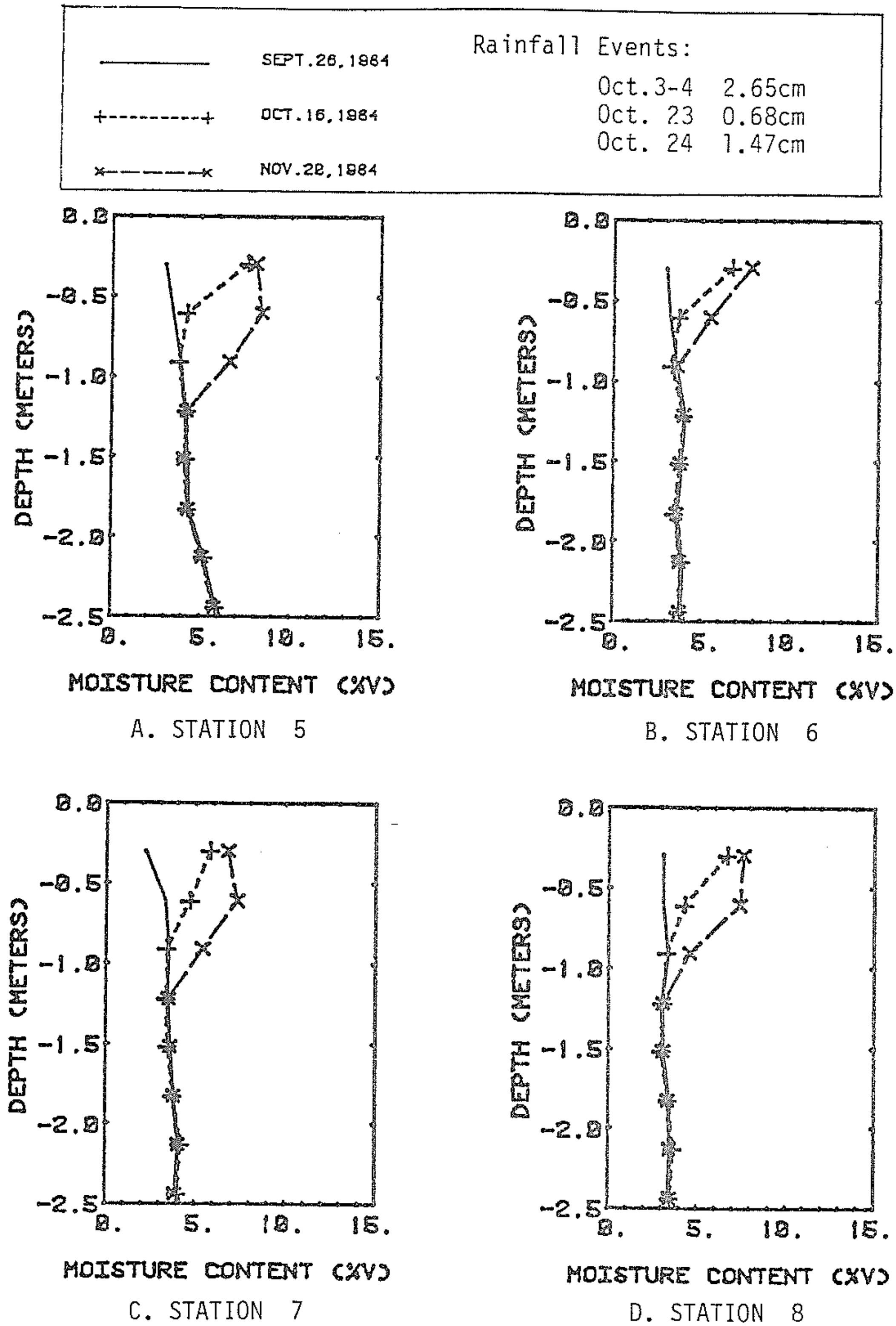

Figure 18. Water Content Profiles in Stabilized Aeolian Sand at Stations 5, 6, 7, 8 Following a Storm Sequence. Stations 5 and 6 are at the Base of a Slope; 7 and 8 are on a Slope; and 5 and 7 are Sparcely Vegetated.

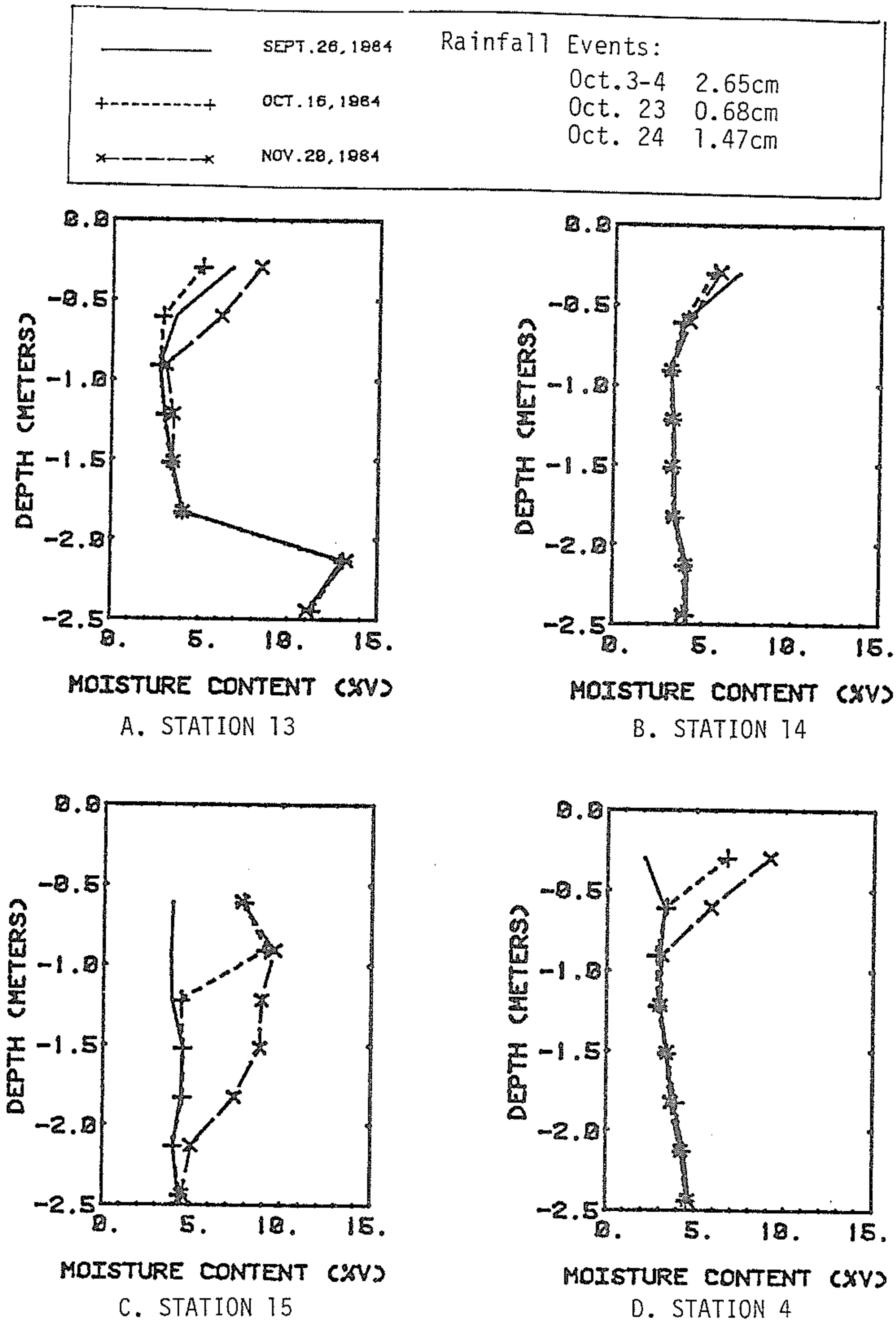

Figure 19. Water Content Profiles in Active Dune Sand at Stations 13, 14, and 5 and Stabilized Aeolian Sand at Station 4. Stations 4 and 13 are on Steep Slopes, 14 is on the Dune Crest, and 15 is in a Swale.

in areas of low vegetation density. At all but one station, number 3, there is an increase in soil moisture to depths of at least 50 cm. The increase in moisture in the lower portion of the profile at stations 2, 11 and 12 is attributed to upward water movement from a rising water table. The differences in initial water content (September 26, 1984) between profiles are attributed mostly to lithologic and stratigraphic variability, as well as vegetation type and density (table 1). A silty layer was encoutered at depths of approximately 30 to 90 cm near station 2, 3, 9 and 10. Grassy vegetation which is especially dominant near stations 2 and 3, may extract moisture from the silty layer. Therefore, it is diffucult to separate the effects of vegetation and soil texture based on moisture content data.

In figure 18, stations 5 and 6 are located at the base of a hillslope whereas stations 7 and 8 are located on the mid-slope (figure 2). Moisture has clearly moved beyond the 1.2 cm depth within approximately one month following the storms of October 1984, except at station 6 which is vegetated. However, in the fall of 1984 the evapotranspiration demand was relatively low, and therefore the difference in moisture between stations 5 and 6 could also be due to textural differences. Station 8 is also located close to vegetation, but there is little difference in moisture content between this profile and that at the less densely vegetated site area, station 7. The soils at these four stations appear to be eolian, although the land surface is generally stablized by vegetation. These profiles contain few fine textured sediments which would impede downward water percolation. The depth of the infiltration of precipitation is nearly the same at stations 5 and 7. However, by integrating the moisture profile curves obtained on November 20, the volume of water behind the wetting front is approximately 15 percent higher at station 5 than at station 7. This minor difference may be due to the topography concentrating moisture at the base of the hillslope.

Figure 19 shows the soil moisture profile after the October 1984 precipitation events for stations 13, 14, and 15 located on the active sand dune (figure 2). Station 14 is located on the dune crest, station 13 is on the middle of the steep slope, and station 15 is located in a relatively level area bordered on two sides by moderately steep slopes. There is a marked variability in moisture stored within the very sparsely vegetated sand dune. The greatest increase in soil moisture following the October storms occurs in the lowland, station 15. At this location the depth of wetting was approximately 2 m; this is much greater than the depth of moisture penetration at any other station during this period. By comparison, moisture content in the profile near the dune crest (station 14) was much less affected by the October rains. The profile at station 13, on the steep dune slope, exhibited a response similar to that at the stabilized eolian dune stations (4, 5, 6, 7, 8) and also at station 1 on the old floodplain. There is no evidence of surface runoff on the dunes, and it would take a rain intensity of about 1700 cm/d to exceed the saturated hydraulic conductivity of the sand. Comparing the results for stations 13, 14, and 15, topography appears to exert a very strong influence on soil moisture storage, if the distribution of rainfall is uniform over the dune sites. In fact, if we calculate the increase of soil moisture as a result of the 2.6 cm of precipitation which fell on October 3 through 6, 1984, the station at the dune crest gained about 0.4 cm, the station on the steep dune slope gained about 2.0 cm, and the station on the swale gained more than 3 cm of water; these increases in moisture amount to about 15, 80 and 120 percent, respectively, of the precipitation. The implications of this variability with respect to lateral soil moisture movement will be discussed later in the report.

Hydraulic Head Measurements

For the period November 1982 through May 1984, pressure head data at station 1 are shown in figure 20 to depths of 244 cm. These data show the same rapid soil-water response to precipitation as the moisture content data in figure 15. That is, both the summer thunderstorms and winter rain and snow melt contribute to rapid, deep infiltration. Even at the 244 cm depth, the pressure head begins to increase following the drought which ended with thunderstorms occurring in late summer of 1983. During June and July 1983, there is some evidence to suggest that plant roots are most active in the zone above about 135 cm. During this period of maximum evapotranspiration, the pressure head is approximately 25 cm less in the zone above the 135 cm depth than below it. During the winter months when the plants are relatively dormant, the pressure head distribution is more uniform vertically. A uniform vertical pressure head distribution indicates predominantly vertical downward flow under the influence of gravity.

Total hydraulic head is essentially equal to the sum of pressure head and elevation head components. Total hydraulic head data, which can be used to infer the direction of soil-water movement, are shown in figures 21 - 36 for each site for the period January 1984 through May 1985. Inasmuch as these records were only completed a short time ago, there has not been a sufficient opportunity for detailed analysis and interpretation.

There are a few general observations which can be made at this time regarding the total hydraulic head data for stations 1 through 15 in figures 21 - 35. But first, to interpret the total hydraulic head graphs, keep in mind that land surface is chosen as the local datum at each station. That is, the stations are not tied into the same elevation, and therefore, the total hydraulic head values between stations should not be compared. For each station, elevation head is zero at the land surface, and positive elevation

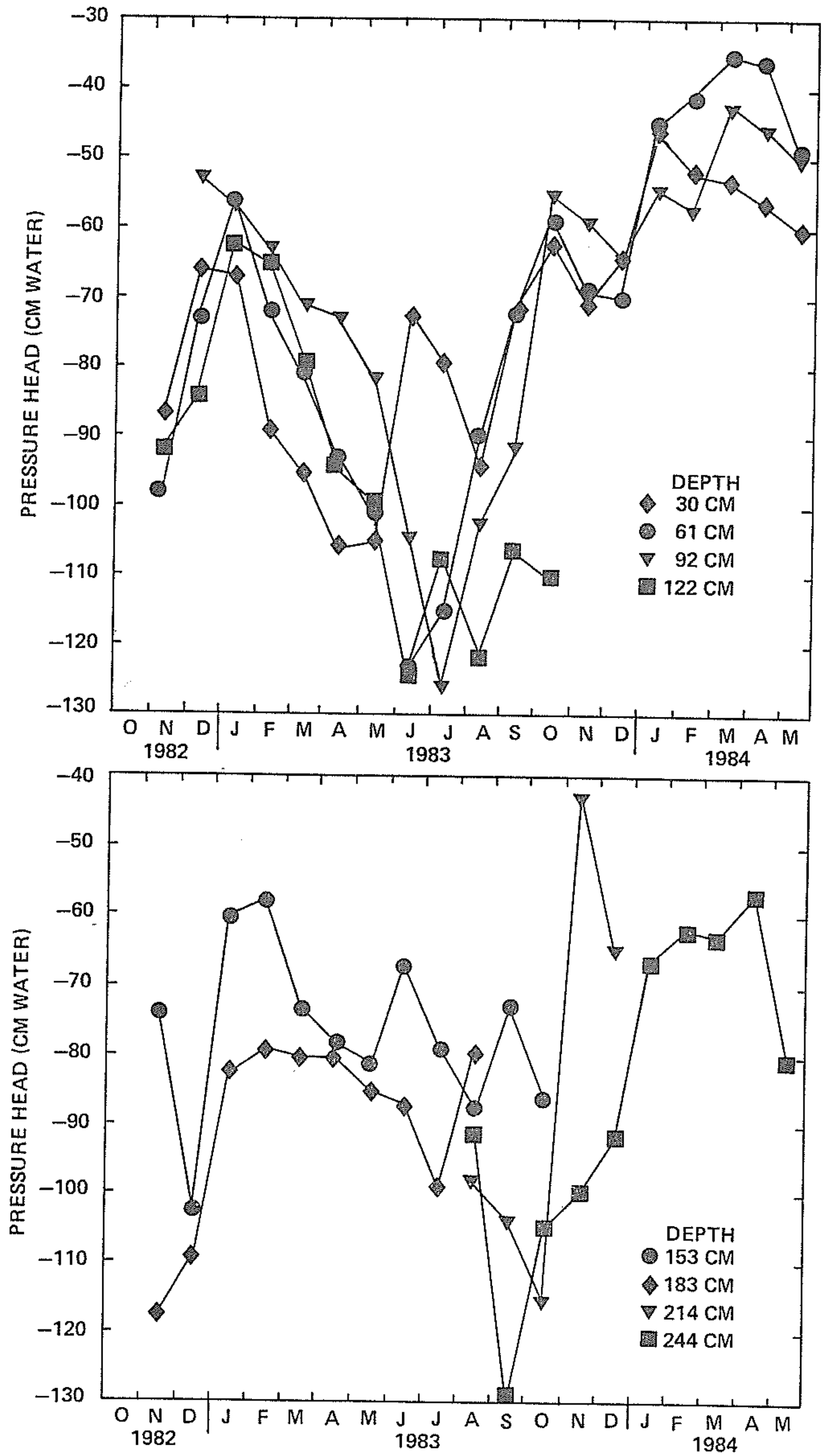

Figure 20. Monthly Average Pressure Head at Station 1 Through May 1984.

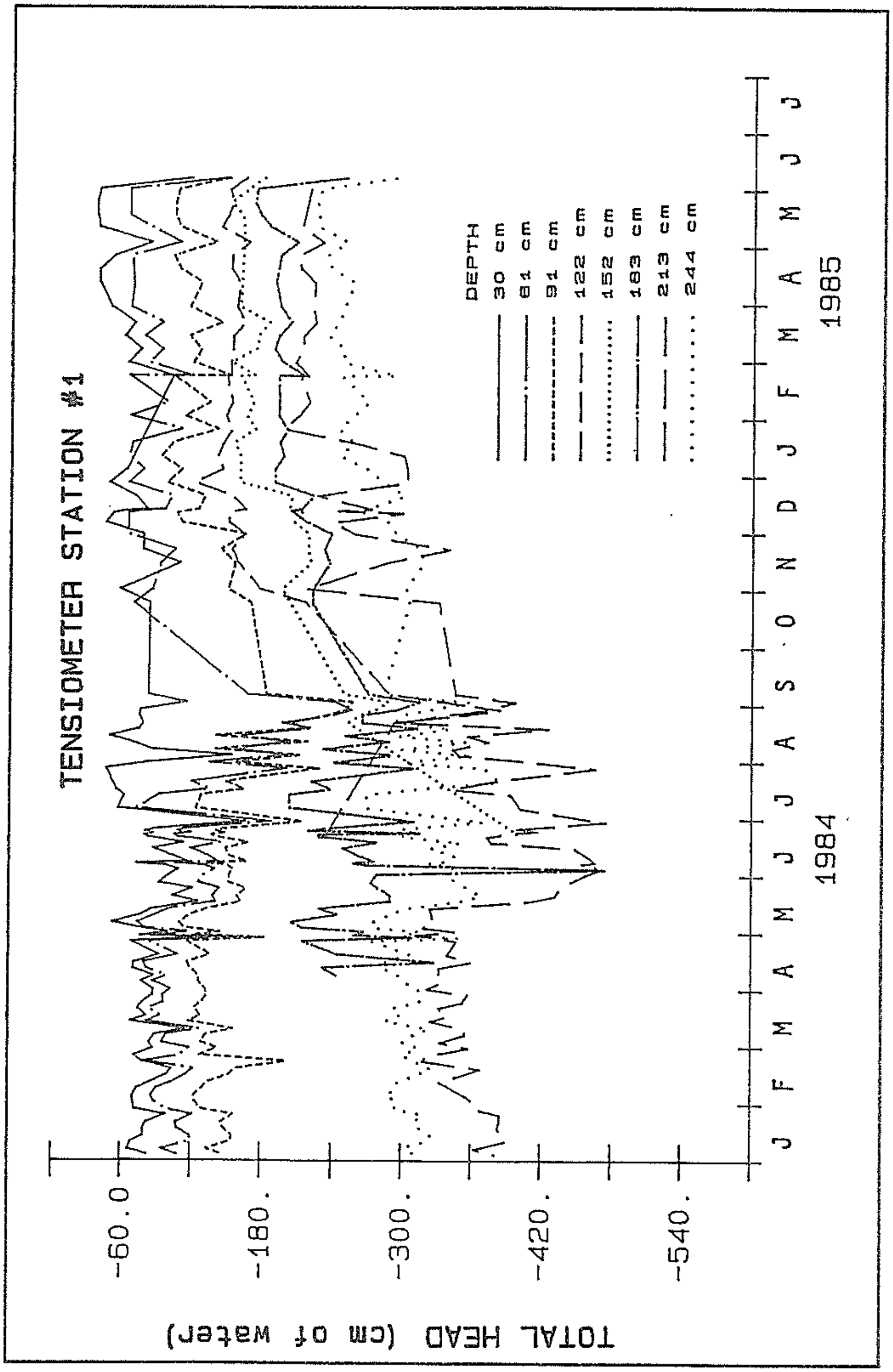

Figure 21. Total Hydraulic Head at Station 1.

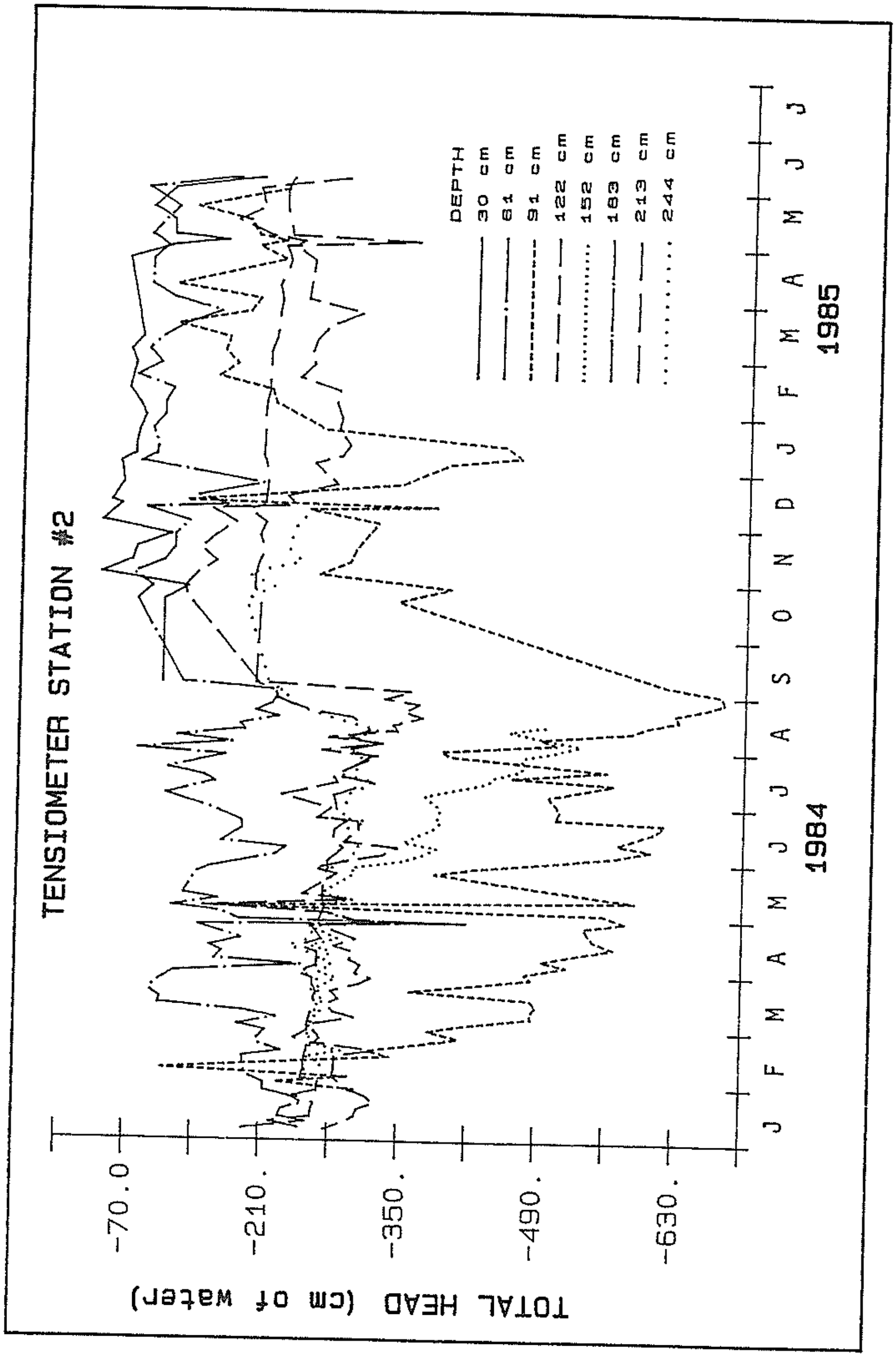

Figure 22. Total Hydraulic Head at Station 2.

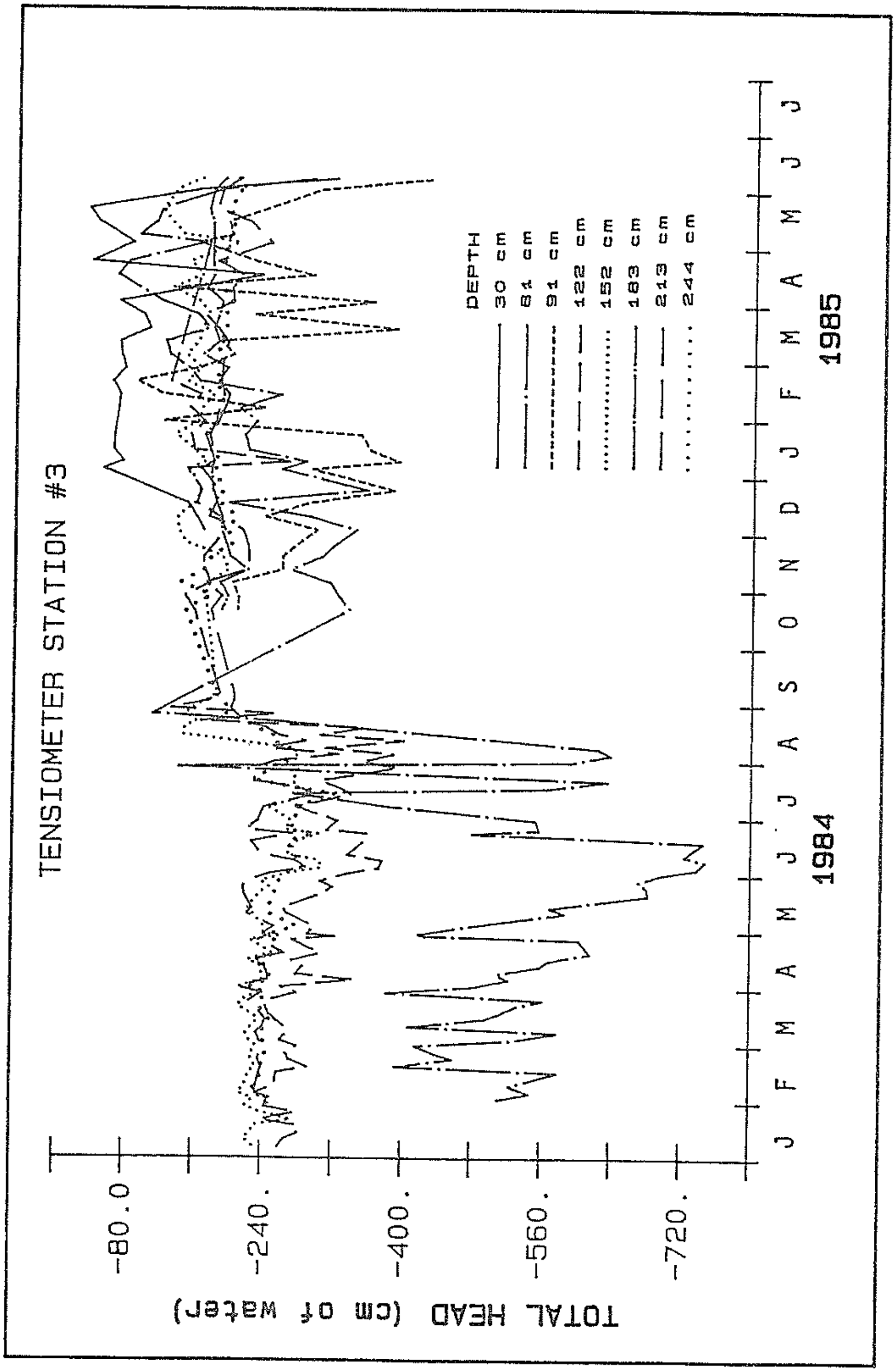

Figure 23. Total Hydraulic Head at Station 3.

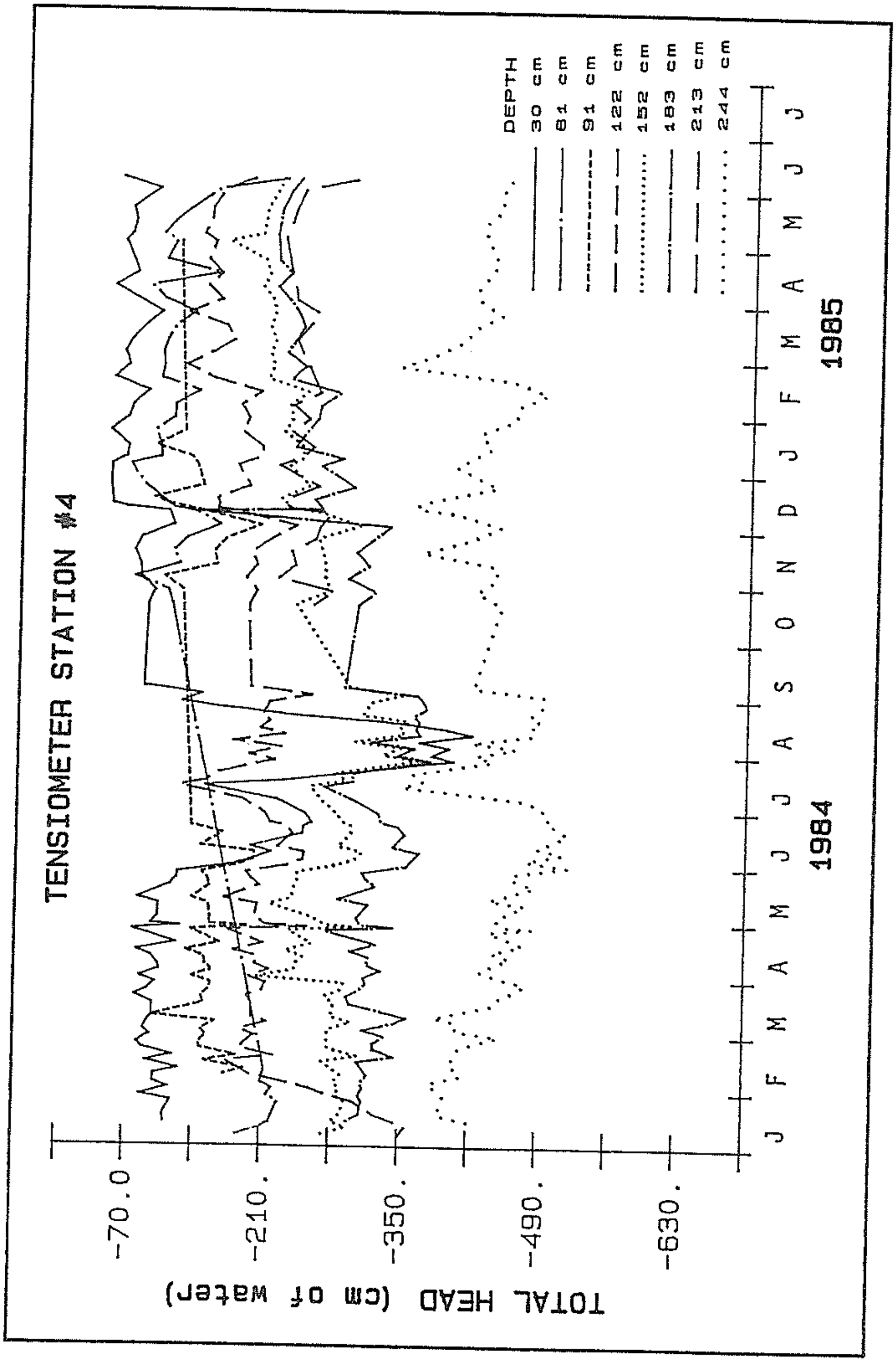

Figure 24. Total Hydraulic Head at Station 4.

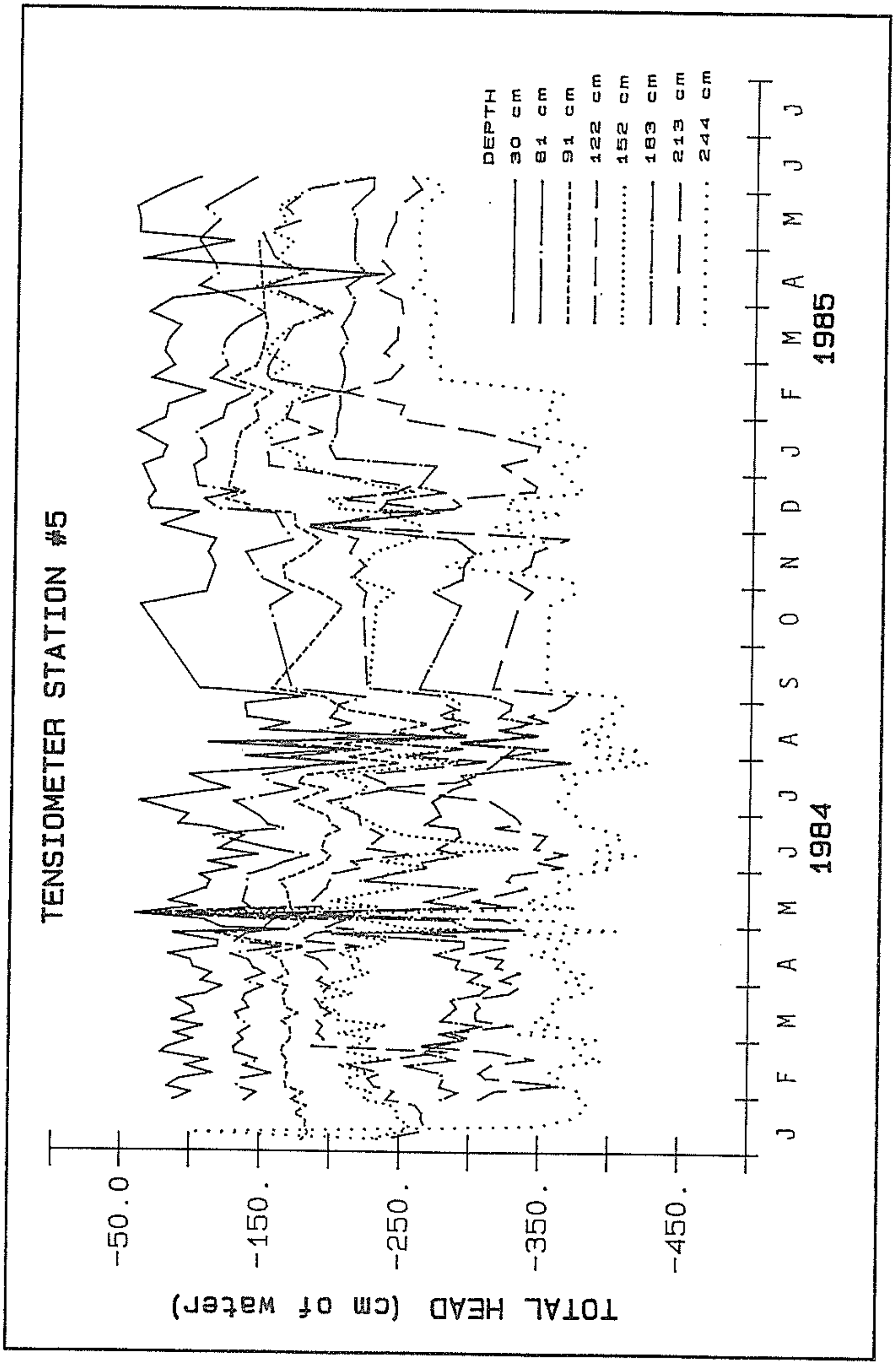

Figure 25. Total Hydraulic Head at Station 5.

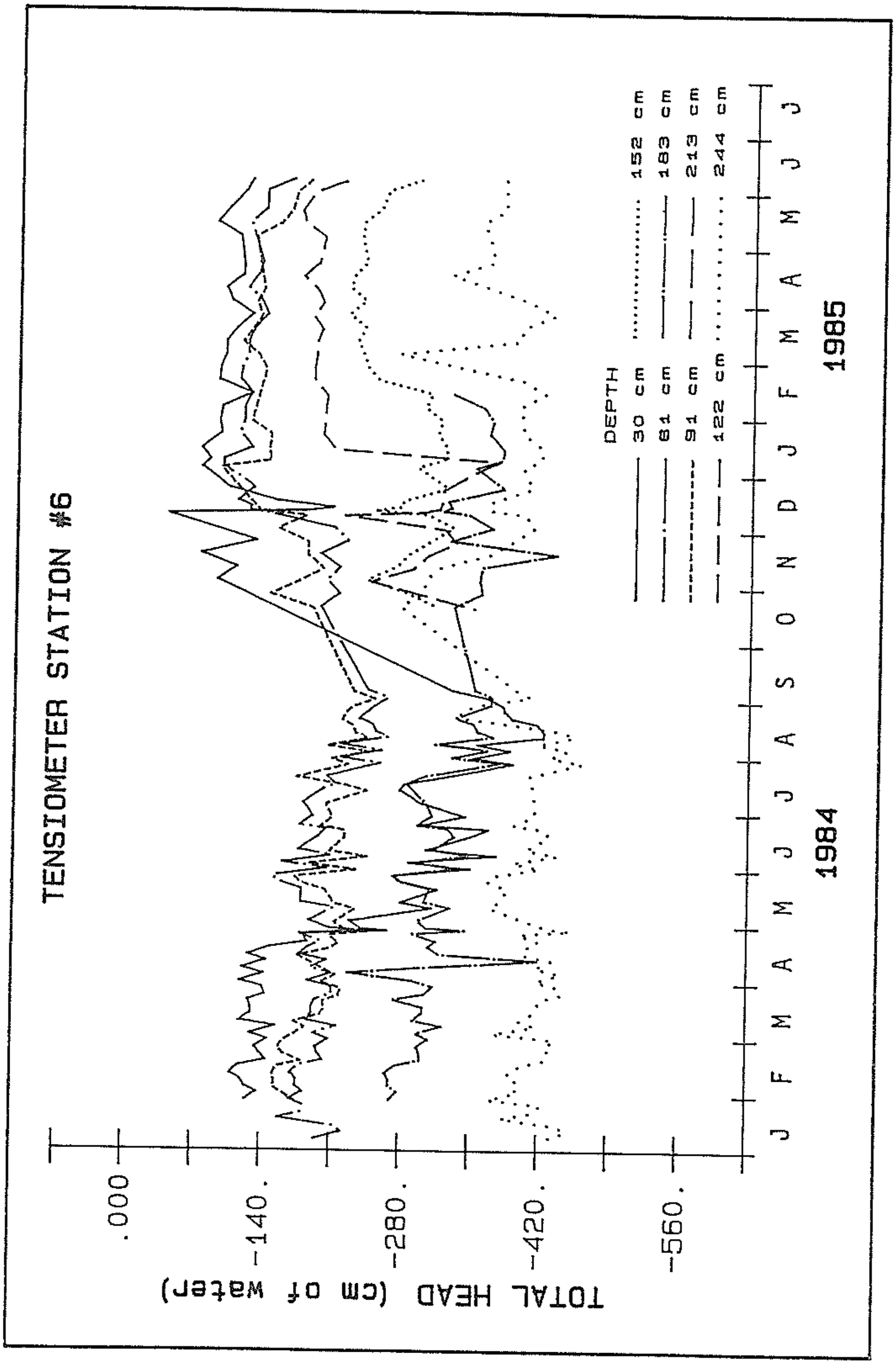

Figure 26. Total Hydraulic Head at Station 6.

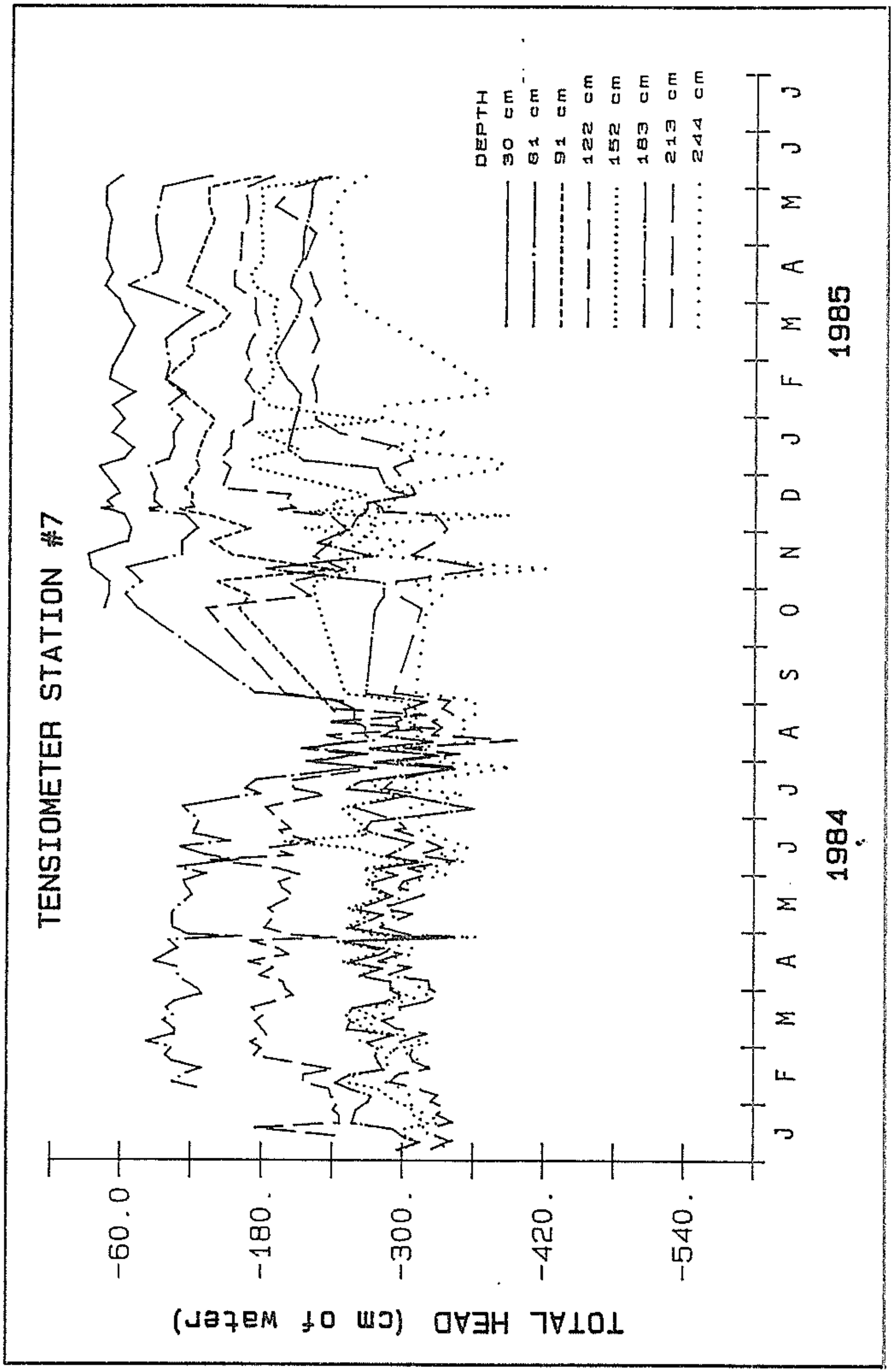

Figure 27. Total Hydraulic Head at Station 7.

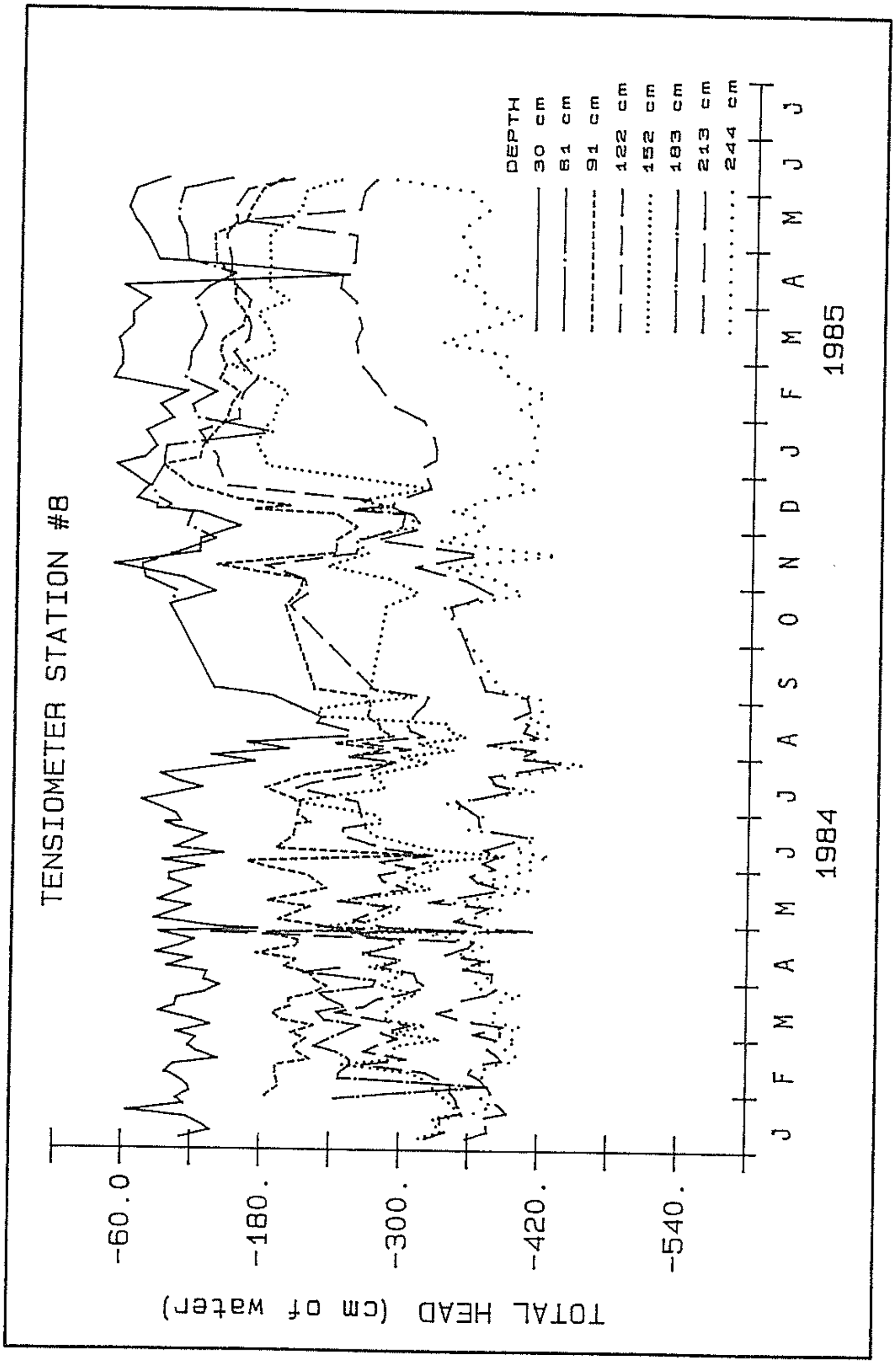

Figure 28. Total Hydraulic Head at Station 8.

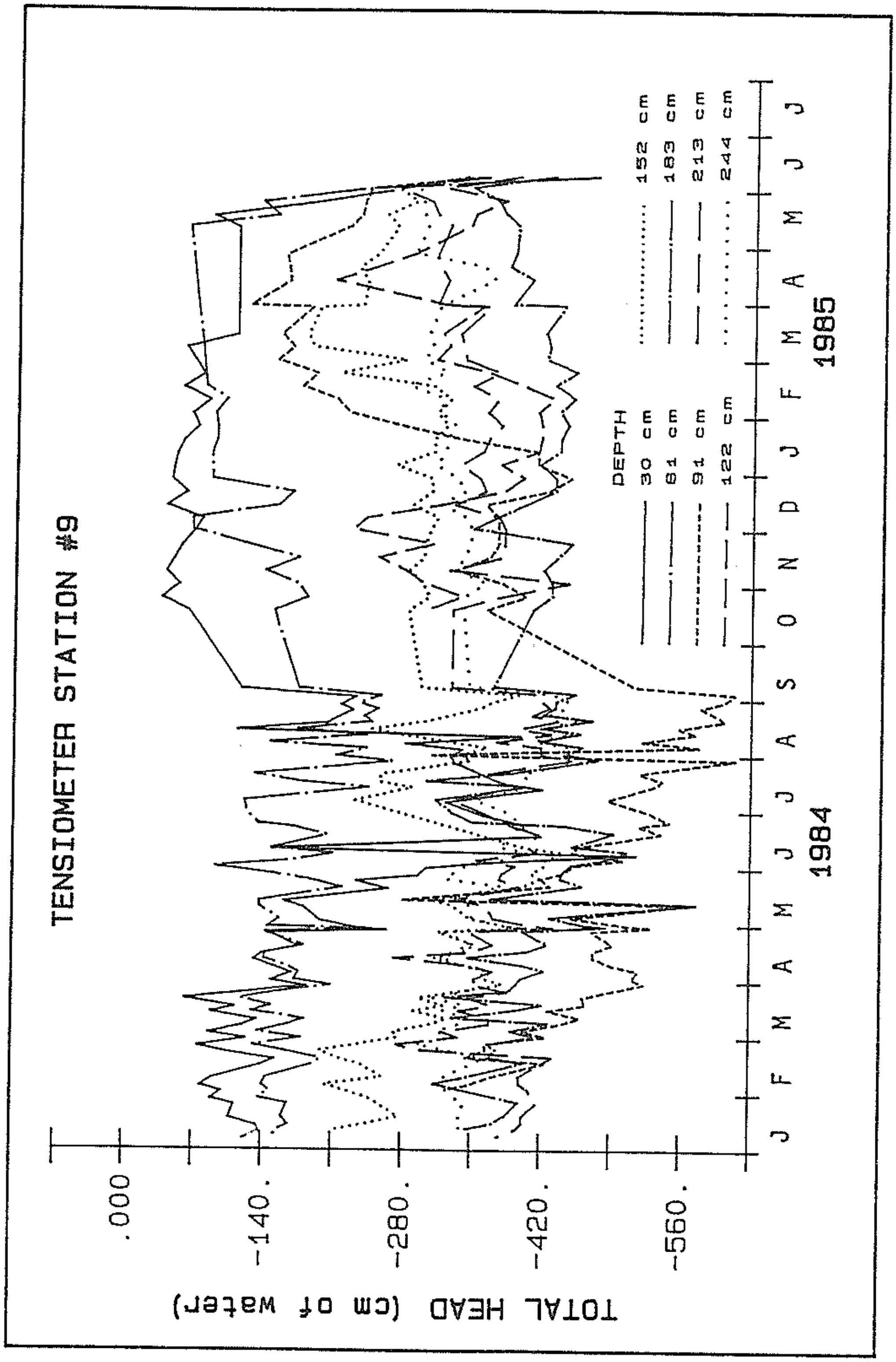

Figure 29. Total Hydraulic Head at Station 9.

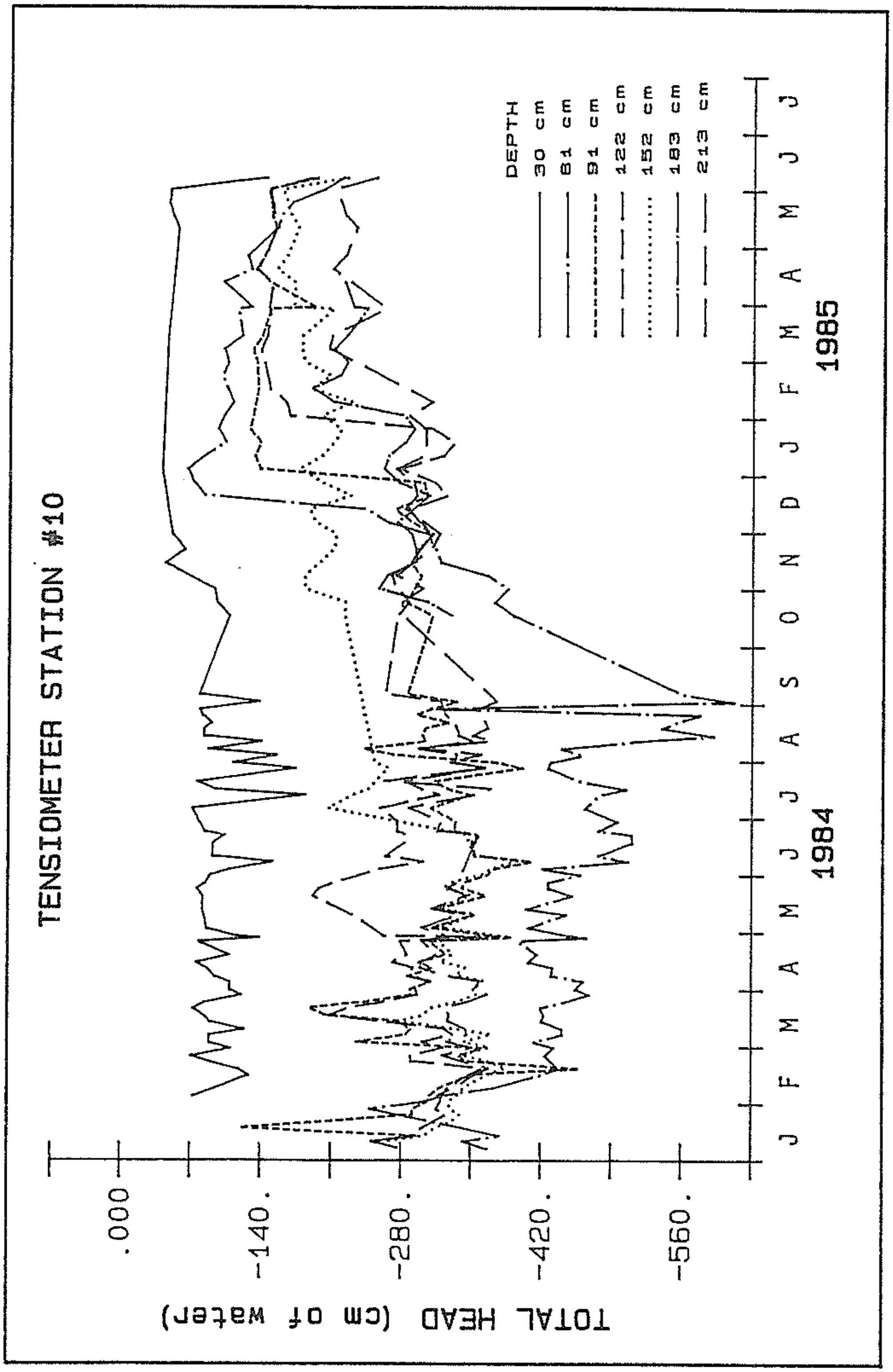

Figure 30. Total Hydraulic Head at Station 10.

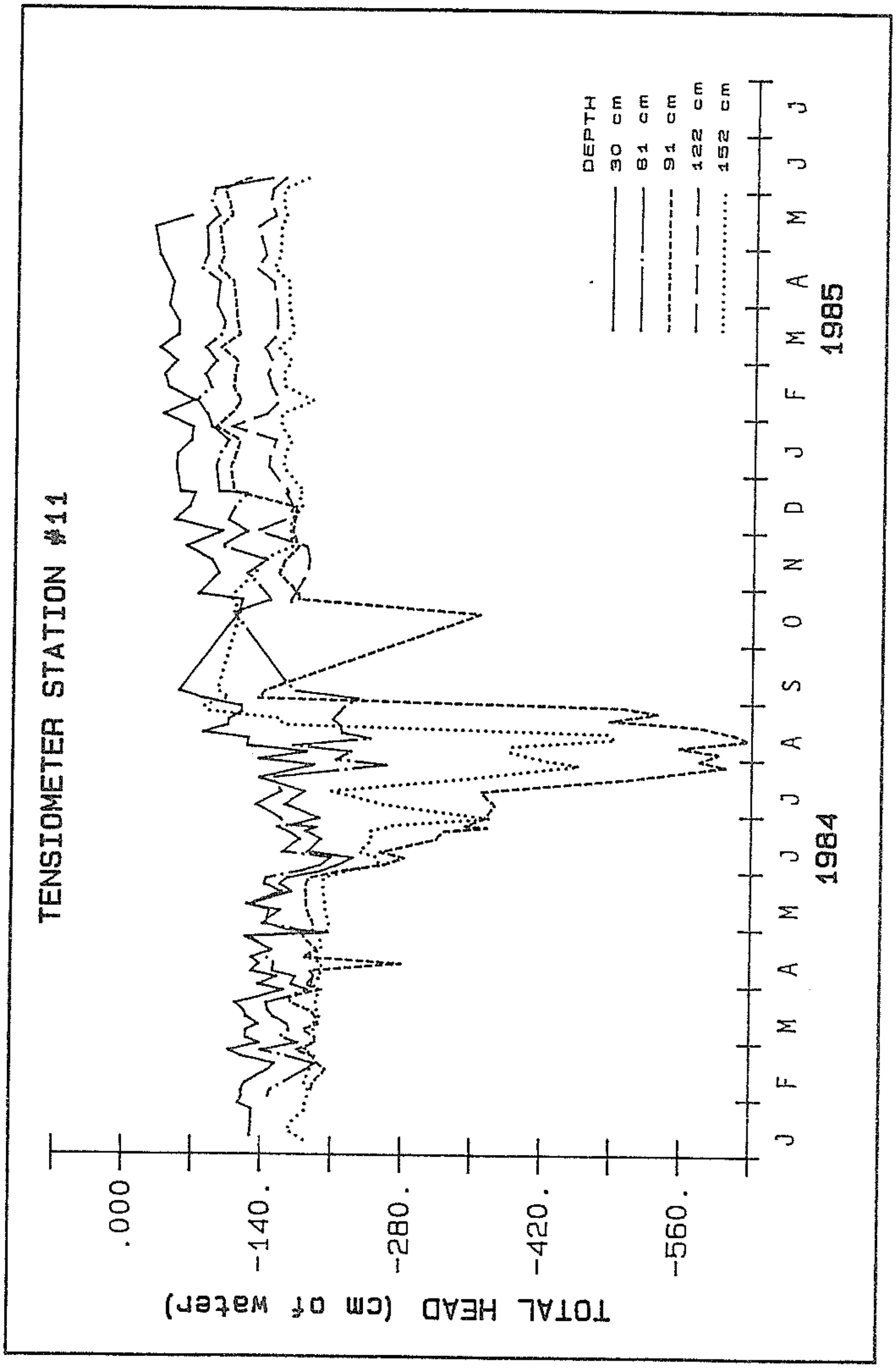

Figure 31. Total Hydraulic Head at Station 11.

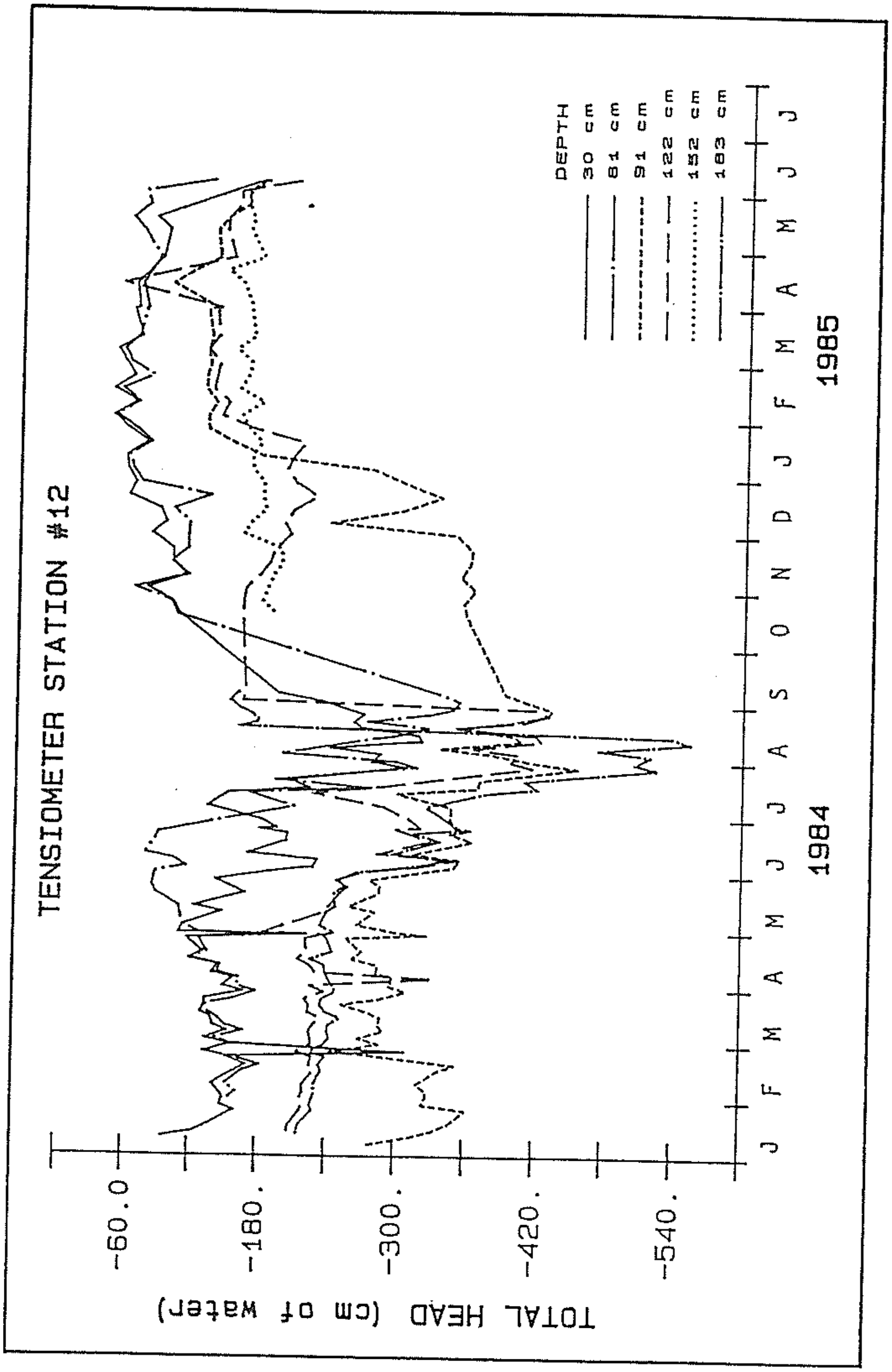

Figure 32. Total Hydraulic Head at Station 12.

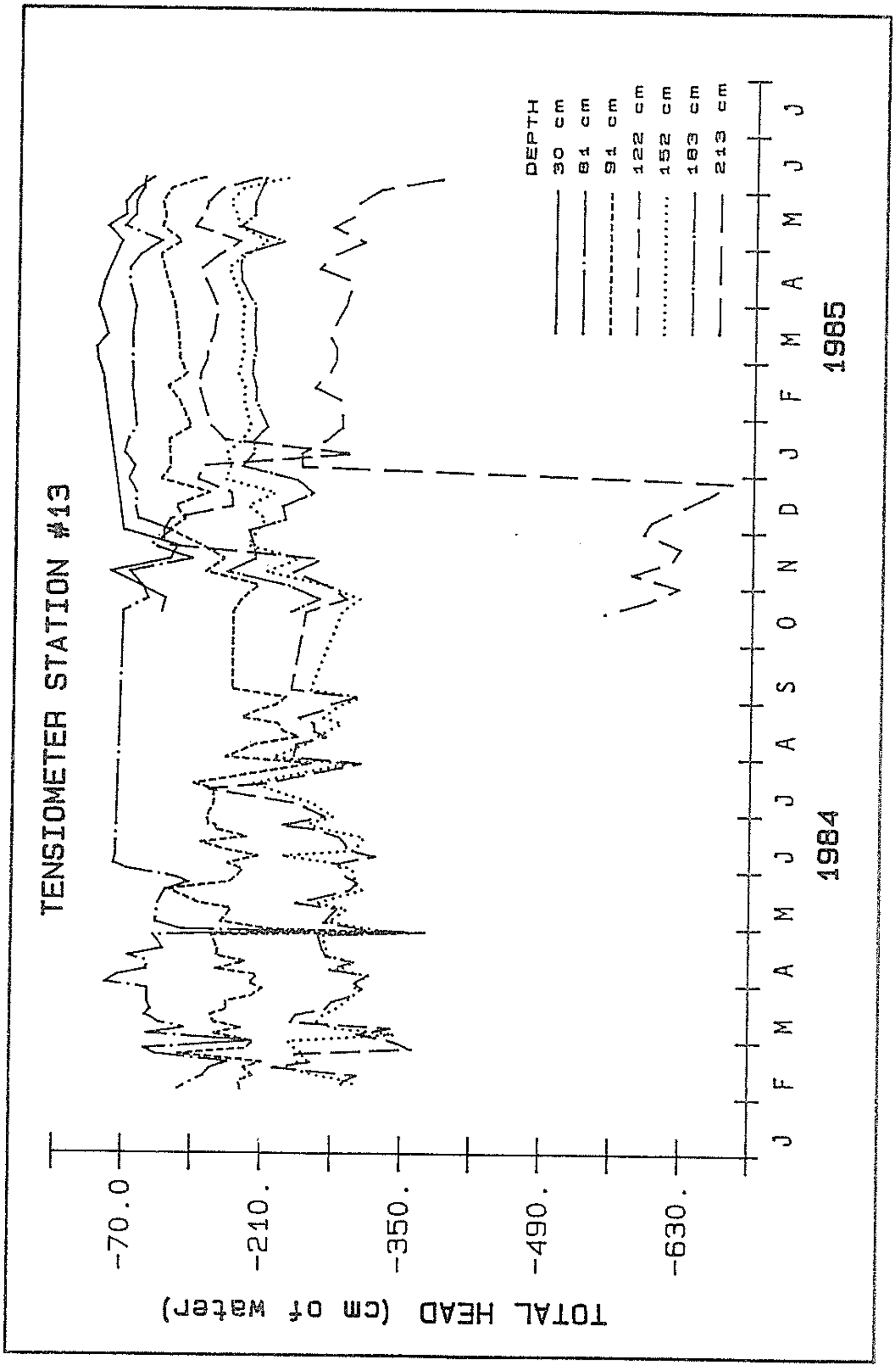

Figure 33. Total Hydraulic Head at Station 13.

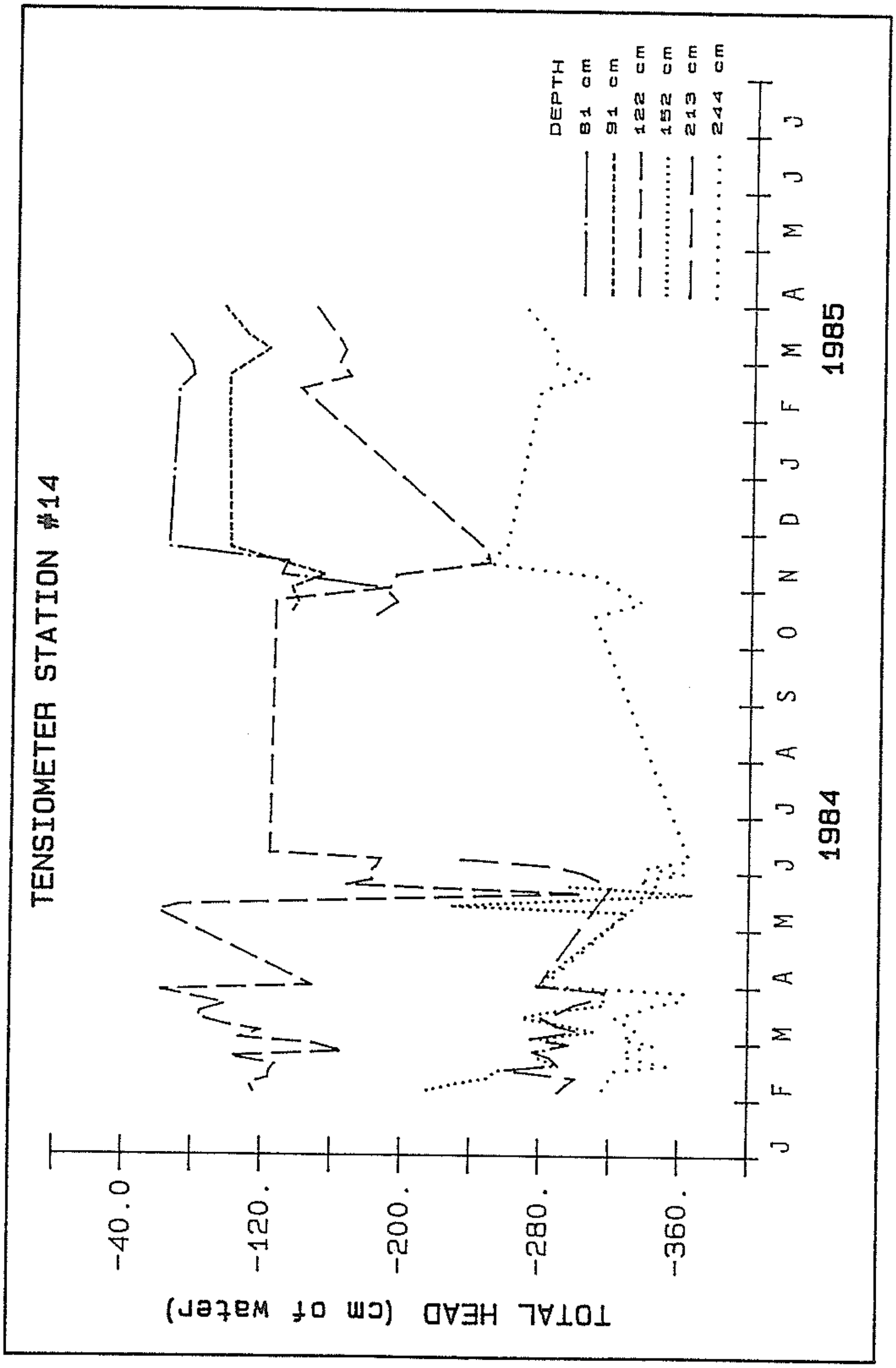

Figure 34. Total Hydraulic Head at Station 14.

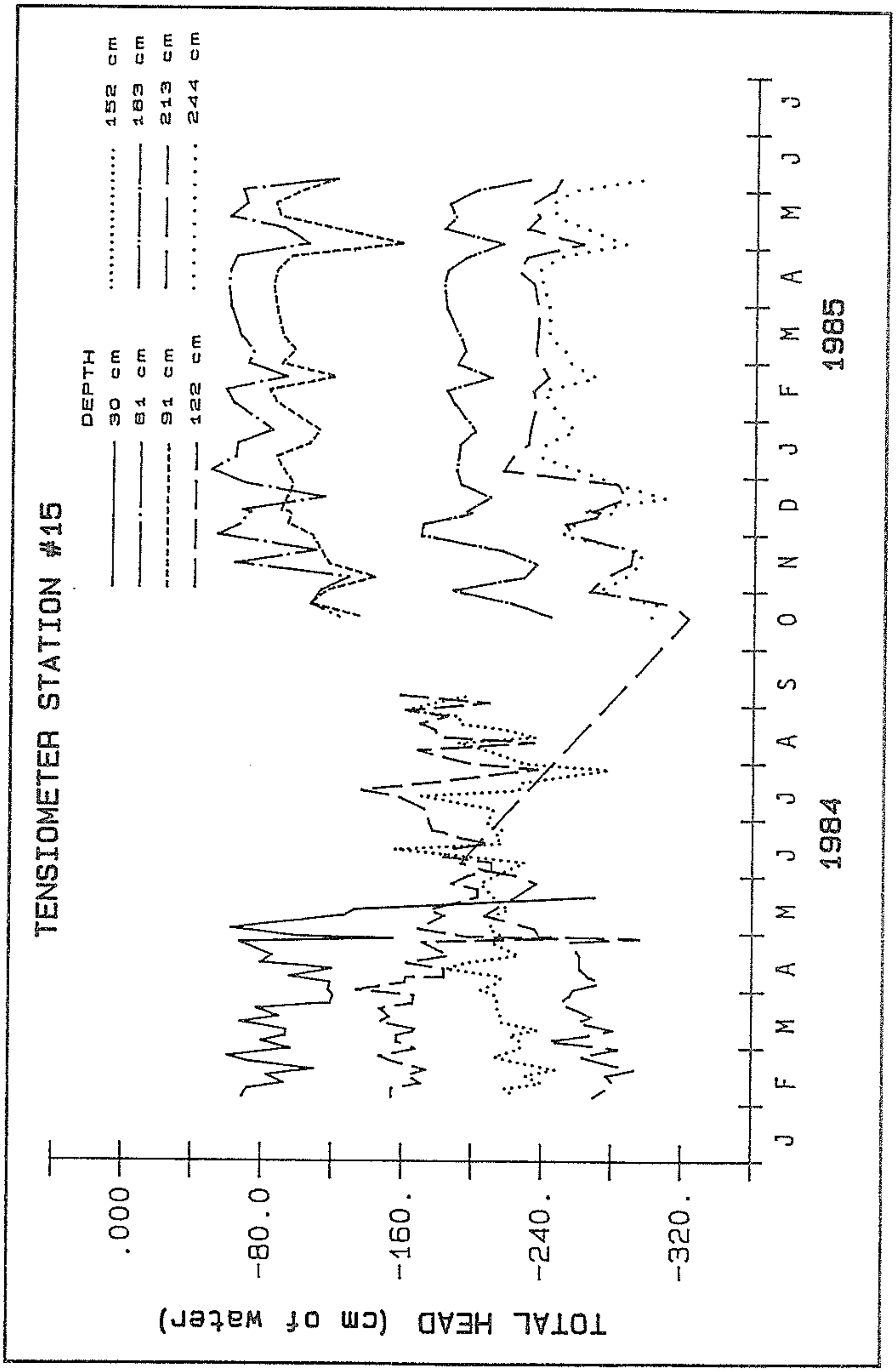

Figure 35. Total Hydraulic Head at Station 15.

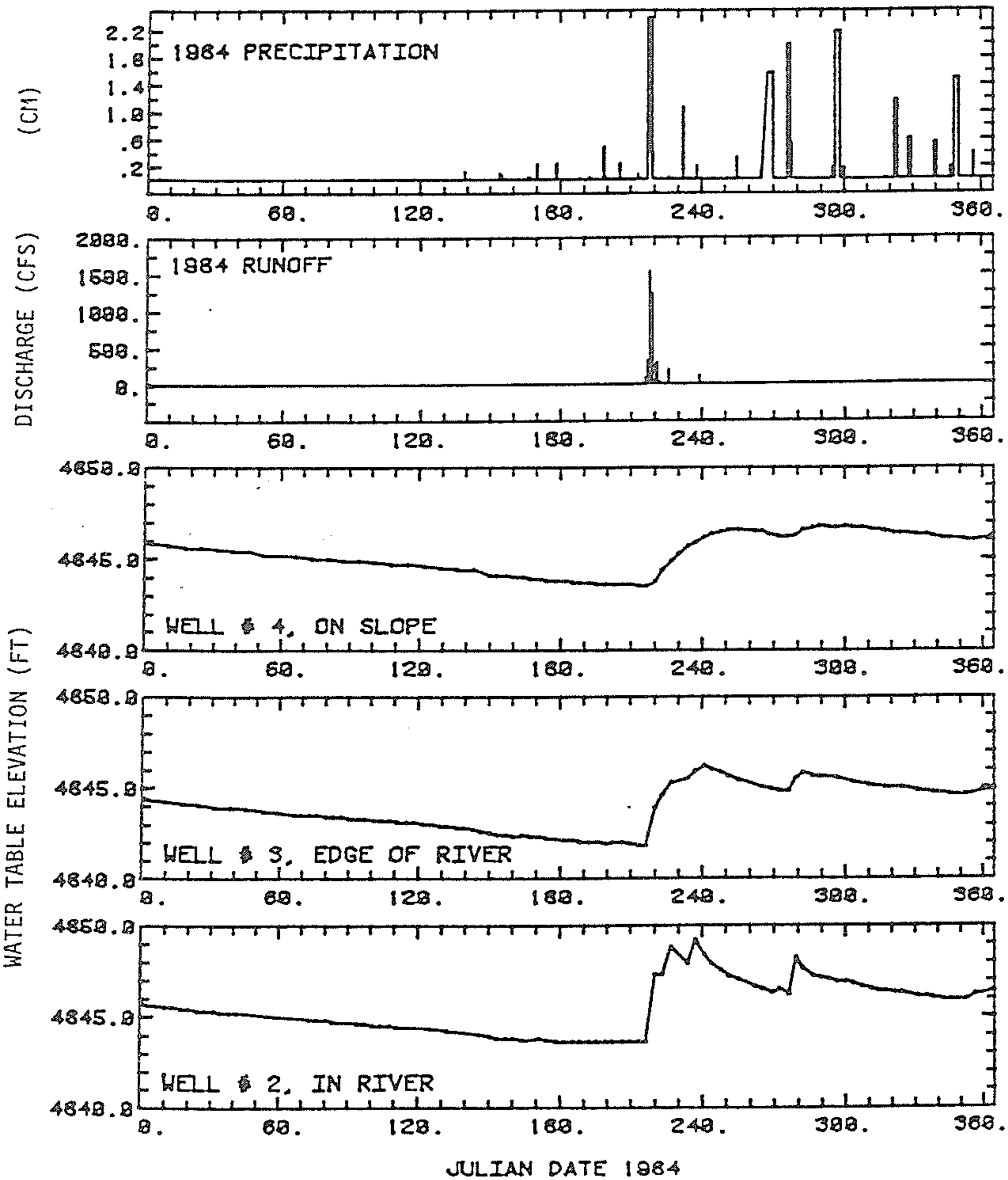

Figure 36. Water Level Hydrographs from Observation Wells.

head values increase upward. When the direction of soil moisture flow is downward, total hydraulic head will decrease with increasing depth below land surface.

In regard to the measurements shown in figures 21 to 35, there is a significant decrease in total head throughout the profile for most locations during the late spring and early summer of 1984 when there was very little precipitation. Subsequently, total head increased at nearly all depths with the beginning of the 1984 thunderstorm season. These results indicate that the rain infiltration affects soil-water potential to depths of as much as 244 cm. These figures also show that total head during the first five months of 1985 is generally greater than for the same period in 1984. This increase is attributed to the greater amount of precipitation which fell in the last months of 1984 and early months of 1985. The tensiometer responses are clearly a reflection of soil moisture conditions as affected by precipitation and evapotranspiration.

The tensiometers also show the influence of the rising water table following channel infiltration in the Rio Salado. Figure 36 shows water level hydrographs of wells which have recording gages, along with precipitation and runoff in the Rio Salado measured in 1984 at the USGS gaging station just downstream from the site. The wells are aligned approximately perpendicular to the channel axis. A major runoff event occurred in early August 1984 which caused a rapid rise in ground water levels. The aquifer response to channel recharge was almost immediate at the channel, causing water levels to increase approximately 170 cm in well number 2 and 140 cm in well number 3. At well 4 about 1 kilometer south of the channel (figure 2), the water table responded to channel recharge after about 4.5 days; at this location the maximum water table rise was only about 90 cm. The deep tensimeters at stations 2, 3, 11, and 12 (figures 22, 23, 31, 32) show the response of the soil to the rising water table. At these locations, the total hydraulic head in the deepest tensiometers increases sharply after runoff occurs, such that the direction of moisture flow is upward in the lower part of the profile. There is no evidence of upward flow throughout the entire profile from the water table to land surface during the period of record.

After the late summer runoff of 1984, there was a period of significant precipitation. During the late fall of 1984 and continuing through to the end of the period of record, May 1985, there was a general trend for downward soil-water movement throughout the site. During this time, most of the graphs in figures 21 - 35 show that total hydraulic head decreases with increasing depth, and vertical hydraulic gradients are near unity. During this moist period, the vegetation was relatively dormant and the potential for ground-water recharge to occur from the winter precipitation was near a maximum. For 1984, approximately 85 percent of the total precipitation for the calendar year occurred from August through December; for comparison, in the previous year at Socorro and Bernardo, only about 52 percent of the total precipitation fell during these five months.

A number of the stations exhibit effects of water withdrawal by plant root systems. For example, at the 91 cm depth at station 2, the total hydraulic head is very low for most of the year (figure 22). Soil-water moved toward this zone from above and below until early in 1985, after which time there was a period of high winter precipitation and a downward gradient throughout the profile. Station 2 however, was located in a zone of relatively low vegetation density, at least on the land surface. Station 3 shows a similar response, except at the 183 cm depth. Station 1 also shows a zone of low total head prior to the wet season; in this case the roots appear to be at a depth of about 213 cm. The rooting depth at the densely vegetated site station 9 appears to be at about 91 cm, whereas at the sparsely vegetated site, station 10, it is near 183 cm. The variability of the zone of water uptake by vegetation may be due to vegetation type, but it may also be associated with the occurrence of silty and clayey horizons which can retain more moisture. Unfortunately, detailed geologic descriptions of soil at each site are not available. However, silty zones several centimeters thick were noted in a trench near station 1 below about 180 cm. The soil contain silt and clay at stations 2, 3, 9 and 10 at least in the upper 60 and 90 cm of the profile. Although the land surface may appear sparsely vegetated, the roots from plants at adjacent areas may extend laterally in clay or silt-rich horizons. Thus, it may be difficult to distinguish the relative importance of soil texture and vegetation.

Recharge

Hydrodynamic Approach. The two methods to calculate recharge which are based upon Darcy's equation comprise the hydrodynamic approaches in this report. One method is based on measured hydraulic conductivity at insitu pressure head and hydraulic gradients; the second method is based on measured hydraulic conductivity at insitu moisture content and assumes a unit hydraulic gradient. These approaches were only applied to station 1, owing to the lack of time available for computation.

Average monthly soil-water pressure head measurements between the 152 to 244 cm depths are used to compute monthly recharge by equation 1 over the period November 1982 to May 1984. In some cases the same tensiometers could not be used throughout the period, because of equipment failure and the subsequent addition of new tensiometers. The average hydraulic gradient is usually slightly greater than unity and the monthly average pressure head ranges from -129 to -35 cm (figure 20), except at the 213.5 cm depth. As indicated in table 4, pressure head at the 213.5 cm depth is lower than at adjacent tensiometers. This may be due to heterogeneity in the profile or a root. A thin, low-permeable zone was found at the 250-cm depth (figure 7).

To calculate recharge, the arithmetic mean monthly pressure head is first determined at each of the depths indicated in table 5. The arithmetic mean pressure head at those depths is substituted into the regression equation fit through insitu K-ψ data in figure 6 to calculate conductivity at each tensiometer depth. An effective unsaturated hydraulic conductivity for the profile is calculated as both a geometric mean and a harmonic mean of the two or three conductivities determined at the tensiometer depths shown in table 5. The monthly average darcian fluxes calculated by these methods are given in table 5, and the geometric mean flux is shown in figure 37. For the geometric-mean case, the effective average conductivity at 20°C was corrected for in situ temperature variations (table 2) by calculating a geometric-mean temperature for the depths and correcting for viscosity. For the harmonic-mean case, conductivities were corrected to average in situ monthly temperature before calculating the harmonic mean. The harmonic mean may give a more reasonable effective average conductivity in the vertical direction (Mualem 1984); however, pressure head measurements, and hence unsaturated hydraulic conductivity, at the 214 cm depth seems anomalously low for a profile which is assumed to be uniform. Therefore, the harmonic mean may give an unrealistically low estimate of recharge, especially if the apparent anomaly at the 214 cm depth is localized due to a discontinuous clay layer or root. Whether the geometric or harmonic mean provides the most accurate estimator of an effective average conductivity for the profile cannot be determined from our investigation. Actual recharge rates are considered to fall between values obtained by these two approaches.

TABLE 4. AVERAGE PRESSURE HEAD AND HYDRAULIC CONDUCTIVITY

Depth / Month	30.5cm		61.0cm		91.5cm		122.0cm		152.5cm		183.0cm		213.5cm		244.0cm	
	(cm)	K(cm/s)	(cm)	K(cm/s)	(cm)	K(cm/s)	(cm)	K(cm/s)	(cm)	K(cm/s)	(cm)	K(cm/s)	(cm)	K(cm/s)	(cm)	K(cm/s)
11/82	-87	1.20×10^{-8}	-98	1.28×10^{-9}	-----	-------	- 92	4.34×10^{-9}	- 74	1.68×10^{-7}	-117	2.71×10^{-11}	----	--------	----	--------
12/82	-66	8.50×10^{-7}	-73	2.05×10^{-7}	-53	1.19×10^{-5}	- 84	2.20×10^{-8}	-102	5.70×10^{-10}	-109	1.38×10^{-10}	----	--------	----	--------
1/83	-67	6.94×10^{-7}	-56	6.47×10^{-6}	-57	5.28×10^{-6}	- 62	1.92×10^{-6}	- 60	2.87×10^{-6}	- 82	3.30×10^{-8}	----	--------	----	--------
2/83	-89	7.98×10^{-9}	-72	2.52×10^{-7}	-63	1.56×10^{-6}	- 65	1.04×10^{-6}	- 58	4.31×10^{-6}	- 79	6.07×10^{-8}	----	--------	----	--------
3/83	-95	2.36×10^{-9}	-81	4.05×10^{-8}	-71	3.08×10^{-7}	- 79	6.07×10^{-8}	- 73	2.05×10^{-7}	- 80	4.96×10^{-8}	----	--------	----	--------
4/83	-106	2.53×10^{-10}	-93	3.54×10^{-9}	-73	2.05×10^{-7}	- 84	2.89×10^{-9}	- 78	7.44×10^{-8}	- 80	4.96×10^{-8}	----	--------	----	--------
5/83	-105	3.10×10^{-10}	-101	6.98×10^{-10}	-31	4.05×10^{-8}	- 99	1.05×10^{-9}	- 81	4.05×10^{-8}	- 85	1.80×10^{-8}	----	--------	----	--------
6/83	-72	2.52×10^{-7}	-123	8.02×10^{-12}	-104	3.80×10^{-10}	-124	6.55×10^{-12}	- 67	6.94×10^{-7}	- 87	1.20×10^{-8}	----	--------	----	--------
7/83	-79	6.07×10^{-8}	-115	4.07×10^{-11}	-126	4.36×10^{-12}	-107	2.06×10^{-10}	- 79	6.07×10^{-8}	- 99	1.05×10^{-9}	----	--------	----	--------
8/83	-94	2.89×10^{-9}	-90	6.51×10^{-9}	-102	5.70×10^{-10}	-121	1.20×10^{-11}	- 88	9.77×10^{-9}	- 79	6.07×10^{-8}	- 98	1.28×10^{-9}	- 91	5.32×10^{-9}
9/83	-71	3.08×10^{-7}	-72	2.52×10^{-7}	-91	5.32×10^{-9}	-106	2.53×10^{-10}	- 73	2.05×10^{-7}	----	--------	-104	3.80×10^{-10}	-129	2.37×10^{-9}
10/83	-62	1.92×10^{-6}	-59	3.52×10^{-6}	-55	7.93×10^{-6}	-110	1.12×10^{-10}	- 86	1.47×10^{-8}	----	--------	-116	3.32×10^{-11}	-105	3.10×10^{-10}
11/83	-71	3.08×10^{-7}	-69	4.62×10^{-7}	-59	3.52×10^{-6}	----	---------	----	--------	----	--------	- 43	9.06×10^{-5}	-100	8.55×10^{-10}
12/83	-64	1.28×10^{-6}	-70	3.77×10^{-7}	-64	1.28×10^{-6}	----	---------	----	--------	----	--------	- 65	1.04×10^{-6}	- 92	4.34×10^{-9}
1/84	-46	4.93×10^{-5}	-45	6.04×10^{-5}	-54	9.72×10^{-6}	----	---------	----	--------	----	--------	-163	2.39×10^{-15}	- 67	6.94×10^{-7}
2/84	-52	1.46×10^{-5}	-41	1.36×10^{-4}	-57	5.28×10^{-6}	----	---------	----	--------	----	--------	-128	2.91×10^{-12}	- 62	1.92×10^{-6}
3/84	-53	1.19×10^{-5}	-35	4.60×10^{-4}	-42	1.11×10^{-4}	----	---------	----	--------	----	--------	-127	3.56×10^{-12}	- 63	1.56×10^{-6}
4/84	-56	6.47×10^{-6}	-38	2.50×10^{-4}	-43	9.06×10^{-5}	----	---------	----	--------	- 69	4.62×10^{-7}	-122	9.83×10^{-12}	- 57	5.28×10^{-6}
5/84	-60	2.87×10^{-6}	-49	2.68×10^{-5}	-50	2.19×10^{-5}	----	---------	----	--------	- 69	4.62×10^{-7}	-169	7.06×10^{-16}	- 81	4.05×10^{-8}

TABLE 5. SUMMARY OF RECHARGE FLUX CALCULATED FROM MONTHLY AVERAGE PRESSURE HEAD, CORRECTED FOR AVERAGE SOIL TEMPERATURE

Month	Depths Averaged (cm)	Hydraulic Gradient	Harmonic Mean Keff(cm/s)	Harmonic Mean q(cm/s)	Geometric Mean Keff(cm/s)	Geometric Mean q(cm/s)
11/82	153,183	2.25	5.42×10^{-11}	1.22×10^{-10}	1.94×10^{-9}	4.37×10^{-9}
12/82	153,183	1.20	2.22×10^{-10}	2.67×10^{-10}	2.18×10^{-10}	2.62×10^{-10}
1/83	153,183	1.64	4.96×10^{-8}	8.13×10^{-8}	2.28×10^{-7}	3.74×10^{-7}
2/83	153,183	1.61	7.92×10^{-8}	1.28×10^{-7}	3.88×10^{-7}	6.25×10^{-7}
3/83	153,183	1.20	6.38×10^{-8}	7.66×10^{-8}	7.98×10^{-8}	9.56×10^{-8}
4/83	153,183	0.94	5.01×10^{-8}	4.71×10^{-8}	5.10×10^{-8}	4.80×10^{-8}
5/83	153,183	1.11	2.39×10^{-8}	2.65×10^{-8}	2.59×10^{-8}	2.88×10^{-8}
6/83	153,183	1.58	2.38×10^{-8}	3.76×10^{-8}	9.40×10^{-8}	1.48×10^{-8}
7/83	153,183	1.58	2.18×10^{-9}	3.44×10^{-9}	9.78×10^{-9}	1.39×10^{-8}
8/83	153,183, 214,244	1.13	3.92×10^{-9}	4.43×10^{-9}	8.93×10^{-9}	1.01×10^{-8}
9/83	153,214, 244	1.57	9.87×10^{-12}	1.55×10^{-11}	6.29×10^{-10}	9.86×10^{-10}
10/83	153,214, 244	1.22	8.97×10^{-11}	1.09×10^{-10}	5.49×10^{-10}	6.71×10^{-10}
11/83	92,214, 244	1.14	2.45×10^{-9}	2.79×10^{-9}	5.99×10^{-7}	6.83×10^{-7}
12/83	92,214, 244	1.15	1.11×10^{-8}	1.28×10^{-8}	1.42×10^{-7}	1.64×10^{-7}
1/84	92,214, 244	1.33	5.73×10^{-15}	7.62×10^{-15}	1.91×10^{-9}	2.54×10^{-9}
2/84	92,214, 244	1.20	6.81×10^{-12}	8.17×10^{-12}	2.42×10^{-8}	2.90×10^{-8}
3/84	92,214, 244	1.31	8.34×10^{-12}	1.09×10^{-11}	6.92×10^{-8}	9.04×10^{-8}
4/84	183,214, 244	0.79	2.51×10^{-11}	1.98×10^{-11}	2.64×10^{-8}	2.09×10^{-8}
5/84	183,214, 244	1.18	1.95×10^{-15}	2.30×10^{-15}	2.37×10^{-10}	2.79×10^{-10}

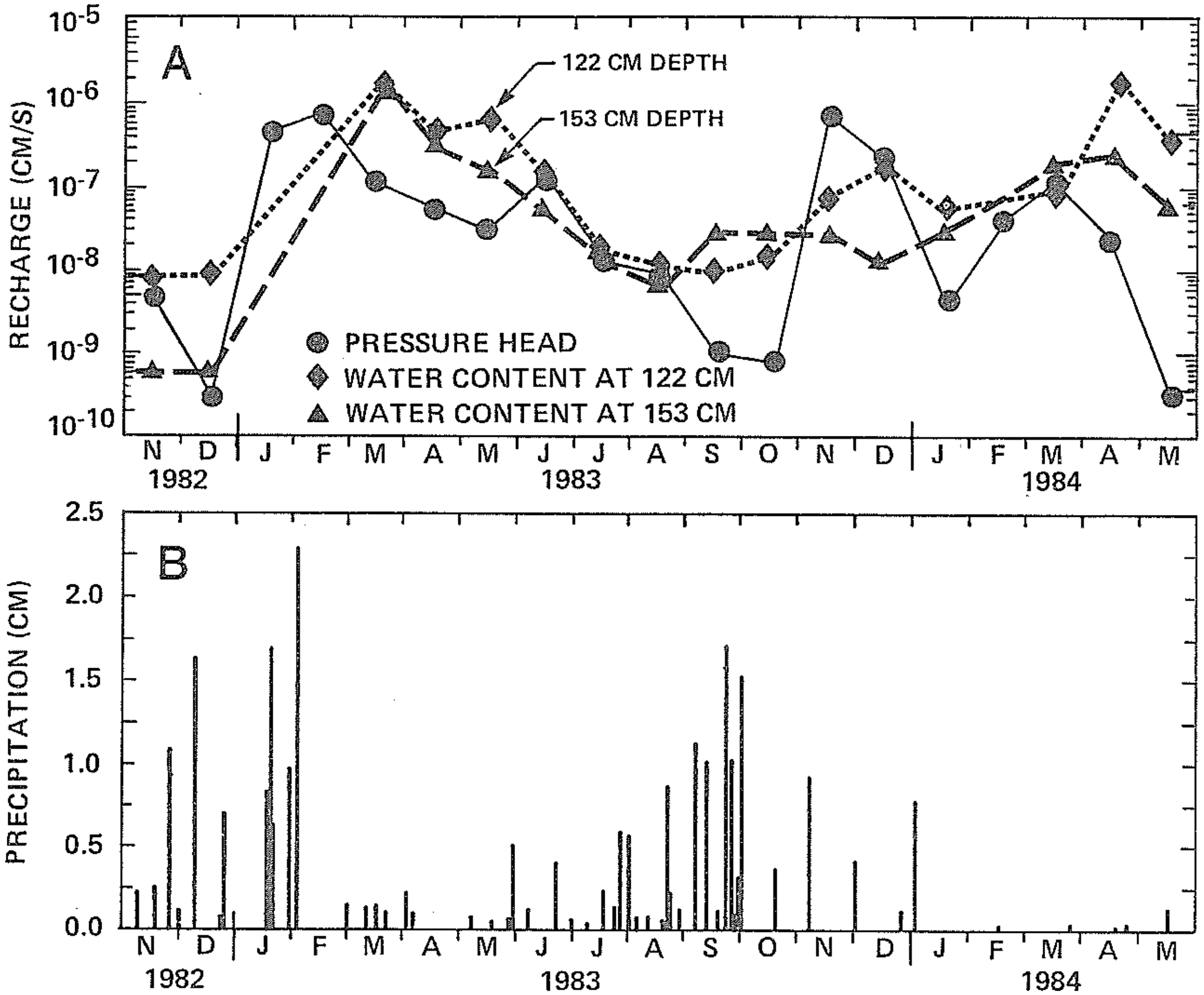

Figure 37. Calculated Soil Moisture Flux November 1982 Through May 1984.

The soil-water flux calculated above is assumed to become recharge when it arrives at the water table, about 5 m below land surface at this location. Owing to the absence of an extensive root system to withdraw moisture below a depth of about 1.5 m, the above assumption appears reasonable.

What is the percent of the precipitation which becomes recharge? This is a difficult question based on the short period of record because the proportion of a particular precipitation event which becomes recharge is dependent upon storm duration, intensity, antecedent moisture content, and evapotranspiration demand.

During the 19 month period November 1982 through May 1984, we estimate that the annual mean flux (arithmetic average of monthly recharge fluxes) is 0.70 cm/yr and 3.66 cm/yr using the harmonic and geometric mean hydraulic conductivities, respectively, from the different depth intervals. Compared with an estimated annual precipitation of 17.9 cm/yr during the same period (only 9 months of the record are from on-site measurements), recharge would comprise 5.0 percent and 26.5 percent of annual precipitation, from the harmonic and geometric mean conductivities, respectively. On the other hand, if we isolate the amount of recharge occuring from about November 1983 through May 1984 and attribute this to the 15.12 cm of precipitation which fell from May 1983 through April 1984 (figure 37), then the percentages of precipitation which become recharge are 0.469 percent and 29.6 percent for the harmonic and geometric mean cases, respectively. After October 1983 tensiometric data from the 92 cm depth were included in the recharge calculation because of the failure of some of the deeper tensiometers (table 4); as a result, recharge may be over estimated. Moreover, recharge from pressure head data may also tend to be overestimated owing to hysteresis.

The other hydrodynamic approach to calculate recharge utilizes water content data at the 122 and 153 cm depths over the same 19 month period. However, there were nearly three months during which time the neutron moisture probe (Troxler 3222 Depth Moisture Gage, Troxler Electronics Laboratory, Inc., Research Triangle Park, N.C.) was out of service due to electronics malfunction. Greater depths were not used for calculations owing to the fact that the access tube was only 220 cm deep until September 1983 and the insitu conductivities were only calculated above the 153 cm depth. Furthermore, the average moisture content at the 183 cm depth was slightly greater than that above, which suggests that the hydraulic properties at that depth may not be the same as those characterized at shallower depths by the instantaneous profile method.

Table 6 shows average volumetric water content and hydraulic conductivity for the 122 and 153 cm depths. The unsaturated hydraulic conductivity represents the average soil-water flux for the month, assuming a unit hydraulic gradient. The distribution of this flux is shown in figure 37. Recharge rates calculated from moisture content data from November and December 1982 appear to be anomalously low, possibly due to non-equilibrium between the moisture in the backfill of the access tube and that in the surrounding soil.

The percentage of precipitation which may cause recharge is calculated from water content data for the same period as in the previous case. During November 1982 through May 1984, the average annual soil-water flux is about 5.17 cm/yr at the 122 cm depth and 4.42 cm/yr at the 153 cm depth. These rates comprise 29.0 percent and 24.7 percent of the average annual precipitation rate, 17.9 cm/yr. On the average, this result agrees favorably with the flux calculated from presure head data using a geometric mean.

Moisture from the summer rains of 1983 (figure 37) appears to penetrate to the 153 cm depth by about September or October. In contrast, pressure head

TABLE 6. AVERAGE VOLUMETRIC WATER CONTENT AND HYDRAULIC CONDUCTIVITY

Month	122cm Depth $\theta(cm^3/cm^3)$	122cm Depth $K(\theta)$cm/s	183cm Depth $\theta(cm^3/cm^3)$	183cm Depth $K(\theta)$cm/s
11/82	0.045	8.05×10^{-9}	0.021	5.68×10^{-10}
12/82	0.046	9.04×10^{-9}	0.023	6.31×10^{-10}
1/83	-----	---------	-----	----------
2/83	-----	---------	-----	----------
3/83	0.090	1.47×10^{-6}	0.088	1.17×10^{-6}
4/83	0.080	4.63×10^{-7}	0.077	3.27×10^{-7}
5/83	0.083	6.55×10^{-7}	0.070	1.45×10^{-7}
6/83	0.070	1.45×10^{-7}	0.061	5.13×10^{-8}
7/83	0.052	1.81×10^{-8}	0.049	1.28×10^{-8}
8/83	0.048	1.14×10^{-8}	0.043	6.39×10^{-9}
9/83	0.047	1.01×10^{-8}	0.056	2.88×10^{-8}
10/83	0.049	1.28×10^{-8}	0.056	2.88×10^{-8}
11/83	0.064	7.26×10^{-8}	0.054	2.28×10^{-8}
12/83	0.069	1.30×10^{-7}	0.052	1.18×10^{-8}
1/84	0.061	5.13×10^{-8}	0.056	2.88×10^{-8}
2/84	-----	---------	-----	---------
3/84	0.086	9.27×10^{-7}	0.070	1.45×10^{-7}
4/84	0.089	1.31×10^{-6}	0.073	2.06×10^{-7}
5/84	0.078	3.67×10^{-7}	0.062	5.76×10^{-8}

data used to calculate recharge in figure 37 are averaged over the 153 to 244 cm depths, and moisture from summer rains does not appear at these depths until about November 1983. The total flow calculated from water content data below the 122 and 153 cm depths from September 1983 to April 1984 is 7.45 and 1.40 cm, respectively. Assuming this flow is due to the 15.12 cm of precipitation during this 8-month period, the recharge would comprise 49.3 and 9.2 percent of precipitation, respectively. Although this period contains months when plants are relatively dormant and conditions seem most favorable for recharge, the result from the 122 cm depth appears too high for an estimate of recharge. One explanation could be error associated with neutron probe measurements. After February 1984 we replaced the neutron probem which had been used for the instantaneous profile tests and all monitoring with another brand (Campbell Pacific Nuclear Corp., model 503, Pacheco, CA). Although it was calibrated in a manner similar to the other probe, there may be slight differences in measured moisture content which translate into large differences in unsaturated hydraulic conductivity. On the other hand, if the flow past the 122 cm depth is reasonable, the reduction in flow between this depth and 153 cm could be due to water uptake by the plants. In general, the sparse root network appears to be distributed above the 150 cm depth.

Temperature Gradient Method. The average temperature over the period of record, November 3, 1983 to May 29, 1984, was 12.2, 12,8, and 13.3°C at depths of 152, 183, and 213 cm below land surface, respectively. For the calculations of recharge, we estimate that the thermal conductivity was 2.09×10^{-3} cal/cm-s-°C, the field wet density was 2.06 g/cc, and the heat capacity was 1.00054 cal/gm-°C. Over the 61 cm vertical distance, the seepage velocity is calculated from equation 3 to be about 21 cm/yr. Assuming an average volumetric water content of 0.06 cm^3/cm^3, the recharge rate would be 1.26 cm/yr or 7.1 percent of precipitation measured during this same period of record. Precipitation during this period was quite low.

This approach has not been extensively applied in the unsaturated zone, and there are several sources of error associated with it. First, it is clear from figure 10 that there are significant seasonal temperature fluctuations. During spring and summer, the direction of the temperature gradient is downward, opposite to that in fall and winter. For the calculations, temperature gradients have been averaged in order to satisfy the assumption of steady state heat flow. Second, the fluid velocity, which is assumed to be constant for the model, may actually vary by more than an order of magnitude, as shown in figure 37. Third, the period of record is rather short, only about seven months; this is too brief to provide annual estimates of recharge. Fourth, the sensitivity of the meter used to read the thermistors was rather poor, because each scale division represented two decreases fahrenheit. Furthermore, the depth of the thermistors is known only to within a few centimenters, and the thermal properties and field moisture content are also only approximate. Although large errors could be expected for these and probably other reasons, the results are not inconsistent with the hydrodynamic approaches.

Deep Drainage

Changes in moisture stored in the profile below the root zone can also indicate recharge. Below the root zone, the decreases in moisture content between all measurements averaged over one year are shown in table 7. The period of record for computing the averages shown in this table extends from January 1984 through May 1985. The depths of measurement varied.

At station 1 the neutron probe access tube was deepened from about 2 m to 5 m in August 1983. For the period November 1982 through May 1984, we can use moisture content data from the 122 cm to 183 cm depths to calculate the

TABLE 7. Deep Drainage January 1984 - May 1985

STATION	PREDOMINANT LITHOLOGY	TOPOGRAPHIC CONDITION	VEGETATION	DEPTH OF MEASUREMENT (CM)	DEEP DRAINAGE (CM/YR)
1	Eolian and Alluvial Sand	Flat	Sparse	213-244	2.93
2	Alluvial Clay and Sand	Flat	Sparse	91-122	3.22
3	"	"	Dense	91-122	1.04
4	Stabilized Eolian Sand	Hillslope	Sparse	213-244	0.86
5	"	Base of Hillslope	Sparse	213-244	1.64
6	"	"	Dense	213-244	1.13
7	"	Hillslope	Sparse	213-244	1.38
8	"	"	Dense	213-244	0.63
9	Alluvial Sand and Clay	Flat (old flood plain)	Dense	213-244	1.38
10	"	"	Sparse	213-244	2.28
11	Alluvial Sand Gravel and Silt	Flat (active channel)	Sparse	30-61	2.17
12	"	"	Dense	30-61	1.71
13	Active Eolian Sand	Slope on Dune	None	213-244	2.53
14	"	Crest of Dune	"	213-244	0.57
15	"	Swale on Dune	"	213-244	1.94

approximate rate of deep drainage for comparison to the hydrodynamic results (figure 37) and the temperature gradient results. The average rate of deep drainage calculated from these depths during this time period is 4.8 cm/yr. The hydrodynamic methods using geometric mean averaging of hydraulic conductivities give a slightly greater value for this period. The drainage for this period (November 1982 through May 1984), is less than that calculated in table 6 for January 1984 through May 1984, presumably due to the smaller amount of precipitation during this period.

The variability of recharge within the instrumented areas may be estimated by the amount of deep drainage for all stations (table 7). Below about 200 cm, the deep drainage rate ranges from about 1.64 cm/yr, at a densely vegetated station in the crest of the sand dune, to 2.93 cm/yr at a sparsely vegetated lowland site underlain by alluvial and eolian sand. Precipitation during this period was below normal during the first nine months of the period, but it was significantly above normal during the winter of 1984-85 and early spring of 1985. Precipitation during the period January 1984-May 1985 fell at the annual rate of about 18 cm/yr, based on the hillside precipitation gage. The deep drainage during the same period, expressed as a percentage of the measured precipitation, would range from approximately 3 percent to 16 percent. Some long duration, low intensity storms which occur in winter and early spring undoubtedly contribute a greater percentage of precitation to deep drainage than short, intense summer thunderstorms. When greater depths of the profile are taken into account the amounts of deep drainage would increase.

In most cases the apparent effect of vegetation in deep drainage was measureable, as indicated by comparing the densely and sparsely vegetated soil-water monitoring stations in table 7. At stations 7 and 8 on the hillslope and 9 and 10 on the flatland, vegetation reduced deep drainage by about 50 percent. Vegetation reduced deep drainage slightly less at station 5 and 6, and 11 and 12. It is possible that plant root systems are much more extensive and uniform below land surface than could be inferred by the distribution of the plants on the surface. The exposure of the site to sun may also affect deep drainage, particularly that drainage which is due to snowmelt. For example, sparsely vegetated Station 11 is in full sun, whereas densely vegetated station 12 is shaded. Vegetation type may not be a clear indicator of deep drainage. The deep drainage at station 9 and 10 consists of desert shrubs and grasses, whereas stations 11 and 12 are in the salt cedar grove. Deep drainage is practically the same at those sites.

In the active dune areas, where the sands are very permeable and the vegetation is extremely sparse, the average deep drainage is not significantly greater than at the other stations. Deep drainage in the dune areas stabilized by vegetation is about the same as in the extremely sparsely vegetated dune areas.

Detailed geologic data and subsurface permeability data are not known for all the stations. This gap makes any conclusions regarding the importance of topography and vegetation rather tenuous at this time. Hydrodynamic Darcian calculations will be undertaken in the near future as time permits.

Tracer Experiments

Flatlands. There may remain some question as to whether the precipitation events, such as those shown in figure 32 in the winter of 1982-83 and summer and fall of 1983, actually caused the flux observed at the various depths just described or whether these fluxes are due to earlier events. Temporal variations in pressure head (figure 20) and calculated recharge (figure 37) show peaks shortly after the peak precipitation periods.

The two peaks are lagged by about ten months in both cases. The same trend is shown by moisture content data in figure 15. At the 30 cm depth there is a rapid increase in water content in early December 1982 after a few winter storms. The long recession in moisture content during 1983 is abated in about August; and in October the moisture increases very sharply, just after a period of considerable rainfall. This same trend propagates to the 60 cm depth. The moisture content responses to depths of 183 cm suggest that moisture propogates downward rather rapidly. The same general conclusion is reached based on pressure head data in figures 20.

The rapid transmission of moisture through the profile is supported from simple hydraulic calculations. For example, we assume a piston-type one-dimensional, gravity flow model used by Warrick et al. (1971) to estimate the velocity of a wetting front, V_{wf}:

$$V_{wf} = K(\theta_o) - K(\theta_i)/(\theta_o - \theta_i) \qquad (9)$$

where θ_o and θ_i are the water content behind and head of the wetting front, respectively. Assuming θ_o = 0.10 cm^3/cm^3 and θ_i = 0.04 cm^3/cm^3, the wetting front would move about 24 cm/d, if the flux at the surface were only sufficient to moisten the soil to 0.10 cm^3/cm^3. A moisture pulse would propogate through about 120 cm of soil in five days or through 5 meters of material to the water table in about 21 days, assuming a constant surface infiltration during this time. The pulse of moisture observed in the profile during March and April 1983 to depths of 183 cm (figure 15), is not shown in the profile at greater depths after September 1983 when deep neutron logging began. Either the pulse passed completely through the profile before September 1983, or the pulse was damped out below the 183 cm depth, or it passed through the profile during the two-month period of no records. The hydrodynamic model suggests the first explanation is possible. However, the quality of tensiometric data and neutron logging data below about the 2 m depth needs to be improved to draw more definite conclusions on the rate of soil-water movement from insitu instrumentation.

During infiltration in an agricultural plot, Warrick et al. (1971) showed, using tracers, that the infiltrated water displaced the antecedent moisture. A field experiment at our site using a bromide tracer supports this concept. A 15 cm diameter x 30 cm long plastic tube was pushed into the soil on November 29, 1983, about three weeks after any significant precipitation. On December 3, 1983, 0.44 cm of precipitation occurred. The tube was excavated on December 16, and no other precipitation occurred between the installation and sampling date. There is a pulse of moisture observed at a depth of 20 to 26 cm, as shown in figure 38. An estimate of the amount of moisture within this peak is nearly equal to that which was recorded as precipitation. This fact, and the long time between this precipitation and the previous storm, suggests that this pulse of moisture is due to the precipitation of December 3. The bromide concentration is not detected below about the 20 cm depth. From this, we infer that the precipitation which infiltrated, and mixed with bromide on the surface, displaced antecedent moisture.

Hillslopes. Not all soil-water movement takes place in a vertical direction, especially on a hillslope. To demonstrate this, a bromide tracer was buried on September 22, 1984, in the undisturbed trenches. There were rains totaling 1.6 cm on September 24 and 2.5 cm on October 3-4; after a 2.4 cm rain on October 22-24, 1984, samples were collected and analyzed by specific ion electrode for bromide concentration. Results are shown in figure 39 for bromide tracer buried at depths of 1, 15 and 50 cm. It appears that the bromide moves with a significant lateral component which was nearly the

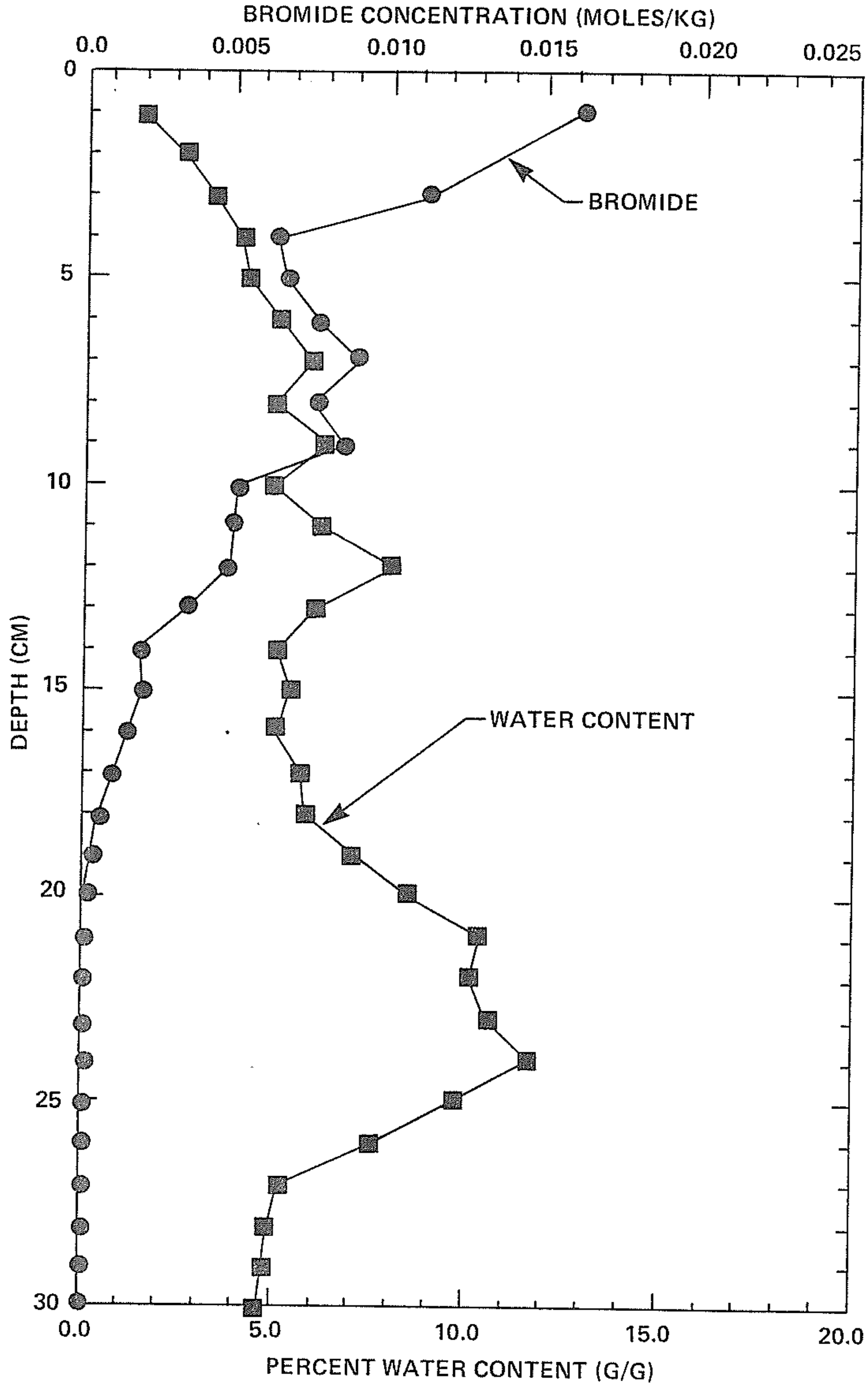

Figure 38. Tracer Movement on Flatlands.

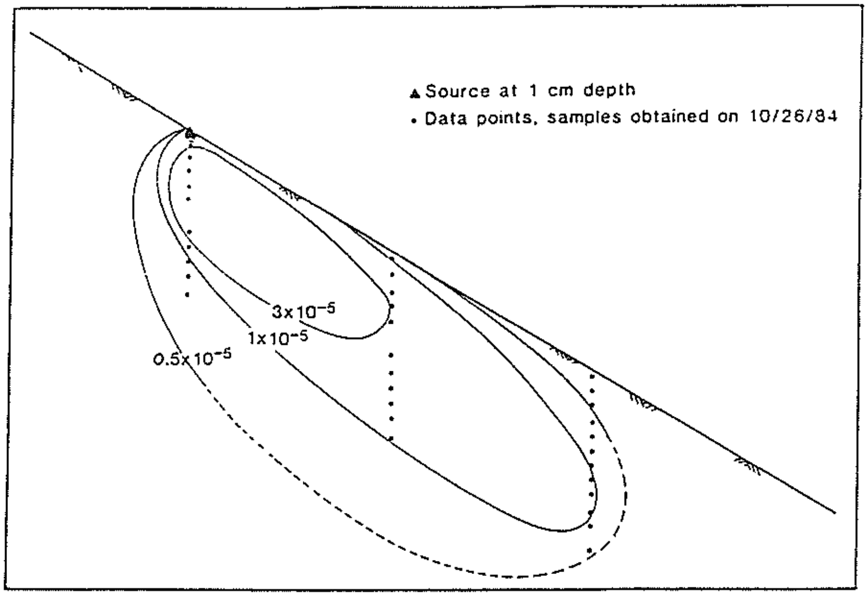

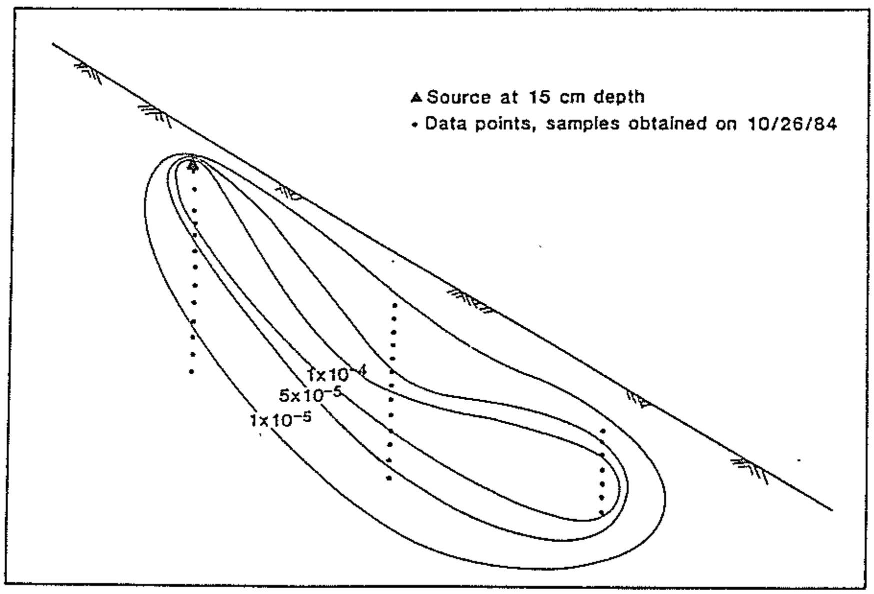

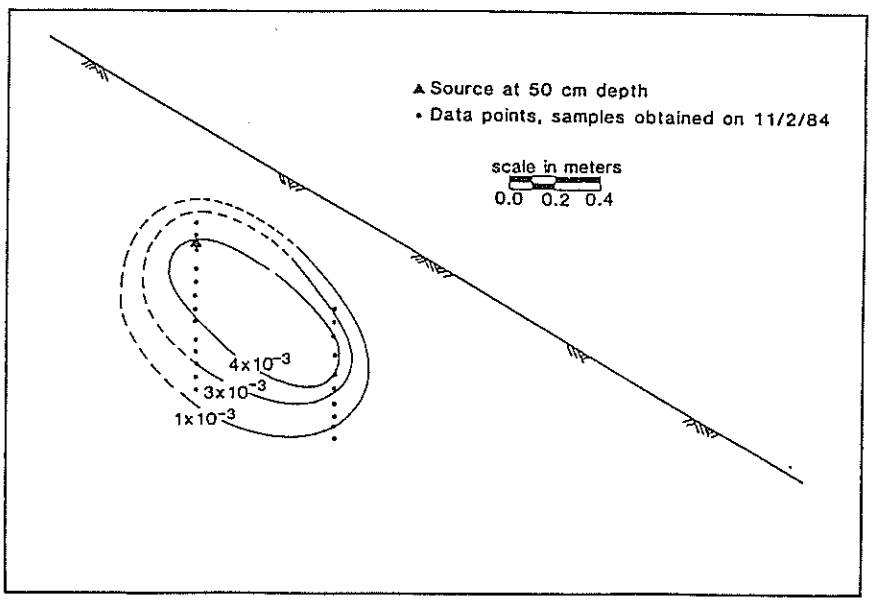

Figure 39. Tracer Movement on a Hillslope.

same direction as both the topographic slope and the direction of stratification dip. To determine whether topography or stratification is primarily responsible for the direction of tracer movement, the results of the tracer experiment the backfilled trench were evaluated. In this experiment even though the stratification was destroyed, there was significant lateral movement of the tracer. From these preliminary results, we conclude that topography has a significant influence on unsaturated flow direction on hillslopes.

Lateral Flow Inferred from Soil-Moisture Data

A similar conclusion regarding lateral flow in the unsaturated zone is inferred from data collected at soil-water monitoring stations 13, 14 and 15 on an active sand dune (figure 19). Station 13 is located on a steep slope, 14 is on the crest of the dune, and 14 is at a slight depression on the flank of the dune. Figure 40 indicates the cumulative depth of precipitation which fell on October 23-24, 1984, and the subsequent increase in soil-water storage. At the crest of the dune, station 14, only about 15 percent of the precipitation infiltrates into the profile. On the slope of the dune, about 80 percent of the precipitation infiltrated. In the lowland where slopes converge slightly toward station 15, more than 120 percent of the amount of water which fell as precipitation appears in the profile. Because there is no evidence of surface runoff, the latter results suggest there are lateral contributions of unsaturated flow from adjacent areas.

Station 1 is located in a flat land area, but it is adjacent to the flank of the sand dune. It is possible that lateral flow from the sand dune slope contributes moisture to the deep part of the profile at this location.

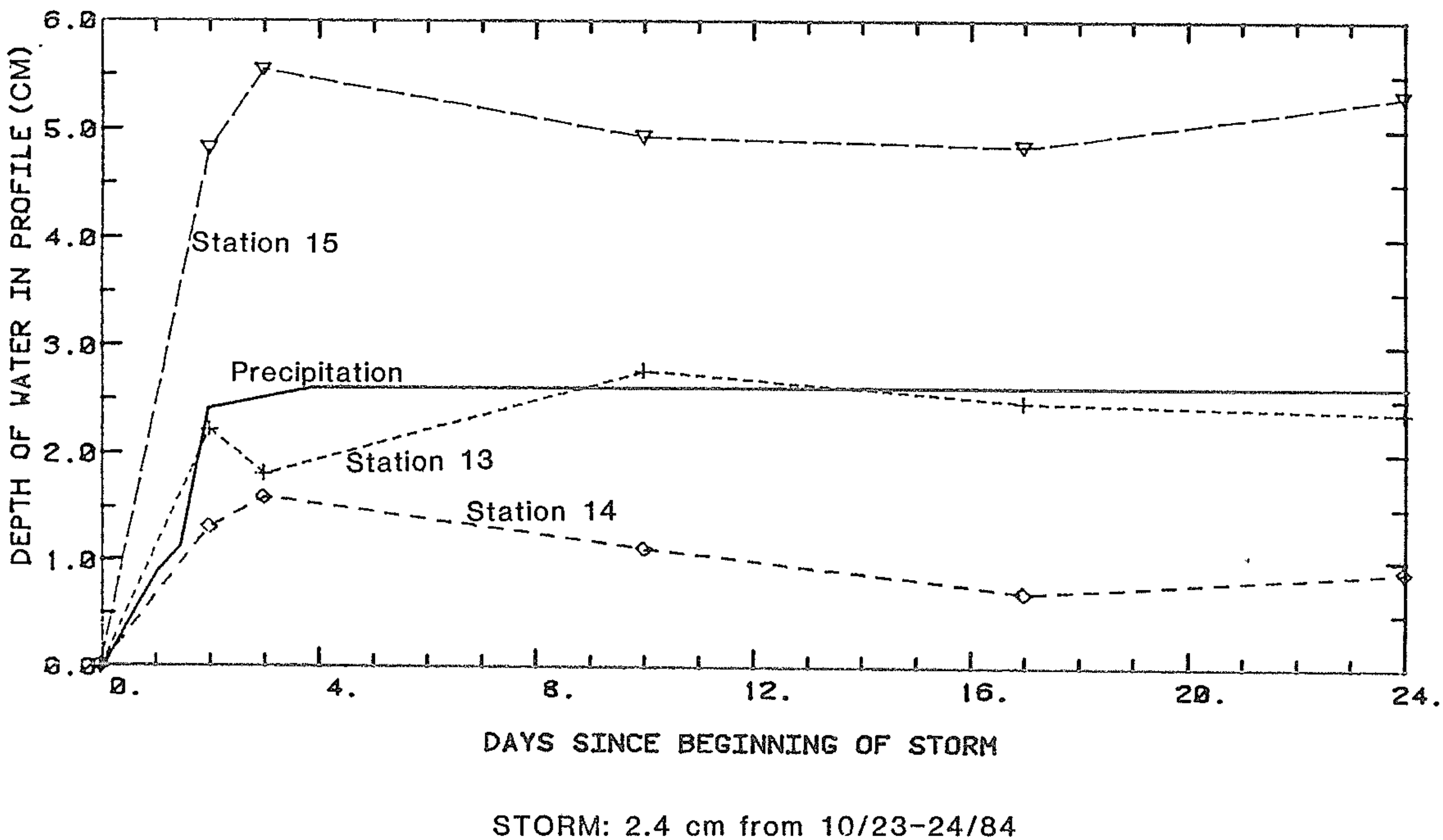

Figure 40. Response of Soil Moisture at Locations on Dune Following 2.6 cm Rainfall Event.

CONCLUSIONS

1. The research area receives approximately 20 cm of precipitation per year. Throughout the year the potential evaporation substantially exceeds precipitation.

2. Soil water content and pressure head data show responses to summer and winter precipitation to depths of more than 2 m below land surface.

3. Recharge, inferred by calculation of moisture fluxes at monitoring station 1, averages about 0.7 or 3.7 cm/yr from November 1982 to May 1984, depending on whether the effective average hydraulic conductivity of the profile is represented by a harmonic or geometric mean.

4. Temperature data are not sufficiently accurate and the existing steady-state methods are not appropriate to calculate recharge in the unsaturated zone at the research site.

5. At station 1, as estimated by drainage of moisture below the root zone, is 4.8 cm/yr. Over the same time period, this result compares very well with the results from the hydrodynamic approach using the geometric mean conductivity.

6. Within the 15 monitoring stations, the maximum deep drainage was 3.22 cm/yr in a flat, unvegetated lowland location underlain by alluvial sand for the period January 1984 through May 1985. The minimum deep drainage was 0.57 cm/yr at the crest of the active sand dune.

7. Lateral movement of soil-moisture occurs on hillslopes underlain by thick permeable, unconsolidated sand. Recharge potential is enhanced in topographically convergent areas.

ACKNOWLEDGEMENTS

We would like to thank the staff of the Sevilleta National Wildlife Refuge for their cooperation and strong support of our research. Ted Stans provided a valuable contribution to the project by identifying the native plants.

REFERENCES

Allison, G.B., W.J. Stone, and M.W. Hughes, 1985, Recharge in karst and dune elements of a semi-arid landscape as indicated by natural isotopes and chloride, J. Hydrology. 76:1-25.

Boyle, J.M. and Z.A. Saleem, 1979, Determination of Recharge Rates using Temperature-Depth Profiles in Wells, Water Resourc. Res. 15(6):1616-1622.

Byers, E. and D.B. Stephens, 1983, Statistical and stochastic analyses of hydraulic conductivity and particle size in a fluvial sand, Soil Sci. Soc. Amer. Proc. 47(6):1072-1080.

Dincer, T., A. Al-Mugrin, and U. Zimmerman, 1974, Study of the Infiltration and Recharge through Sand Dunes in Arid Zoneswith Special Reference to the Stable Isotopes and Thermo-nuclear Tritium, J. Hydrology. 23:79-109.

Enfield, C.G., J.J.C. Hsieh, and A.W. Warrick, 1973, Evaluation of Water Flux above a Deep Water Table using Thermocouple Psychrometers, Soil Sci. Soc. Amer. Proc. 37:968-970.

Freeze, R.A., 1969, The Mechanism of Natural Ground-Water Recharge and Discharge, 1. One-dimensional, Vertical, Unsteady, Unsaturated Flow above a Recharging or Discharging Ground-Water Flow System, Water Resour. Res. 5(1):153-171.

Gupta, S.K., K.K. Tanji, D.R. Nielsen, J.W. Biggar, C.S. Simmons, and J.L. MacIntyre, 1978, Field Simulation of Soil-Water Movement with Crop Water Extraction, Univ. Cal., Dept. of Land, Air and Water Resour., Water Science and Engineering Paper No. 4013, 121 pp.

Hanks, R.J., A. Klute, and E. Bresler, 1969, A Numeric Method for Estimating Infiltration, Redistribution, Drainage and Evaporation of Water from Soil, Water Resour. Res. 5:1064-1069.

Hawley, J.W., 1983, Site Identification for Low-Level Radioactive Waste Disposal in New Mexico, Report to the Radioactive Waste Consultation Committee of the New Mexico State Legislature, February 18, 1983.

Higuchi, M., 1984, Numerical Simulation of Soil-Water Flow During Drying in a Nonhomogeneous Soil, J. Hydrology. 71:303-334.

Hillel, D., V.D. Krentos, and Y. Stylianou, 1972, Procedure and Test of an Internal Drainage Method for Measuring Soil Hydraulic Characteristics In Situ, Soil Sci. 114(5):395-400.

Hillel, D., 1980, Fundamentals of Soil Physics, Academic Press, New York, 411 pp.

Jensen, K.H., 1983, Simulation of Water Flow in the Unsaturated Zone including the Root Zone, Inst. of Hydrodynamics and Hydraulic Eng., Technical University of Denmark, Series Paper No. 33, 259 p.

Jury, W.A., L.H. Stolzy, and P. Shouse, 1982, A Field Test of the Transfer Function Model for Predicting Solute Transport, Water Resour. Res. 18(2):369-375.

Kirkham, R.R. and G.W. Gee, 1983, Measurement of Unsaturated Flow Below the Root Zone at an Arid Site, Proc. Conf. on Characterization and Monitoring of the Vadose Zone, National Water Well Association.

Klute, A., R.E. Danielson, D.R. Linden, and P. Hamaker, 1972, Ground-Water Recharge as affected by Surface Vegetation and Management, Colorado State University, Colorado Water Resour. Res. Inst. Compl. Rep., No. 41, 48 pp.

Krishnamurthi, N., D.K. Sunada, and R.A. Longenbaugh, 1977, Mathematical Modeling of Natural Groundwater Recharge, Water Resour. Res. 13(4):720-724.

Longenbaugh, R.A., 1975, Computer Estimates of Natural Recharge from Soil Moisture Data, High Plains of Colorado, Colorado State University, Colorado Water Resour. Res. Inst. Compl. Rep., Series No. 64, 58 pp.

Longmire, P.A., B.M. Gallaher, and J.W. Hawley, 1981, Geological, Geochemical, and Hydrological Criteria for Disposal of Hazardous Wastes in New Mexico, New Mex. Geol. Soc., Spec. Pub. No. 10, p. 93-102.

Machette, M.N., 1978, Geologic Map of the San Acacia Quadrangle, Socorro County, New Mexico, U.S. Geol. Surv., Geologic Quadrangle Map GQ-1415.

Marthaler, H.P., W. Vogelsanger, F. Richard, and P.J. Wierenga, 1983, A Pressure Transducer for Field Tensiometers, Soil Sci. Soc. Amer. Jour. 47:624-627.

Maxey, G.B. and T.E. Eakin, 1949, Ground Water in White River Valley, White Pine, Nye, and Lincoln Counties, Nevada, Nevada State Engineer, Water Resour Bull., No. 8, 59 pp.

Meyboom, P., 1966, Estimates of Ground-Water Recharge on the Prairies, Symp. on Hydraulic Resour. of Canada, Water Resour. of Canada, University of Toronto Press.

Mualem, Y., 1984, Anisotropy of unsaturated soils, Soil Sci. Soc. Amer. J. 48(3):505-509.

Reddel, D.L., 1967, Distribution of Ground-Water Recharge, Tech. Rep. No. AER 66-67 DLR91, Agricultural Engineering Department, Colorado State University, Fort Collins, Colorado.

Saffigna, P.G., D.R. Keeney, and C.B. Tanner, 1977, Lysimeter and Field Measurements of Chloride and Bromide Leaching in an Uncultivated Loamy Sand, Soil Sci. Soc. Amer. J. 41:478-482.

Sammis, T.W., D.D. Evans, and A.W. Warrick, 1982, Comparison of Methods to Estimate Deep Percolation Rates, Water Resour. Bull. 18(3):465-470.

Stallman, R.W., 1963, Computation of Ground-Water Velocity from Temperature Data, in U.S. Geol. Surv. Water Supply Paper 1544-H, p. 36-46.

Stephens, D.B., S.P. Neuman, S. Tyler, K. Lambert, D. Watson, R. Knowlton, E. Byers, and S. Yates, 1983, Insitu Determination of Hydraulic Conductivity in the Vadose Zone using Borehole Infiltration Tests, Tech. Compl. Rep., Project B-073-NMEX, N.M. Water Resour. Res. Inst., Las Cruces, NM, 165 pp.

Stephens, D.B. and K.R. Rehfeldt, 1984, Evaluation of closed-form analytical models to calculate unsaturated hydraulic conductivity in a fine sand, submitted to Soil Sci. Soc. Amer.

Stephens, D.B., 1985, A field method to determine unsaturate hydraulic conductivity using flow nets, Water Resour. Res., in press.

U.S. Department of Agriculture, 1972, New Mexico Water Resources: Assessment for Planning Purposes, 22 maps, Soil Conservation Service.

Vomocil, J.A., 1965, Porosity, in Methods of Soil Analysis Part 1, C.A. B.ack et al. (eds.), Amer. Soc. Agro., Madison, WI, p. 299-314.

Warrick, A., J.W. Biggar, and D.R. Nielsen, 1971, Simultaneous Solute and Water Transfer for Unsaturated Soil, Water Resour. Res. 7:1216-1225.

Watson, P., P. Sinclair, and R. Waggoner, 1976, Quantitative Evaluation of a Method for Estimating Recharge to the Desert Basins of Nevada, J. Hydrology. 31:335-357.

Winograd, I.J., 1981, Radioactive Waste Disposal in Thick Unsaturated Zones, Science. 212(4502):1457-1463.